To the Graduate Council:

I am submitting herewith a thesis written by Kenneth E. Ebel entitled "Preliminary Thermal Design of The OC-5 Graphite Irradiation Creep Test Capsule and Accompanying Bench Test." I recommend that it be accepted in partial fulfillment of the requirements for the degree of Master of Science, with a major in Nuclear Engineering.

Hall C. Roland

Hall C. Roland, Major Professor

We have read this thesis
and recommend its acceptance:

James C Robinson

Paul N Stevens

Accepted for the Council:

L Evans Reed

Vice Chancellor
Graduate Studies and Research

Thesis
E
.E24
cop. 2

# PRELIMINARY THERMAL DESIGN OF THE OC-5 GRAPHITE IRRADIATION CREEP TEST CAPSULE AND ACCOMPANYING BENCH TEST

A Thesis

Presented for the

Master of Science

Degree

The University of Tennessee, Knoxville

Kenneth E. Ebel

August 1977

1328451

# ACKNOWLEDGEMENTS

This work was performed for the Metals and Ceramics Division at the Oak Ridge National Laboratory, which is operated by Union Carbide Corporation for the Energy Research and Development Administration.

The author expresses deep appreciation to Dr. H. C. Roland who served as advisor throughout the project. His guidance and encouragement are genuinely appreciated.

The contributions of many other individuals in making this work possible are gratefully acknowledged. Specifically, I would like to thank Ron L. Senn and John A. Conlin who provided stimulating discussions and helpful suggestions throughout this work, and Walter E. Eatherly whose support made this work possible.

I would also like to thank Ann D. Peach for patiently typing this thesis, Michael and Damon Falconnier for the graphics, and E. J. Allen for his advice on preparing this thesis.

# ABSTRACT

This report is of a preliminary nature and is intended to provide information necessary for the swift completion of the design of the 1250°C Irradiation Creep Capsule, designated as the OC-5 capsule. Included are the thermal design specifications of the OC-5 capsule along with the preliminary thermal design. This report also contains the thermal design of a bench test which is to be used to verify the thermal design of the OC-5 capsule. In particular, the bench test is to check the constancy of the radiant emissivity of the tungsten reflector under simulated capsule conditions.

TABLE OF CONTENTS


| CHAPTER | | PAGE |
|---|---|---|
| I. | INTRODUCTION | 1 |
| II. | OC-5 IRRADIATION CREEP CAPSULE | 9 |
| | 2.1 Initial Restrictions | 9 |
| | 2.2 Assumptions and Materials | 10 |
| | 2.3 Gross Lattice Computational Model of the OC-5 Capsule | 11 |
| | 2.4 Redesign of the OC-5 Capsule | 19 |
| | 2.5 Axial Shift of the Gamma Heating Distribution | 24 |
| | 2.6 Refinement of Axial Resolution | 29 |
| | 2.7 Parameter Evaluation | 33 |
| | 2.8 Conclusion | 49 |
| III. | BENCH TEST | 55 |
| | 3.1 Design Requirements | 57 |
| | 3.2 Assumptions and Simplifications | 58 |
| | 3.3 Thermal Design | 59 |
| | 3.4 Angular Temperature Variation | 62 |
| | 3.5 Thermal Effect of Discontinuities | 67 |
| | 3.6 Experimental Operation Guide | 69 |
| | 3.7 Conclusion | 70 |
| IV. | SUMMARY | 96 |
| LIST OF REFERENCES | | 97 |
| VITA | | 99 |

# LIST OF TABLES


| TABLE | | PAGE |
|---|---|---|
| 2-1. | Material Properties Used in the Thermal Analysis of the OC-5 Irradiation Capsule . . . . . | 13 |
| 3-1. | Radial Temperature Distribution of the Bench Test as Calculated Using the GENGTC and HEATING 5 Codes. . | 61 |
| 3-2. | Calculated Radial Temperature Distributions for Various Bench Test Coolant Temperatures . . . . . | 71 |
| 3-3. | Calculated Radial Temperature Distributions for Various Radiant Emissivities of the Unpolished Tungsten Surface. . . . . | 72 |
| 3-4. | Figure Reference with Parameters for Use in Controlling the Radial Temperature Distribution of the Bench Test During Operation. . . . . | 74 |

# LIST OF FIGURES


| FIGURE | | PAGE |
|---|---|---|
| 1-1. | Characteristic Creep Behavior of Graphite. . . . . | 2 |
| 1-2. | 900°C Irradiation Creep Capsule Radial Cross Section and Specimen Axial Cross Section. . . . . | 4 |
| 1-3. | 900°C Irradiation Creep Capsule Control Specimen Axial Cross Section . . . . . | 5 |
| 1-4. | 900°C Irradiation Creep Capsule Specimen and Control Specimen Axial Cross Section Enlargement. . . . . | 6 |
| 2-1. | Simplified Model Cross Section of the OC-5 Capsule . . . | 12 |
| 2-2. | Neon-Argon Gas Mixtures Thermal Conductivity, B. H. Montgomery 9/17/73 . . . . . | 14 |
| 2-3. | Helium-Argon Gas Mixtures Thermal Conductivity. B. H. Montgomery 9/17/73 . . . . . | 15 |
| 2-4. | Helium-Neon Gas Mixtures Thermal Conductivity. B. H. Montgomery 9/17/73 . . . . . | 16 |
| 2-5. | Gamma Heating Rate. Position E-5 of the ORR Reactor. . . | 17 |
| 2-6. | OC-5 Capsule Computational Model Cross Section. . . . . | 18 |
| 2-7. | OC-5 Capsule Computational Model Cross Section with Thermal Radiation Reflector . . . . . | 20 |
| 2-8. | Comparison for Heater Effectiveness. Heater power of approximately 3.94 watt/cm . . . . . | 21 |
| 2-9. | OC-5 Capsule Computational Model Cross Section after Removal of Heaters . . . . . | 25 |

FIGURE PAGE

2-10. Axial Dimensional Variation of Outer Gas Gap-Coarse Resolution. . . . . 26

2-11. Gamma Heating Rate at Beginning and End of 14 Day Reactor Power Cycle . . . . . 27

2-12. Specimen Central Temperature Distribution at the Beginning of the Reactor Power Cycle and the End with the Capsule Unshifted and Shifted 5 cm . . . 28

2-13. Comparison of Axial Resolution of the Specimen Central Temperature Distribution. . . . . 31

2-14. Example of Resolution vs. Curve Approximation in HEATING 5 Code. . . . . 32

2-15. Specimen Central Temperature Distribution Before and After Refinement of the Outer Gas Gap-Fine Resolution. . . . . 34

2-16. Axial Dimensional Variation of Outer Gas Gap-Fine Resolution. . . . . 35

2-17. Comparison of Specimen Central Temperature Distributions for Several Polished Tungsten Emissivities and Corresponding Gas Mixtures . . . . . 40

2-18. Comparison of Thermocouple Temperature Distributions for Several Polished Tungsten Emissivities and Corresponding Gas Mixtures. Distributions Obtained at a Radius of 2.896 cm Between Specimen Columns . . 41

FIGURE PAGE

2-19. Comparison of Specimen Central Temperature Distributions for Several Polished Tungsten Emissivities and Corresponding Gas Mixtures at End of Reactor Power Cycle . . . . . 42

2-20. Comparison of Thermocouple Temperature Distributions for Several Polished Tungsten Emissivities and Corresponding Gas Mixtures at End of Reactor Power Cycle. Distributions Obtained at a Radius of 2.896 cm between Specimen Columns . . . . . 43

2-21. Comparison of Specimen Central Temperature Distributions for Various Gas Mixtures and Polished Tungsten Emissivity of 0.3 . . . . . 44

2-22. Comparison of Specimen Central Temperature Distributions for Various Gas Mixtures and Polished Tungsten Emissivity of 0.5 . . . . . 45

2-23. Comparison of Specimen Central Temperature Distributions for Two Gas Mixtures and Polished Tungsten Emissivity of 0.8. . . . . 46

2-24. Final Simplified Model Cross Section of the OC-5 Capsule. 50

2-25. Axial Distribution of Specimen Central Temperature and Thermocouple Temperatures at Two Possible Locations. Thermocouple Locations are at a Radius of 2.896 cm . . . . . 51

2-26. Axial Distribution of Specimen Temperature at Four Cross-Sectional Locations. . . . . 52

FIGURE PAGE

3.1 Simplified Bench Test Cross Section. . . . . 60

3.2 Cross-Sectional Bench Test Temperature Distribution. . . 63

3.3 Angular Variation of Nusselt's Number vs. Reynold's Number for Cylinder in Cross Flow . . . . . 65

3.4 Circumferential Temperature Variation Due to Variation in Forced Convection Coefficient. . . . . 66

3.5 Axial Temperature Distribution with 0.638 cm Discontinuity in Dummy Graphite Specimen. . . . . 68

3-6. Cross-Sectional Temperature Distributions - Variation in Polished Tungsten Emissivities . . . . . 73

3-7. Cross-Sectional Temperature Distributions - Variation in Heater Power. Polished Tungsten Emissivity of 0.1 . . . . . 75

3-8. Cross-Sectional Temperature Distributions - Variation in Heater Power. Polished Tungsten Emissivity of 0.15 . . . . . 76

3-9. Cross-Sectional Temperature Distributions - Variation in Heater Power. Polished Tungsten Emissivity of 0.3 . . . . . 77

3-10. Cross-Sectional Temperature Distributions - Variation in Heater Power. Polished Tungsten Emissivity of 0.5 . . . . . 78

3-11. Cross-Sectional Temperature Distributions - Variation in Coolant Flow. Polished Tungsten Emissivity of 0.1 . . . . . 79

FIGURE PAGE

3-12. Cross-Sectional Temperature Distributions - Variation in Coolant Flow. Polished Tungsten Emissivity of 0.15 . . . . . 80

3-13. Cross-Sectional Temperature Distributions - Variation in Coolant Flow. Polished Tungsten Emissivity of 0.3. . . . . 81

3-14. Cross-Sectional Temperature Distributions - Variation in Coolant Flow. Polished Tungsten Emissivity of 0.5. . . . . 82

3-15. Cross-Sectional Temperature Distributions - Variation in Gas Mixture. Polished Tungsten Emissivity of 0.15 . . . . . 83

3-16. Cross-Sectional Temperature Distributions - Variation in Gas Mixture. Polished Tungsten Emissivity of 0.3. . . . . 84

3-17. Cross-Sectional Temperature Distributions - Variation in Gas Mixture. Polished Tungsten Emissivity of 0.5. . . . . 85

3-18. Cross-Sectional Temperature Distributions - Variation in Polished Tungsten Emissivity and Heater Power for Dummy Specimen Temperature of 1219$^{o}$C. . . . 86

3-19. Cross-Sectional Temperature Distributions - Variation in Polished Tungsten Emissivity and Coolant Flow for Dummy Specimen Temperature of 1219$^{o}$C. . . . . 87

FIGURE PAGE

3-20. Cross-Sectional Temperature Distributions - Variation in Polished Tungsten Emissivity and Gas Mixture for Dummy Specimen Temperature of 1219°C. . . . . 88

3-21. Cross-Sectional Temperature Distributions - Variation of Heater Power and Coolant Flow for Polished Tungsten Emissivity of 0.15 and Gas Mixture of Neon plus 0.4 Mole Fraction Helium . . . . . 89

3-22. Cross-Sectional Temperature Distributions - Variation of Heater Power and Coolant Flow for Polished Tungsten Emissivity of 0.3 and Gas Mixture of Neon plus 0.4 Mole Fraction Helium . . . . . 90

3-23. Cross-Sectional Temperature Distributions - Variation of Heater Power, Coolant Flow, and Gas Mixture for Polished Tungsten Emissivity of 0.15. . . . . 91

3-24. Cross-Sectional Temperature Distributions - Variation of Heater Power and Coolant Flow for Polished Tungsten Emissivity of 0.3 and Gas Mixture of Neon plus 0.2 Mole Fraction Helium. . . . . 92

3-25. Proposed End Design of the Bench Test. Preliminary Design. . . . . 95

# CHAPTER I

## INTRODUCTION

Graphite, due to its low neutron cross section, is used as the moderator in several nuclear reactor systems. The neutron flux and the temperature gradients in the graphite moderator blocks result in time varying differential growth which, in turn, causes stresses. Fortunately, graphite has the ability to creep under irradiation, relaxing the stress intensity. Knowledge of these effects allows the graphite blocks to be designed in such a way that the stresses remain below critical levels for fracture and hence help form a dimensionally stable core.

The characteristic creep behavior, Figure 1-1, consists of a quasi-elastic transient component, which is rapidly recovered if the stress is removed during irradiation, followed by a steady-state non-recoverable component, during which the strain increases linearly with fluence. The transient and the steady-state creep strains are proportional to the applied stress and equal in magnitude for tensile or compressive stresses, and increase with increasing irradiation temperature over the interval of 500°C to 1200°C.[1]

Probably the most useful technique in investigating irradiation induced creep is one in which the sample is loaded in tension or compression, to a known stress, in an irradiation capsule and the strain is recorded as a function of neutron fluence. A series of such experiments at different stresses and temperatures, for a given type graphite, will completely characterize the creep behavior. This

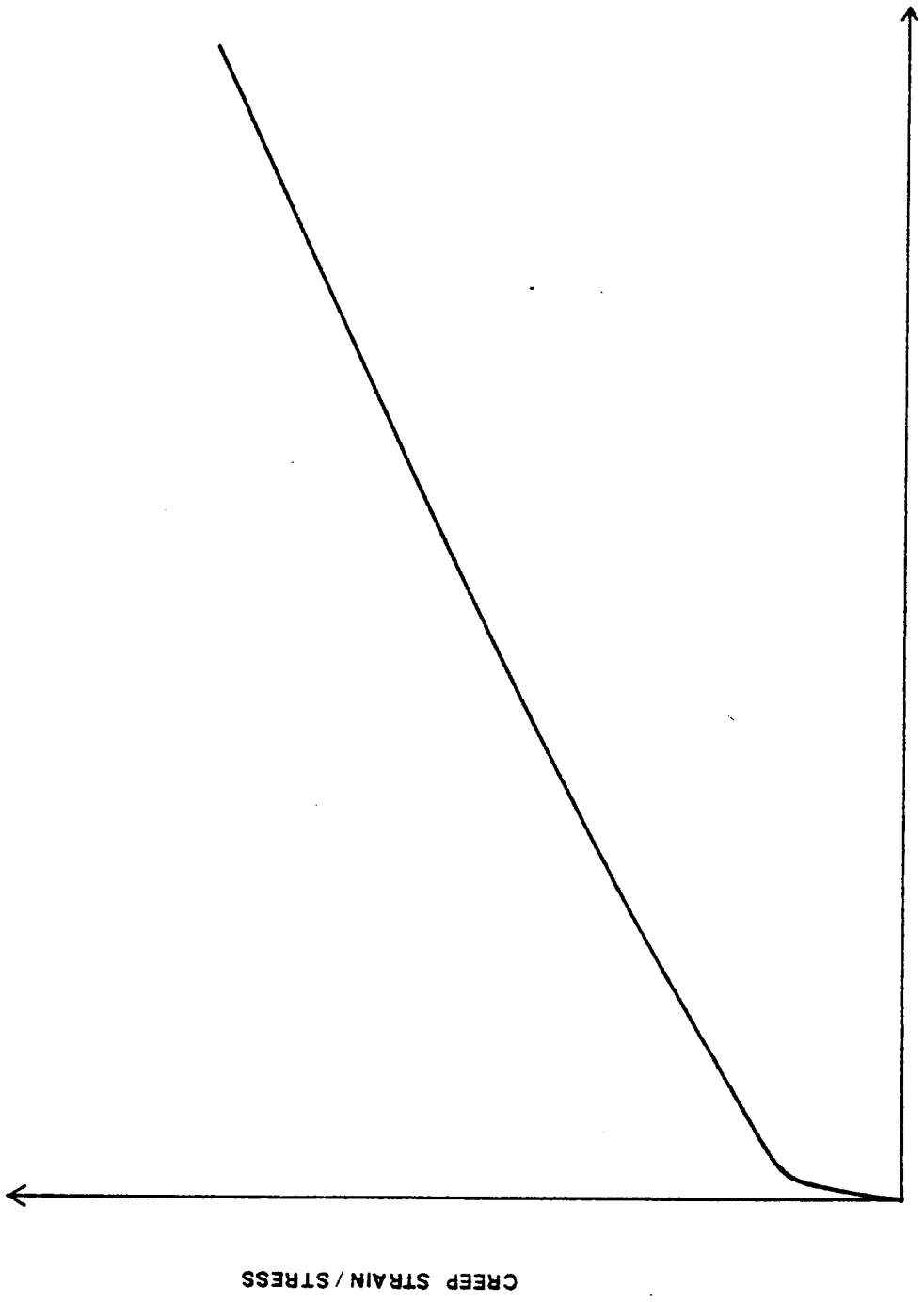



Figure 1-1. Characteristic Creep Behavior of Graphite.

has the disadvantage of high cost and experimental difficulties, i.e. the unreliability of continuous in-pile strain measuring devices. The use of strings of samples loaded to a constant stress, without a continuous strain read-out, is a less expensive modification of the first technique. The creep strain is measured when the capsule is disassembled and further strain measurements require reencapsulation and reirradiation. This technique has the disadvantage of producing a small number of strain readings on each sample which makes accurate measurement of the transient creep period difficult. A third technique is the use of self straining assemblies in which stress is applied to the specimen through the differential in the irradiation induced dimensional change rates between the specimen and a pad, sleeve, or spacer made from a different type of carbon material. The advantages are low cost and simplicity with the disadvantage of not knowing the stress during irradiation. In all three techniques, unstressed samples are irradiated with the creep samples and the creep strain is obtained by subtracting the dimensional change in the unstressed samples from the strain in the stressed samples. Also in all three techniques, a series of experiments at different stresses and temperatures, for a given type graphite, is needed to characterize the creep behavior.[1]

A series of three experiments was begun at Oak Ridge National Laboratory several years ago in which the second technique mentioned above is being used. The capsules used in the experiments are of the same basic design with minor modifications. This basic design is that of the OC-2 capsule, shown in Figures 1-2, 1-3, and 1-4. It consists

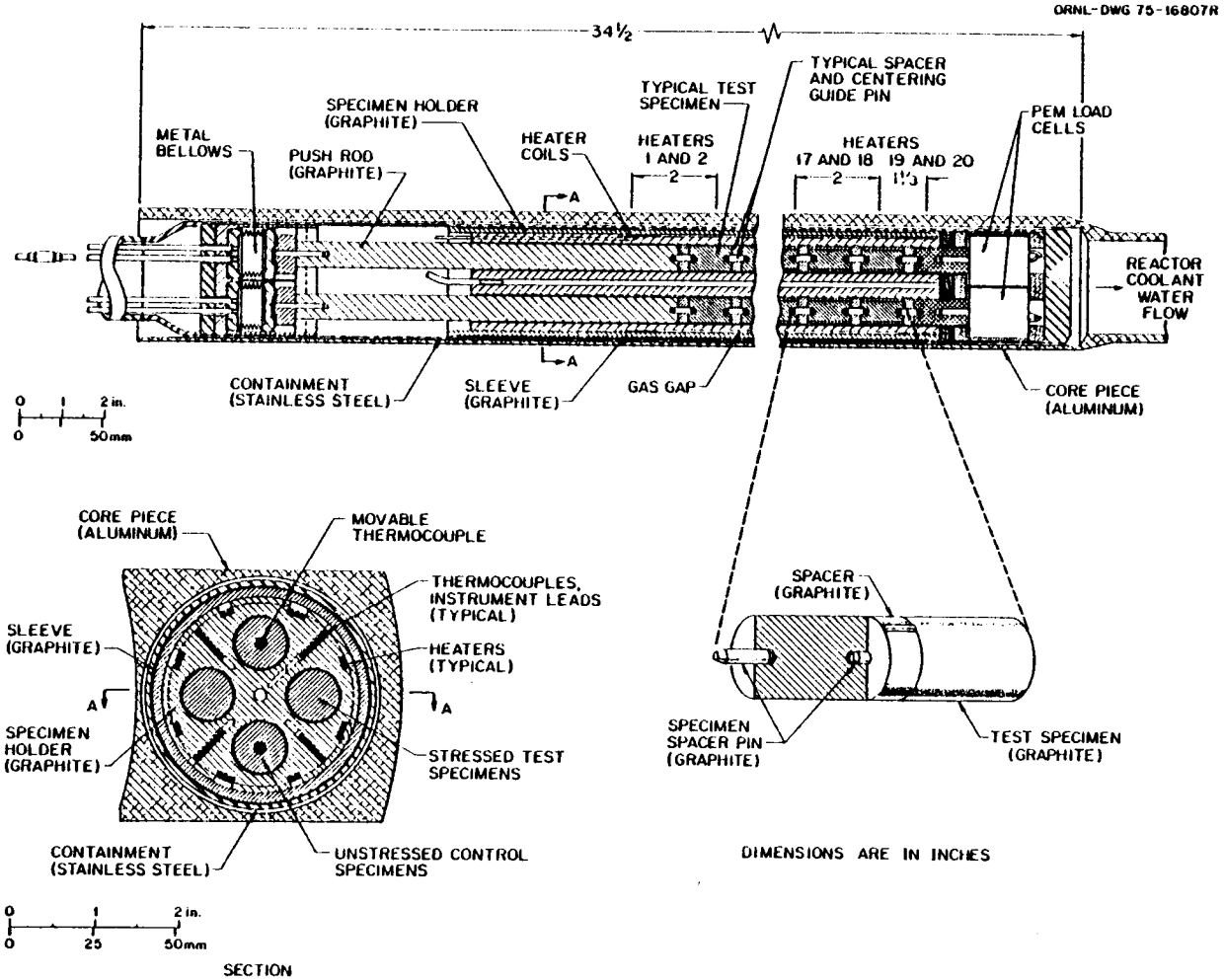



Figure 1-2. 900°C Irradiation Creep Capsule Radial Cross Section and Specimen Axial Cross Section.

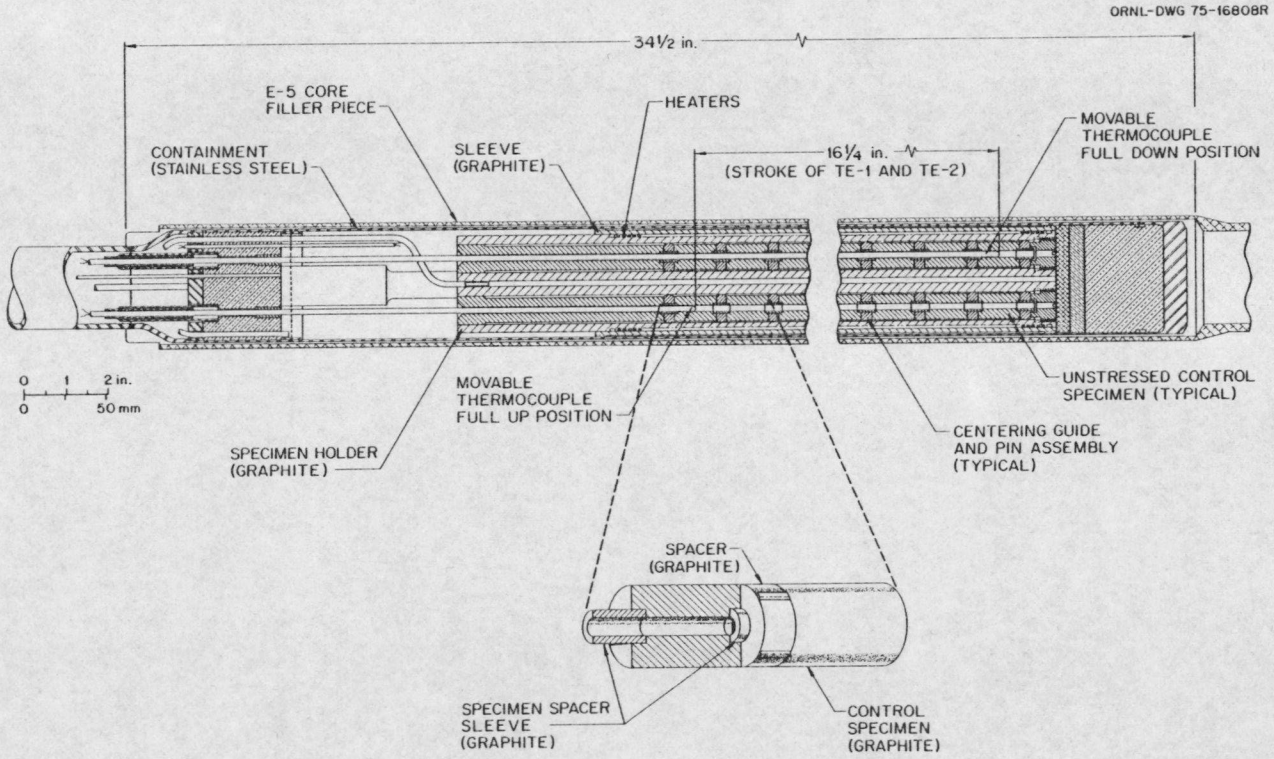



Figure 1-3. 900°C Irradiation Creep Capsule Control Specimen Axial Cross Section.

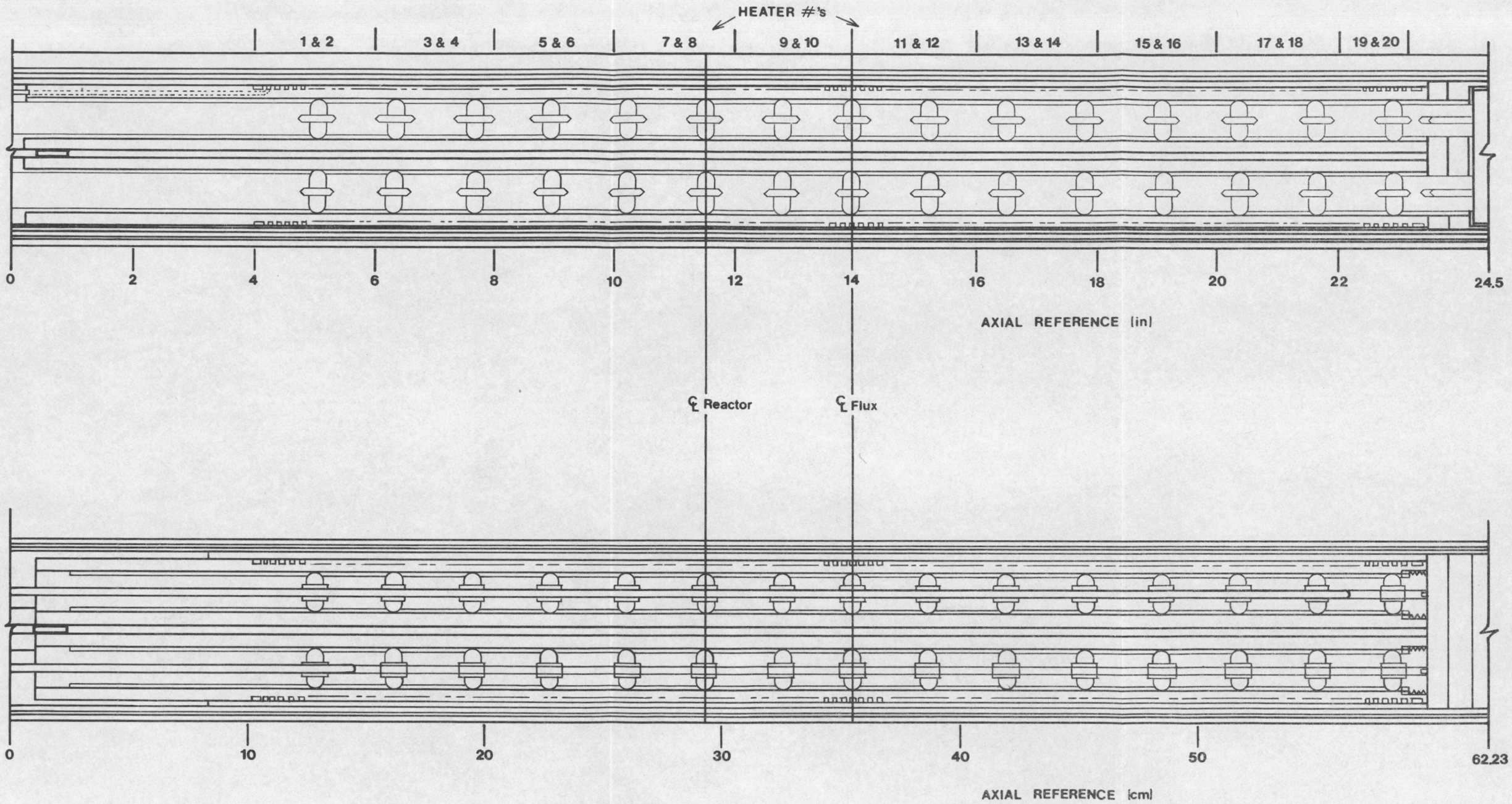



Figure 1-4. 900°C Irradiation Creep Capsule Specimen and Control Specimen Axial Cross Section Enlargement.

of a pressurized bellows arrangement at the top of the two specimen columns (creep specimens) to produce the stress and a pressure sensor at the bottom to determine whether or not the stress is being transmitted through the column. Two other specimen columns (control specimens) are unstressed. Thermocouples are placed at intervals between the specimen columns and a moveable thermocouple within each of the control specimen columns. A series of individually controlled heaters along the length of the capsule provide for temperature control of the specimens. Three capsules are planned such that constant temperatures of 600°C, 900°C, and 1250°C can be maintained within the specimens.

Chapter II covers the thermal analysis and preliminary design of the third experiment, designated the OC-5 irradiation creep capsule, with design specimen temperatures of 1250°C. Several of the problems are discussed which arose due to this extremely high temperature, along with the redesign these problems necessitated.

Chapter III deals with the design of a bench test needed to determine whether or not the thermal radiation reflector, used in the redesign of the capsule, will retain its properties throughout the operation of the OC-5 experiment. The last section of this chapter consists of results obtained by varying pertinent parameters in an effort to aid in controlling the temperature distribution during operation of the bench test.

This report only deals with the preliminary thermal design of the OC-5 capsule and the bench test. Further analysis of the ends of both the capsule and the bench test may be required.

Should the bench test return favorable results, only small changes in the gas composition and gas gaps may be required to complete the gross lattice analysis of the OC-5 capsule. At this point, a brief fine lattice analysis will be needed to complete the thermal design.

# CHAPTER II

## OC-5 IRRADIATION CREEP CAPSULE

Several years ago a series of three experiments was begun at the Oak Ridge National Laboratory and designed to investigate irradiation creep behavior in graphite. Each experiment consists of a capsule under irradiation containing four strings of samples, two under pressure and two unloaded. The three capsules are planned such that constant temperatures of 600°C, 900°C, and 1250°C can be maintained within the specimens.

This chapter covers the gross lattice thermal analysis and design of the 1250°C capsule, where the term gross lattice is used to indicate that the analysis was done on a rough model of the capsule. Although the design is not completed in every detail, further analysis and design must await the completion of the bench test (Chapter III).

### 2.1 Initial Restrictions

The restrictions placed upon the design of the OC-5 irradiation creep capsule were initially as follows:

1. The specimen temperature of 1250°C was to be achieved by simply adjusting the gas gaps and gas composition in the general design of the 600°C and 900°C irradiation creep capsules (Figures 1-2, 1-3, and 1-4).
2. The maximum temperature on the heaters was not to be in excess of 950°C.
3. The maximum temperature on the thermocouples located between the specimen columns was not to be in excess of 950°C.

During the process of design, it became evident that the first restriction had to be relaxed in order to satisfy the other two restrictions and, after completing the rough design, had to be virtually eliminated due to the ineffectiveness of the heaters.

## 2.2 Assumptions and Materials

In order to reduce computer time, and therefore cost of analysis, several simplifying assumptions were made for use in the gross lattice description.

End effects were neglected due to the thermal insulation and greatly reduced gamma heating at the ends and the placement of the ends some distance beyond the specimen region.

Each string of samples was assumed to be a continuous solid cylindrical sample. This is a fair assumption for the gross lattice description because the specimens and spacers are of approximately the same material; however, a more accurate description should be used during the fine lattice analysis

The heater regions were assumed to be a continuous material with a smeared density and conductivity, which were obtained from the fine lattice calculations for the 600$^{o}$C capsule.[2] This assumption may be somewhat questionable as to accuracy, however, it was necessary to make the computer calculations for the entire capsule possible. Fortunately, this became unimportant due to the elimination of the heaters at a later stage of the development.

Because of the very low flow rates involved (a few cubic centimeters per minute) and laminar flow, the sweep gas in the capsule was assumed stagnant.

The capsule was assumed to have adiabatic radial planes of symmetry which occur every $45^{o}$ (.7854 radians). This assumption was reasonable because of the symmetrical arrangement of the capsule (see Figure 1-2).

The thermocouples were neglected. This was a fair assumption because of the comparatively small volumes and masses involved and their location on adiabatic planes; however, they should be included in the fine lattice analysis.

The model arrived at after these simplifying assumptions had been invoked is shown in Figure 2-1. It was from this model that the computer calculational model was obtained and the gross lattice thermal design made.

The revelant material properties are listed in Table 2-1 and Figures 2-2, 2-3, and 2-4. The approximate gamma heating curve for the Oak Ridge Research Reactor (ORR) at position E-5 is shown in Figure 2-5.

## 2.3 Gross Lattice Computational Model of the OC-5 Capsule

The computer code initially used was HEATING $3^{3}$; however, after the nodal limit for this code was exceeded, HEATING $5^{4}$ was used. The coordinate system used in both of these codes was R-$\Theta$-Z and the unit system used was in.-min.-$^{o}$F-radian-lb.-Btu.

The capsule model using the HEATING 3 code is shown in Figure 2-6, for a particular axial position. The axial dimensional variations, not shown, occur in the outer gas gap. In constructing Figure 2-6 from Figure 2-1, it was desired to have the same cross sectional areas and perimeters of the specimen and surrounding gas gap; however, as the

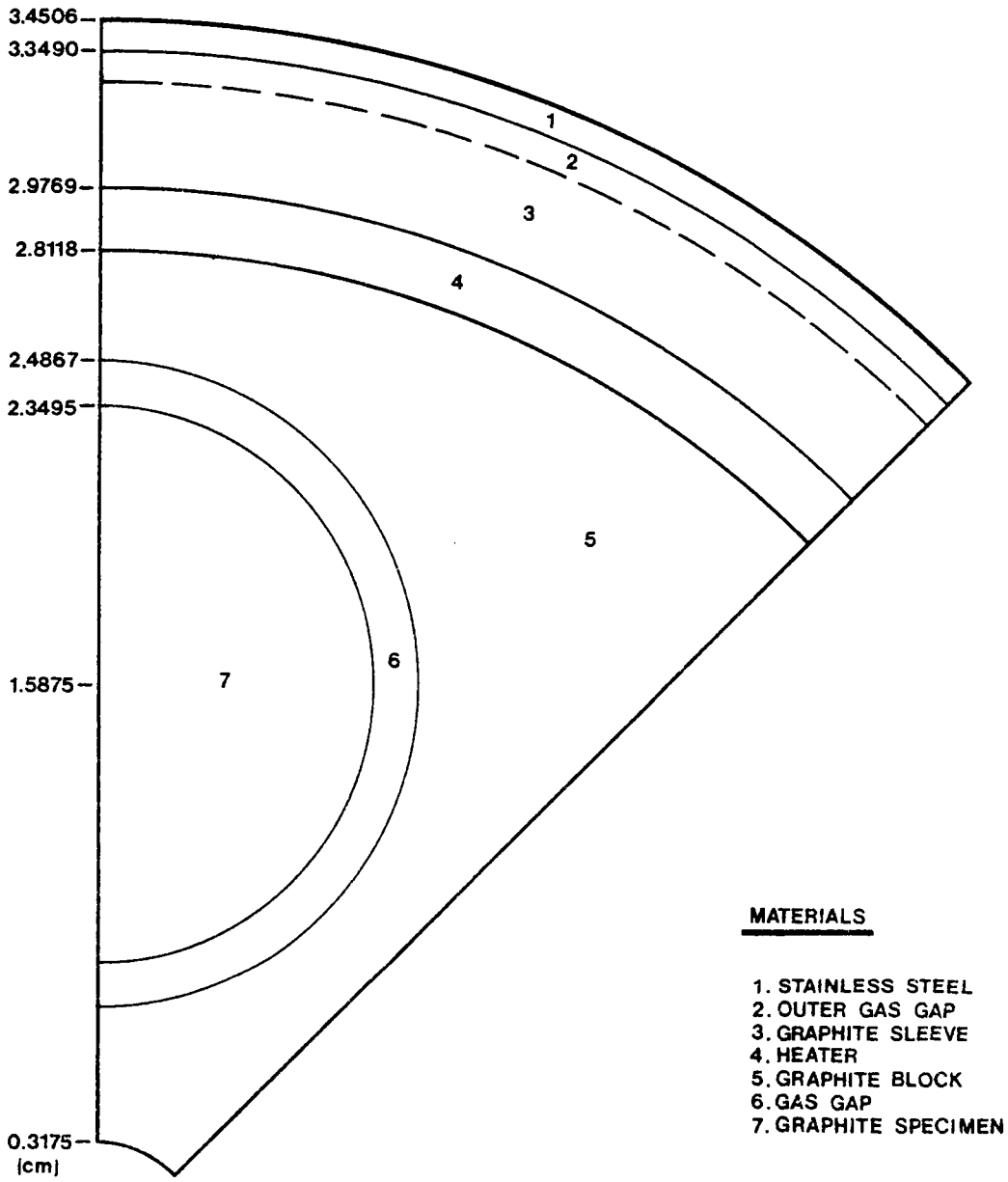



Figure 2-1. Simplified Model Cross Section of the OC-5 Capsule.

TABLE 2-1

MATERIAL PROPERTIES USED IN THE THERMAL ANALYSIS
OF THE OC-5 IRRADIATION CAPSULE

| Material | Density ($gm/cm^3$) | Radiant Emissivity | Conductivity | |
|---|---|---|---|---|
| | | | Conductivity (BTU/min-in-$^oF$) | Temperature ($^oF$) |
| Stainless Steel | 7.85 | 0.7 | 0.01111 | 32 |
| | | | 0.01306 | 212 |
| | | | 0.01514 | 572 |
| Graphite | 1.79 | 0.9 | 0.025 | constant |
| Tungsten | 19.3 | 0.7[a] | 0.1139 | 500 |
| | | | 0.1028 | 1000 |
| | | | 0.09305 | 1700 |
| | | | 0.08917 | 2400 |
| Heater Region | 1.79 | 0.9 | 0.008[b] | constant |
| Sweep Gas | 0.0 | 0.0 | Figures 2-2, 2-3, and 2-4 | |

| Coolant | Temperature ($^oF$) | Coefficient of Forced Convection (BTU/min-$in^2$-$^oF$) |
|---|---|---|
| Water | 118 | 0.6181 |

[a]The radiant emissivity of polished tungsten is estimated to be 0.15.

[b]Smeared value obtained by reference to the OC-3 Irradiation Capsule thermal analysis.

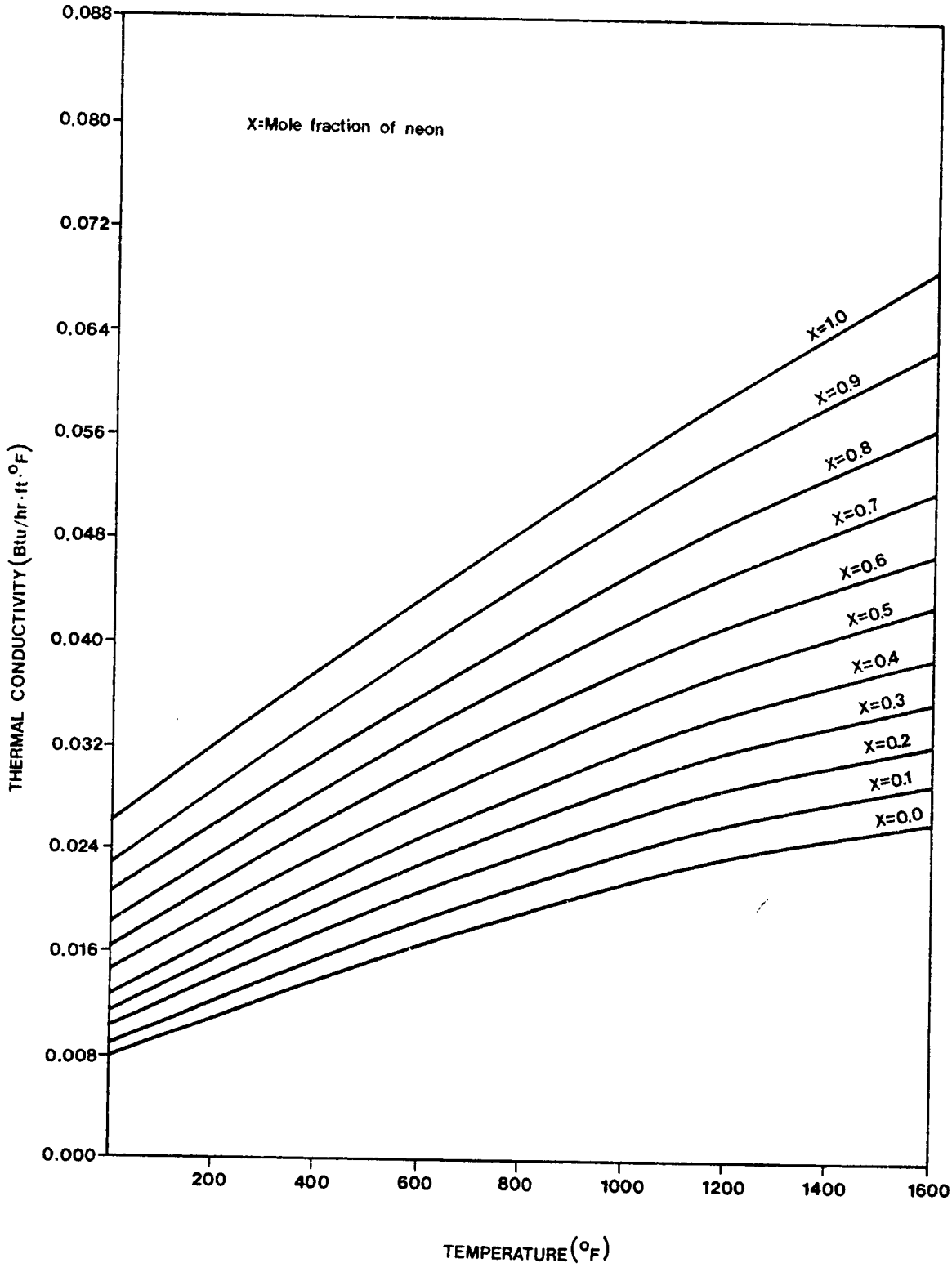



Figure 2-2. Neon-Argon Gas Mixtures Thermal Conductivity.
B. H. Montgomery 9/17/73.

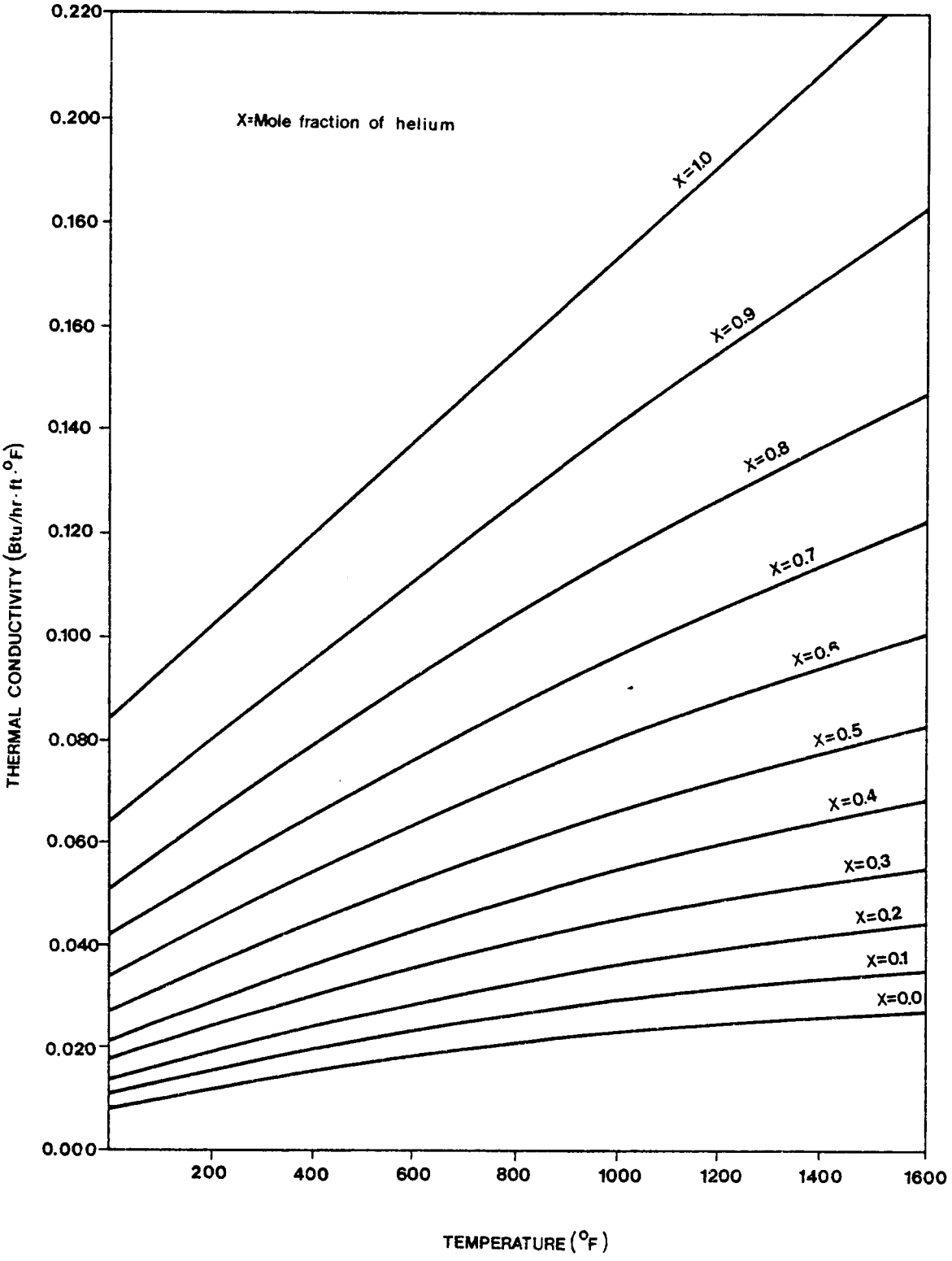



Figure 2-3. Helium-Argon Gas Mixtures Thermal Conductivity.
B. H. Montgomery 9/17/73.

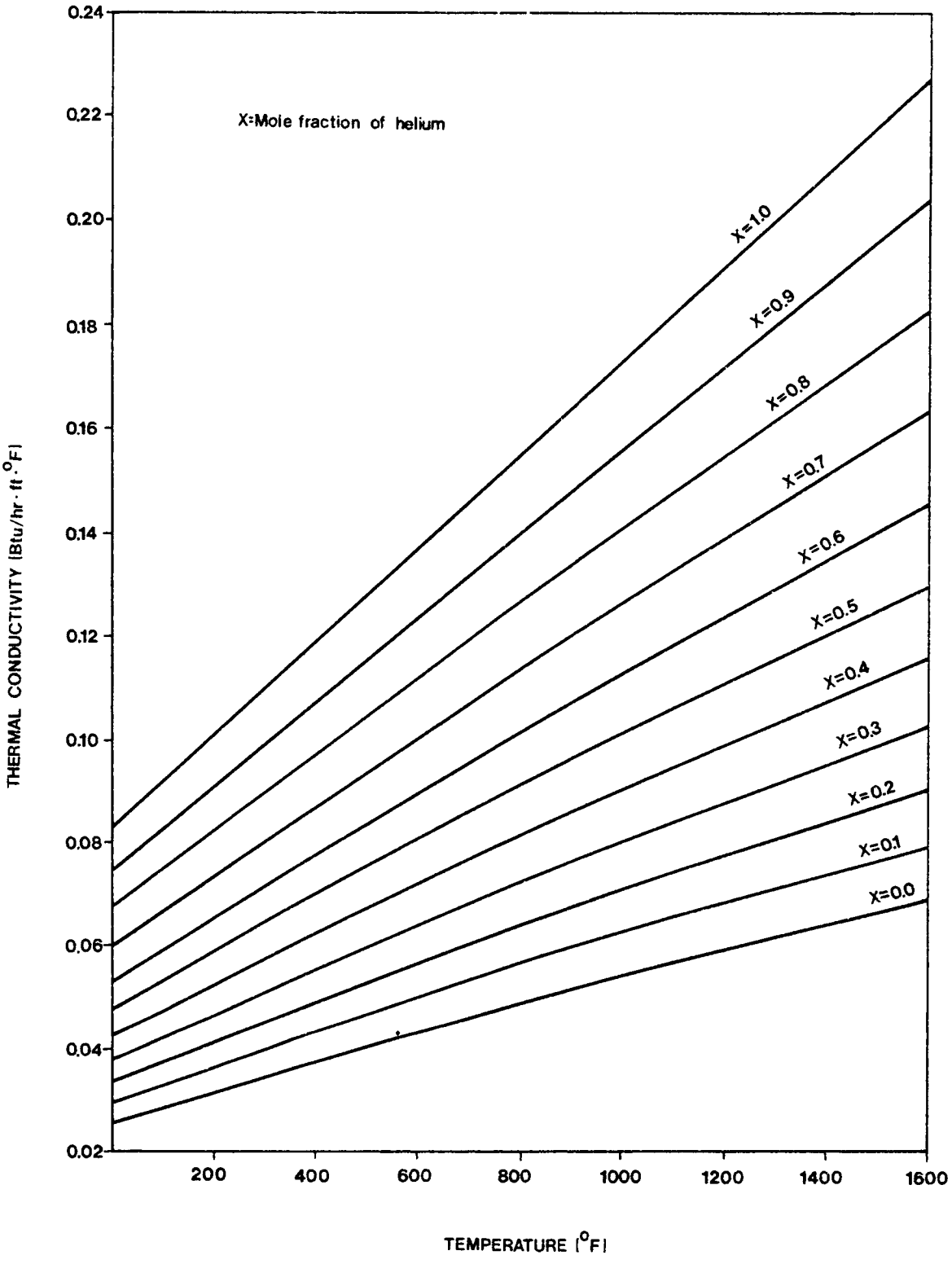



Figure 2-4. Helium-Neon Gas Mixtures Thermal Conductivity.
B. H. Montgomery 9/17/73.

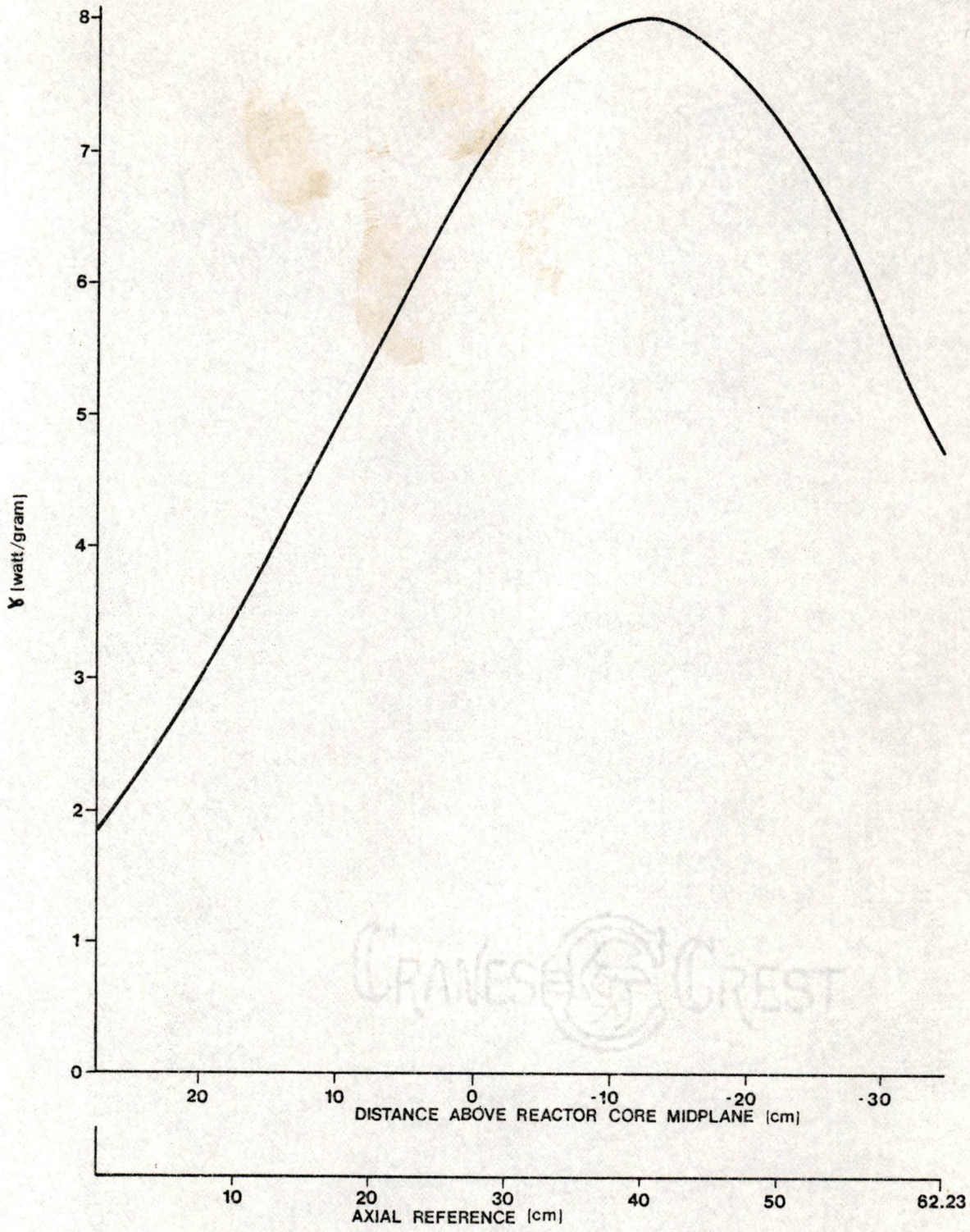



Figure 2-5. Gamma Heating Rate. Position E-5 of the ORR Reactor.

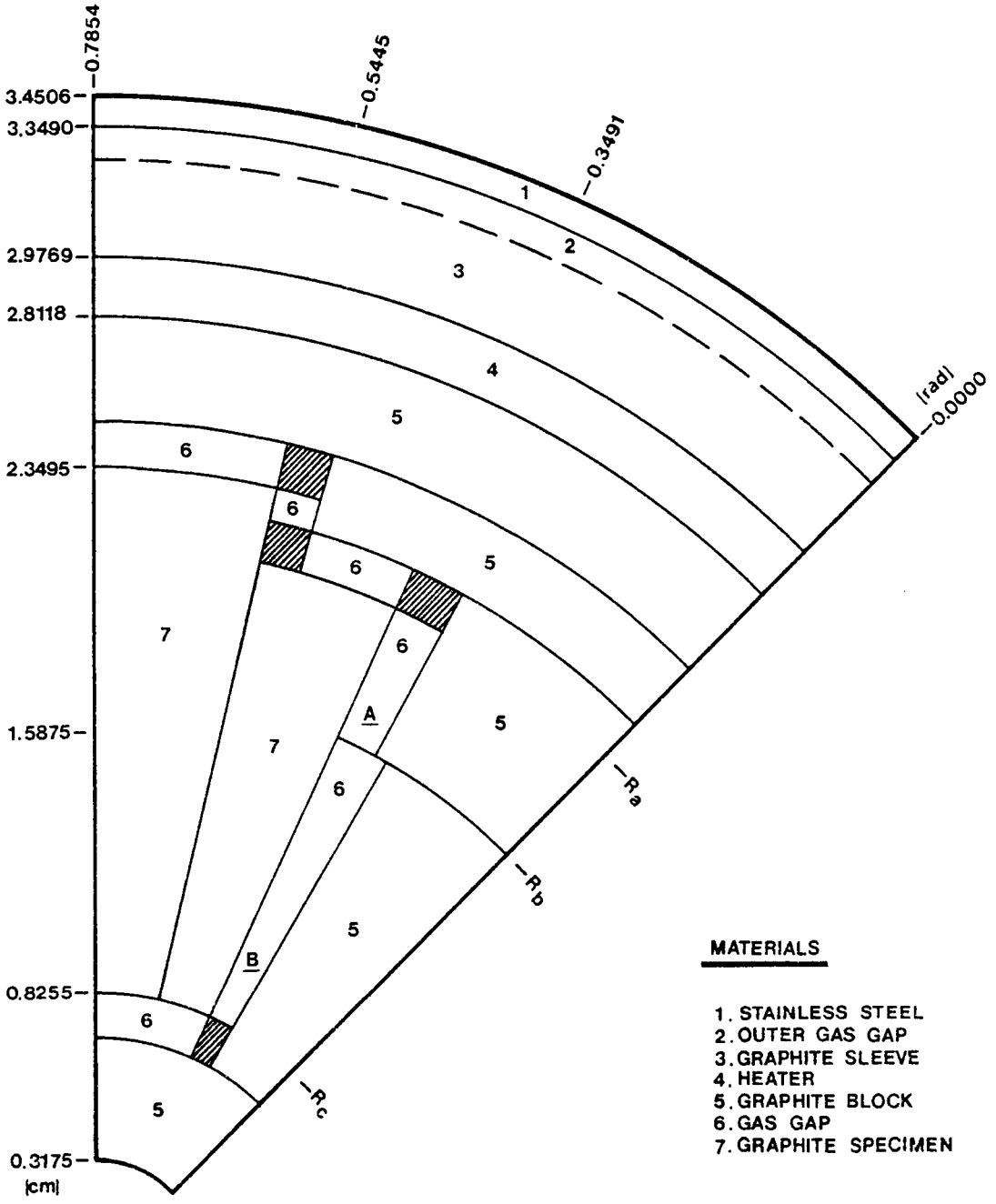



Figure 2-6. OC-5 Capsule Computational Model Cross Section.

equations involved were indeteriminate, an approximation was obtained by trying several simple configurations. A closer approximation could have been obtained, but that would have required additional specimen and gap regions where each region greatly increases the number of nodes and hence, the cost of analysis.

The undefined regions in Figures 2-6, 2-7, and 2-8, designated by hash marks, were placed in the computational models to more closely approximate the cross-sectional areas of the materials involved. The heating codes ignore these regions and place the appropriate temperature on the next surface along the direction of heat transfer.

In addition to the need for identical cross-sectional areas and perimeters because of their influence on heat production and transference, it was necessary to describe the radially extended gas gap adjacent to the specimen such that its dimensions were most accurate in the region of maximum heat transfer. The method by which this was accomplished is discussed in section 2.7.

## 2.4 Redesign of the OC-5 Capsule

After temperature distributions had been obtained for various gas mixtures and gas gaps, it was concluded that the specimen temperature of 1250$^{o}$C could not be reached without violating the second and third restrictions, section 2.1, due to the effect of thermal radiation across the gas gap adjacent to the specimens. It was, therefore necessary to redesign the region immediately around the specimens incorporating a thermal radiation reflector, i.e. a material with a

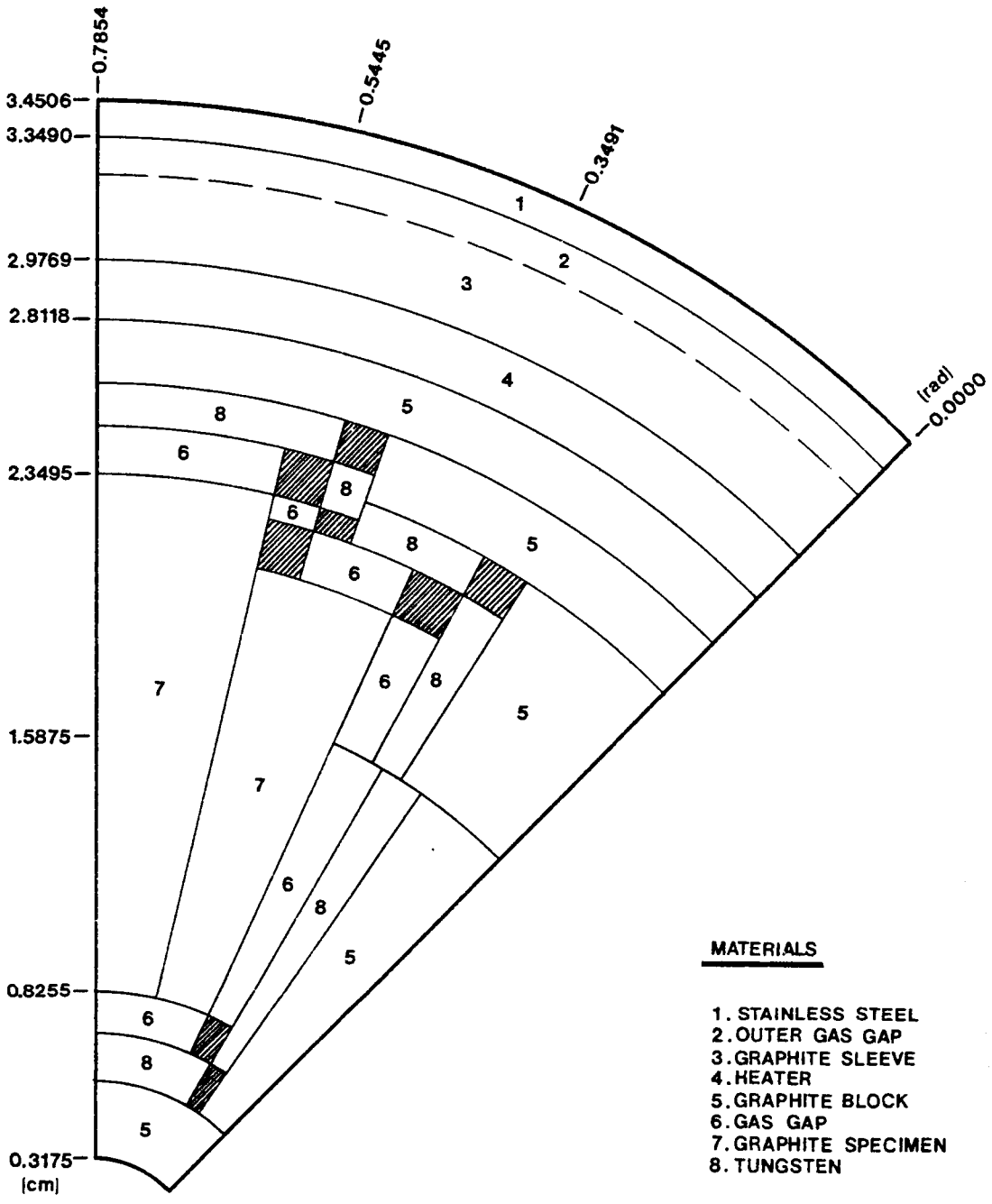



Figure 2-7. OC-5 Capsule Computational Model Cross Section with Thermal Radiation Reflector.

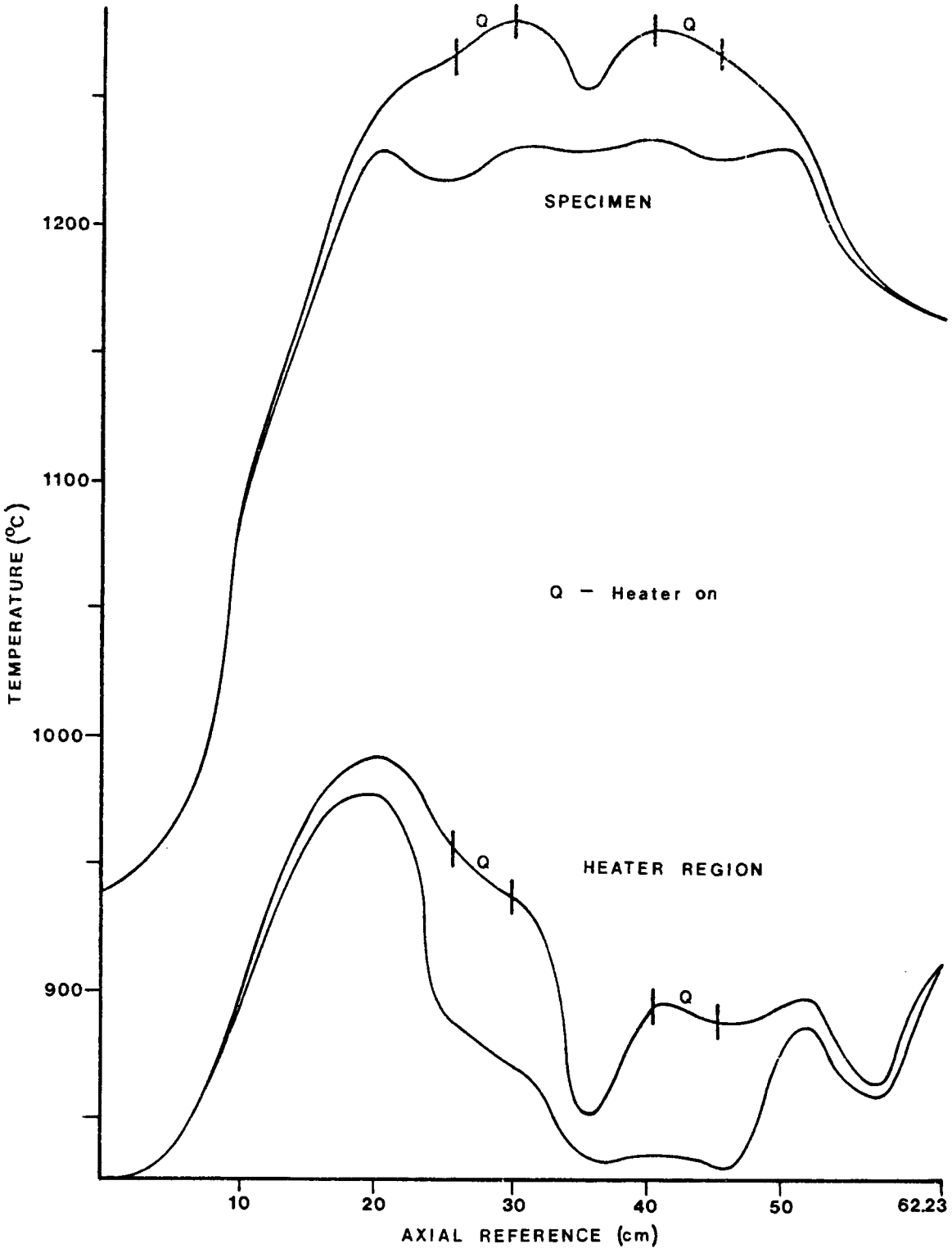



Figure 2-8. Comparison for Heater Effectiveness. Heater power of approximately 3.94 watt/cm.

low radiant emissivity. The material decided upon was polished tungsten with an estimated radiant emissivity of 0.15.

Although information about polished tungsten is somewhat scarce, previous experience indicates that under ideal conditions and at somewhat lower temperatures, tungsten will maintain its properties and polish in the presence of graphite.[5] Because the value of radiant emissivity was obtained by using that of a tungsten filament as a reference, there is some question as to its accuracy. In order to obtain greater confidence in the estimate of radiant emissivity and the characteristics of polished tungsten under the OC-5 capsule conditions, a bench test was proposed and designed (Chapter III).

Because of the large gamma absorption of tungsten, it will partially shield the specimens. This shielding effect, which is expected to be small[6], will not be investigated in the bench test; however, an indication of its magnitude could be obtained using the code XSDRNPM of the AMPX module[7], should more accurate gamma heating rates be desired for the fine lattice thermal analysis.

The addition of the tungsten cylinder between the specimens and the graphite block substantially increased the number of nodes and necessitated a change from the HEATING 3 code to the HEATING 5 code. An example of the computational model of the capsule for the HEATING 5 code is shown in Figure 2-7 for a particular axial position. The axial dimensional variation, not shown, occurs in the outer gas gap. A 0.0038 cm (0.0015 in.) gap has been placed between the tungsten tube and the graphite block, not visible, in order to approximate the gap which will occur because of the differences in the thermal expansion of graphite and tungsten at the steady-state temperatures obtained.

The approximate design arrived at consisted of the basic design used in the 600°C and 900°C capsules with the following changes:

1. A 0.13716 cm (0.054 in.) thick gas gap surrounding the specimens,
2. a 0.13716 cm (0.054 in.) thick tungsten tube around the specimens, with the inner surface polished and the outer surface in contact with the graphite block,
3. the outer gas gap varying from 0.0178 to 0.1143 cm (0.007 to 0.045 in.) width in steps of 5.08 to 10.16 cm (2 to 4 in.), and
4. a gas mixture composed of neon plus 0.4 mole fraction helium.

In order to obtain the effectiveness of the heaters, two heaters were modeled with a power of approximately 3.937 watts per cm (10 watts/in.) of heater wire. These were located between the axial positions of 25.4 to 30.48 cm (10 to 12 in.) and 40.64 to 45.72 cm (16 to 18 in.). This was accomplished by specifying the volumetric heating rate which would be produced in those regions should the heaters be contained within them (see section 2.7). The axial variation of (1) the specimen central temperature, and (2) the maximum temperature of the heater region, before and after the heaters were turned on, is shown in Figure 2-8.

At this point, it was decided that the heaters would not be effective enough to justify their presence, because of the high cost and complexity the heaters added to the capsule, and therefore, the capsule should be redesigned without them. However, an alternative method should be found, if possible, to compensate for the shifting gamma heating due to the lifting of the control rods during the reactor power cycle of approximately fourteen days.

## 2.5 Axial Shift of the Gamma Heating Distribution

The new gross lattice computational model of the capsule is shown in Figure 2-9 for a particular axial position. The axial dimensional variation occurs in the outer gas gap, Figure 2-10.

The final approximate design arrived at by gross lattice thermal analysis consisted of the basic design with the following exceptions:

1. No heaters,
2. a 0.13716 cm (0.054 in.) thick gas gap surrounding the specimens,
3. a 0.13716 cm (0.054 in.) thick tungsten tube around the specimens, with the inner surface polished and the outer surface a close fit with the graphite block,
4. the outer gas gap varying as in Figure 2-10, and
5. the sweep gas mixture composed of neon plus 0.3 mole fraction helium.

Now that the gross lattice design of the capsule had been obtained using the gamma heating rate obtained at the beginning of the reactor power cycle, the effect of core aging during the power cycle was sought. It was found that, by shifting the position of the capsule axially as the gamma heating distribution shifted, a fairly flat temperature distribution could be maintained along the specimens. Figure 2-11 shows the gamma heating distribution at the beginning and end of the reactor power cycle where the end of cycle distribution is a best guess approximation.[8] Figure 2-12 shows the specimen central

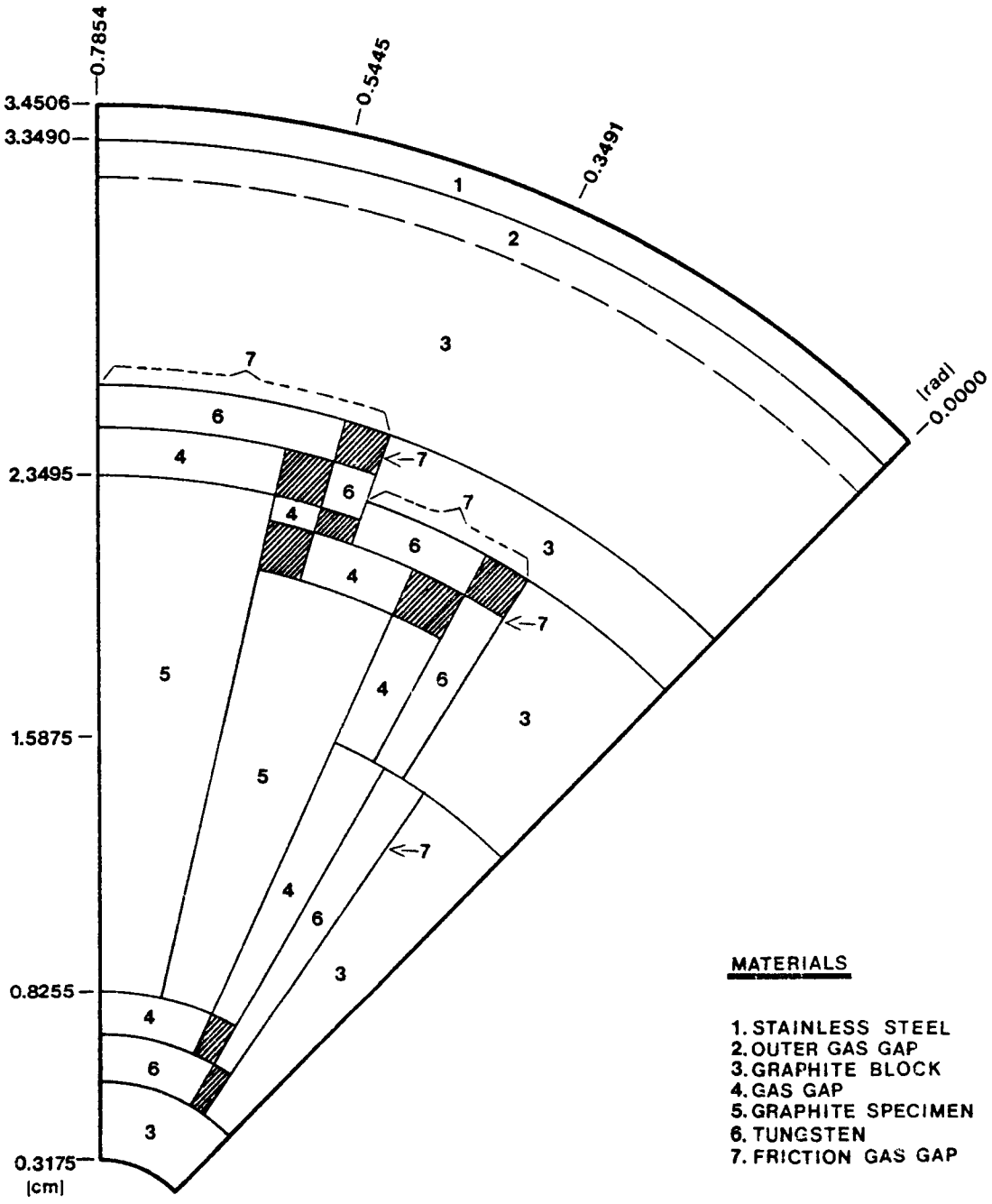



Figure 2-9. OC-5 Capsule Computational Model Cross Section after Removal of Heaters.

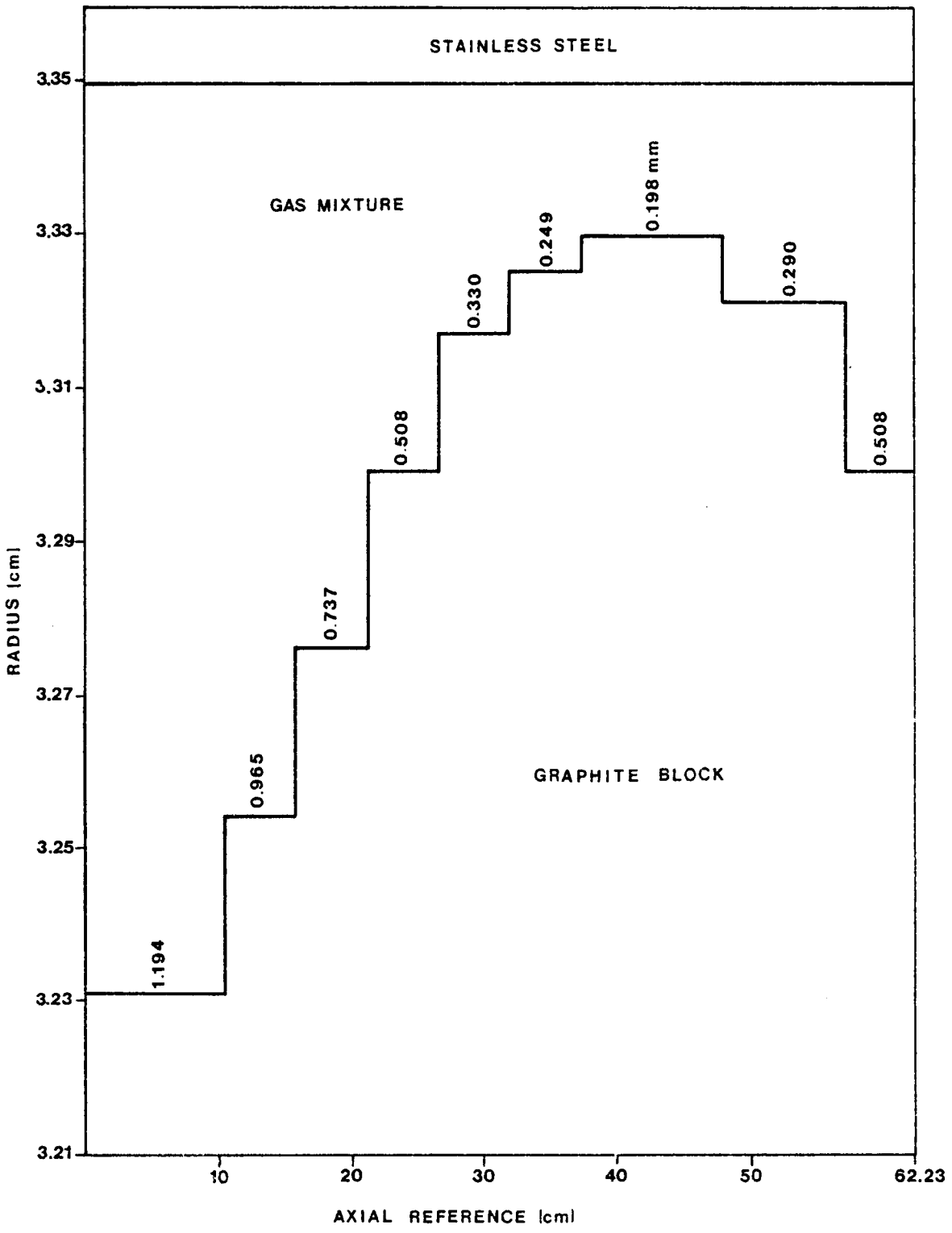



Figure 2-10. Axial Dimensional Variation of Outer Gas Gap-Coarse Resolution.

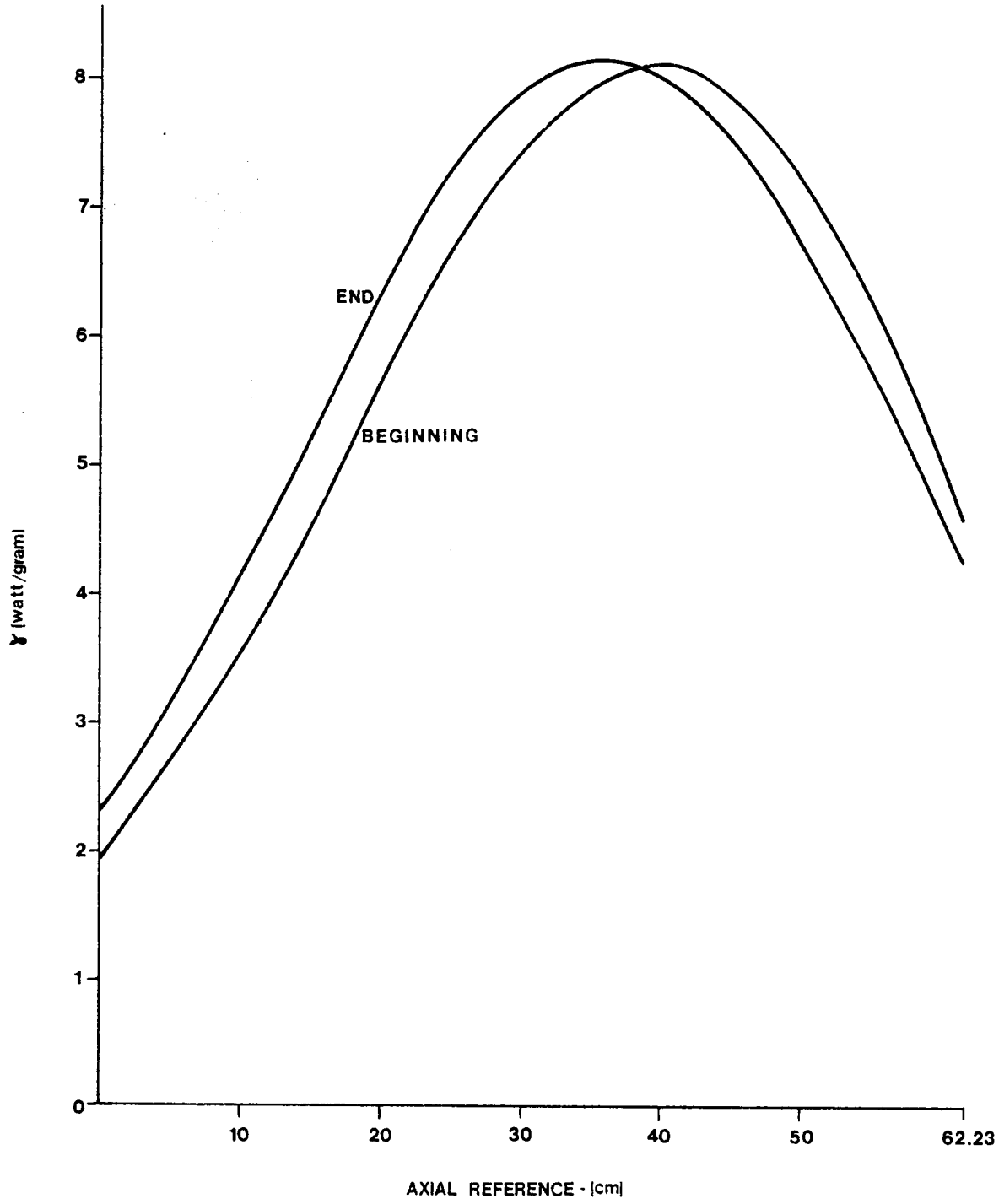



Figure 2-11. Gamma Heating Rate at Beginning and End of 14 Day Reactor Power Cycle.

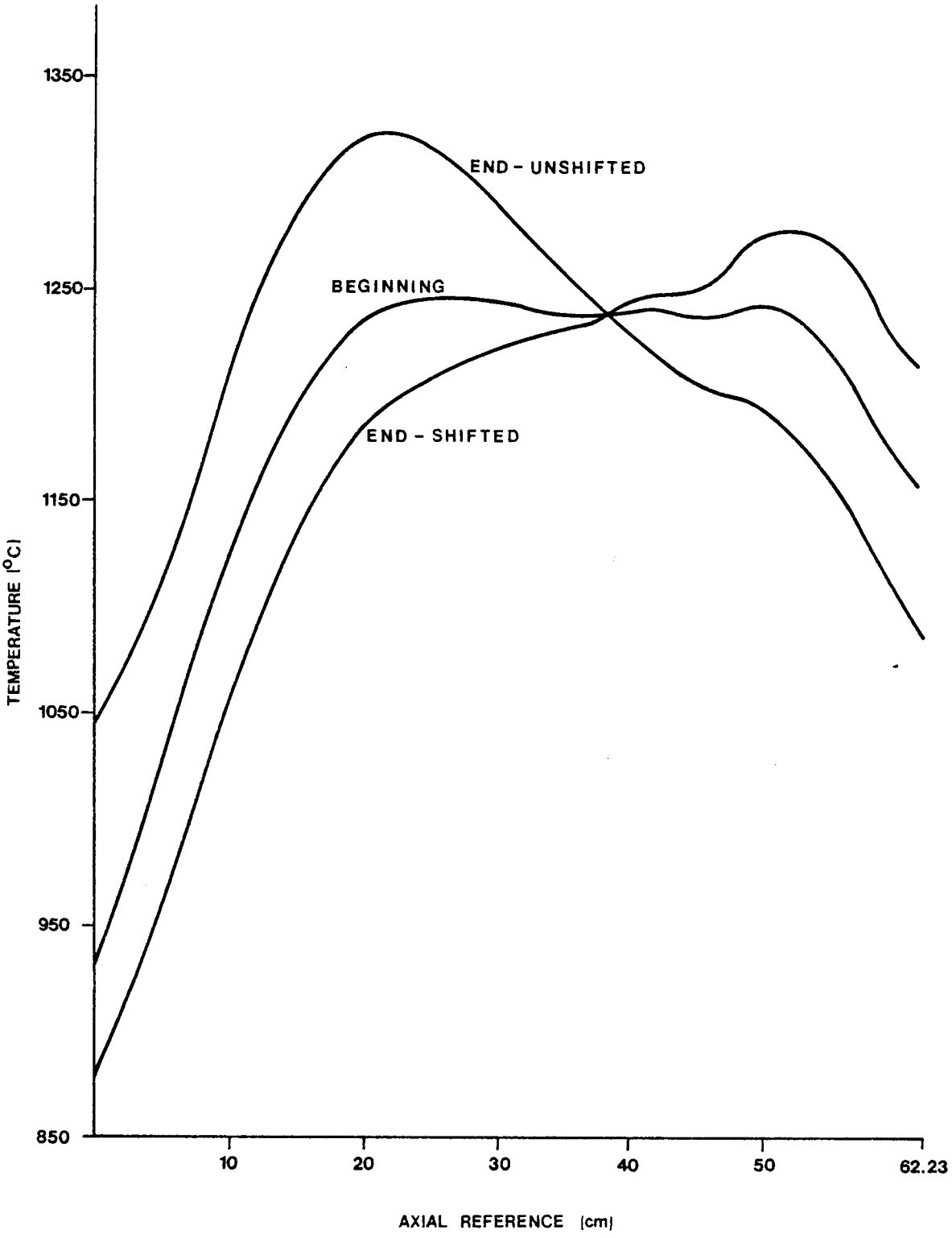



Figure 2-12. Specimen Central Temperature Distribution at the Beginning of the Reactor Power Cycle and the End with the Capsule Unshifted and Shifted 5 cm.

temperature distributions for the two gamma heating distributions just mentioned and a third for the end of cycle gamma heating with the capsule shifted 5.08 cm (2 in.).

As shown in Figure 2-12, shifting the capsule axially as the control rods are raised gives reasonable control in maintaining the specimen temperature distribution close to the initial values. This provides an acceptable alternative to the use of the heaters. In order to accommodate this axial shift, the capsule must be shortened by 5.08 cm (2 in.) because of the limited space within the core of the ORR Reactor.

Up to this point in the design study, the axial description of the capsule used in the computer codes had ranged from 0 to 62.23 cm (0 to 24.5 in.). The shortening of the capsule required a shortening of this model which was accomplished by dropping the top 5.08 cm. The model used for the remainder of the analysis had an axial range of 5.08 to 62.23 cm (2 to 24.5 in.). This change only affected the temperature distributions of the upper end of the capsule substantially, 5.08 to 15.24 cm (2 to 6 in.), and therefore, had little effect on the previous information gained, since the specimens of interest start at 20.32 cm (8 in.).

## 2.6 Refinement of Axial Resolution

In an attempt to better describe the specimen temperature distribution, it was found that increasing the axial resolution changed the calculated temperature distributions. This change consisted of slightly higher temperatures and some temperature peaking

in the upper and lower specimen regions. Figure 2-13 demonstrates the effect on the specimen temperature distribution of approximately doubling the axial resolution.

Doubling the axial resolution exceeded the nodal capacity of HEATING 5. Therefore, the model of the capsule was split into two separate parts along the axial lattice position of 40.64 cm (16 in.) and hence, two separate computer runs were needed to describe the temperature distrbution. This particular lattice position was chosen because of the approximately adiabatic conditions along it. The discontinuity in temperature calculated at this point was approximately $2^{o}C$ and was due to the slightly nonadiabatic nature of this position. This discontinuity was removed from the temperature distribution, Figure 2-13, and replaced by the mean value.

The lower temperatures and smoother temperature distribution obtained from the coarser resolution were caused by the method in which the heating codes evaluate the heating rate. The heating codes determine the heating rate for each nodal position by averaging the heating rates of the midnodal positions on each side of the node in question. This method is fairly accurate when the gamma heating rate has a low curvature; however, there may be a substantial error in the calculated heating rate at any node where the curvature is high, as shown in Figure 2-14.

Increasing the axial resolution not only enhanced the accuracy of the temperature distributions obtained, but also provided an excellent opportunity to demonstrate the effect of decreasing outer gas gap step lengths. Decreasing the step lengths allowed for smaller

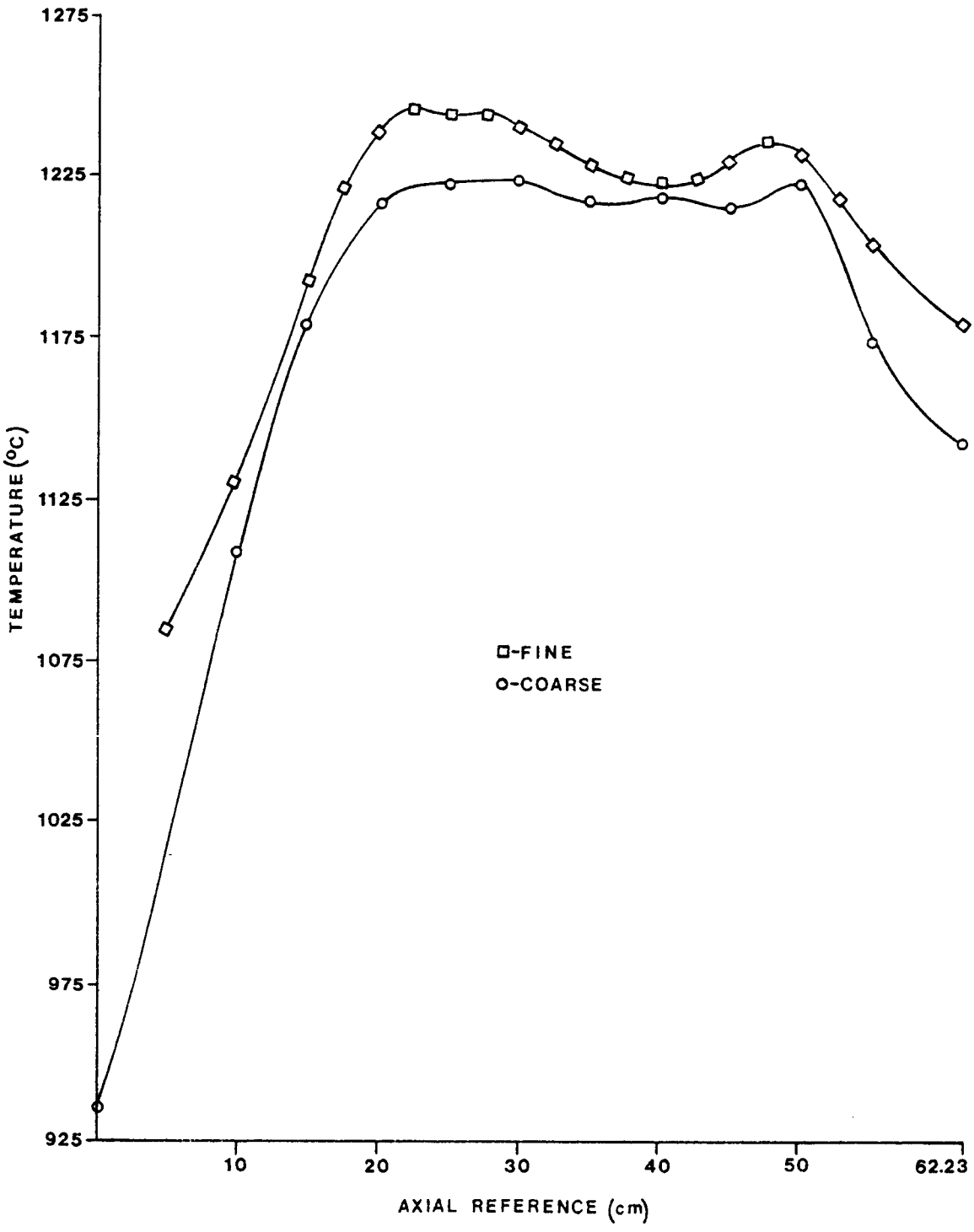



Figure 2-13. Comparison of Axial Resolution of the Specimen Central Temperature Distribution.

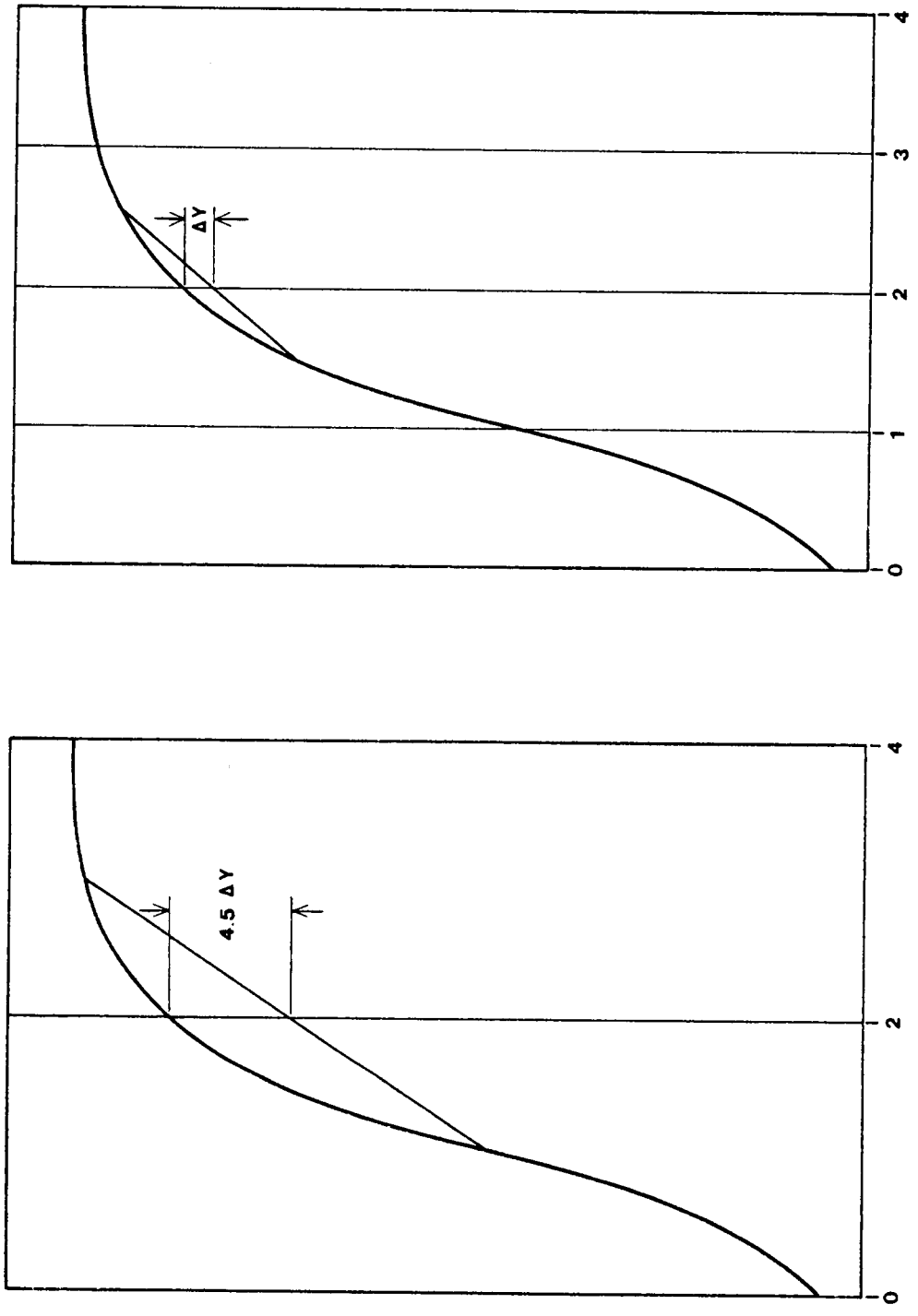



Figure 2-14. Example of Resolution vs. Curve Approximation in HEATING 5 Code.

changes in the gas gap and hence, as can be seen in Figure 2-15, a smoother temperature distribution. The specimen central temperature distributions in Figure 2-15 were produced using the outer gas gap configurations of Figures 2-10 and 2-16 where Figure 2-16 correpsonds with the smoother temperature distribution.

## 2.7 Parameter Evaluation

The remainder of this chapter deals with the methods by which some of the computer input parameters were obtained and, in some cases, an indication of the temperature sensitivity to these parameters.

Gas Mixture Conductivity. As can be seen by Figures 2-2, 2-3 and 2-4 (p. 14, 15, 16), the various gas conductivities are only plotted up to the temperature of 871°C (1600°F); however, the specimens reach a temperature of 1250°C. Therefore, the curves in these figures were linearly extrapolated to the temperature of 1315°C (2400°F).

Dimensioning the Radially Extended Gas Gap. In order to obtain a model of the capsule suitable for use in the heating codes, it was necessary to have a radially extended gas gap adjacent to the specimens. This type of gap produces a computationaly higher rate of thermal radiation at the outer end and a lower rate at the inner end than would be experienced in the actual capsule.

Therefore, the gap needed to be modeled such that its thickness would be more accurate in the outer section of the gap, where most of the heat transfer takes place. This was accomplished by splitting the gap into two sections, (see Figure 2.6, p. 18), and calculating the angles as follows:

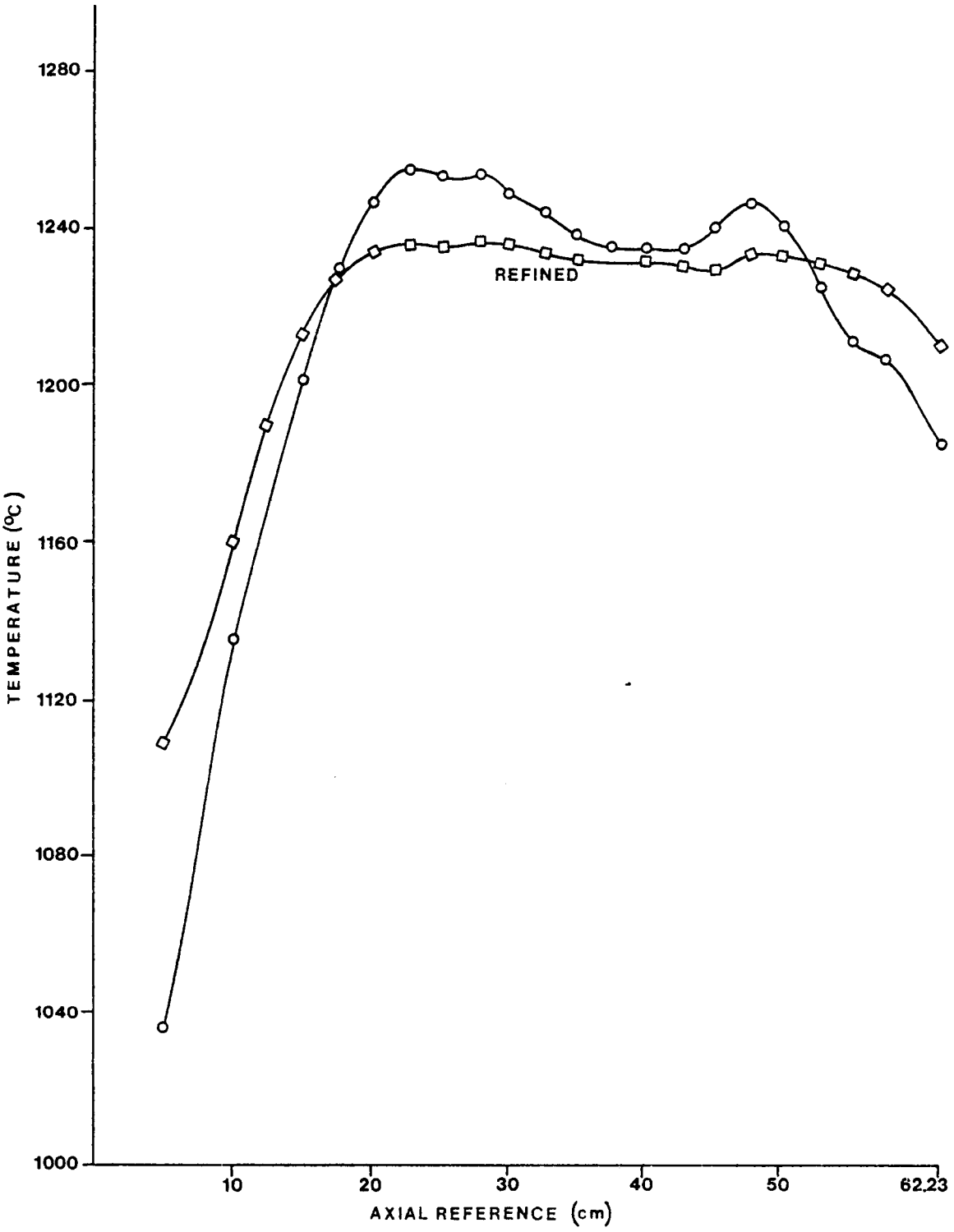



Figure 2-15. Specimen Central Temperature Distribution Before and After Refinement of the Outer Gas Gap-Fine Resolution.

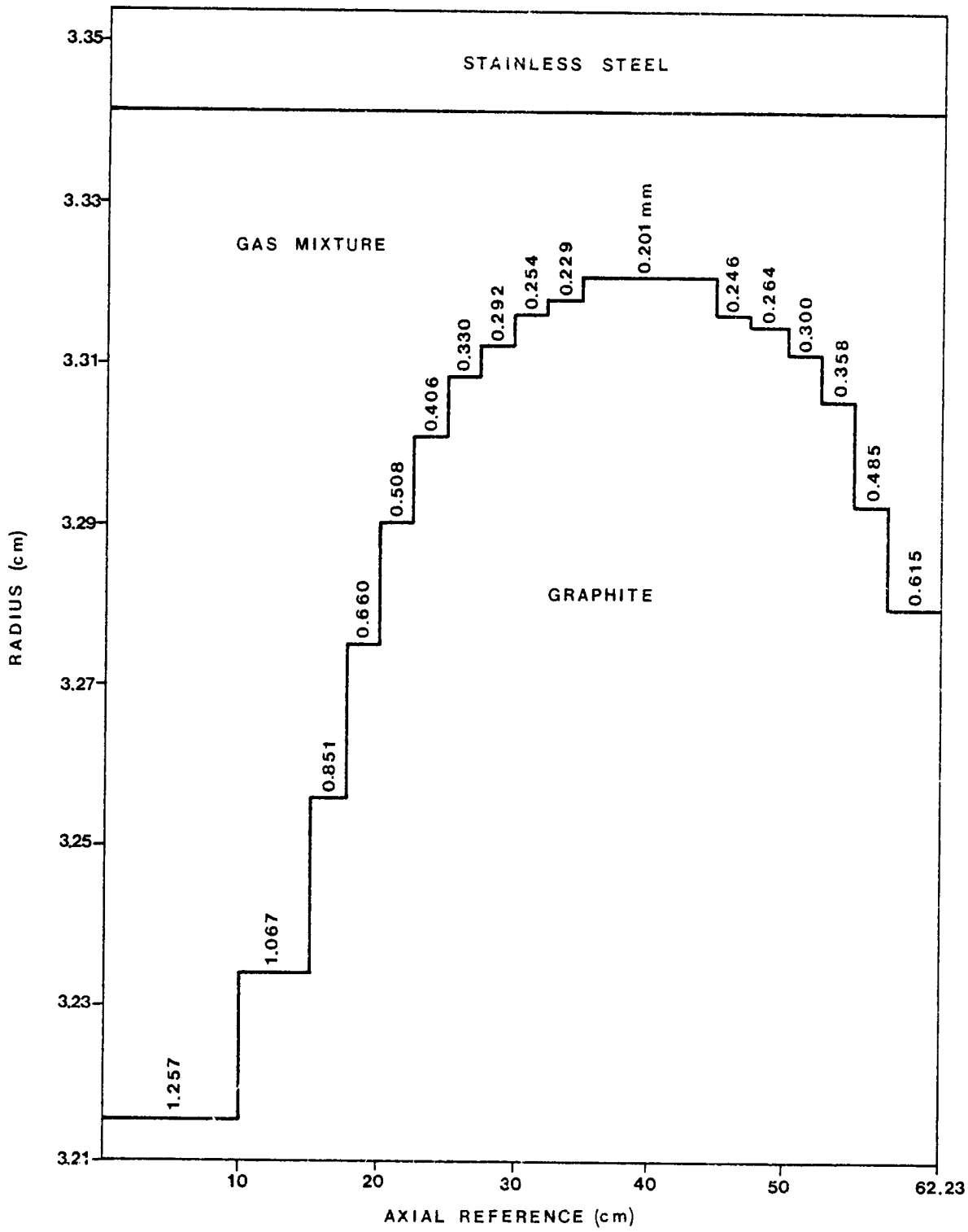



Figure 2-16. Axial Dimensional Variation of Outer Gas Gap-Fine Resolution.

Gap A:

$$\Theta_{small} = \Theta_{large} - \frac{\text{Gap Width}}{.7(R_a - R_b) + R_b}$$

$$\Theta_{small} = \Theta_{large} - \frac{\text{Gap Width}}{0.7R_a + 0.3R_b}$$

which placed the appropriate gap width three tenths the length of the gap from the outer end.

Gap B: Although the same procedure would have been appropriate here, it would have created a large difference in thickness between the inner end of the outer gap and the outer end of the inner gap. Therefore, the gap was adjusted such that the appropriate gap width is located in the center of the gap.

$$\Theta_{small} = \Theta_{large} - \frac{\text{Gap Width}}{0.5(R_b - R_c) + R_c}$$

$$= \Theta_{large} - \frac{\text{Gap Width}}{0.5(R_b + R_c)}$$

Gas Gaps. Three rules of thumb were used when dealing with gas gaps where sensitivity refers to the change in the temperature difference per unit gap width change:

1. Increasing the gap width, decreases the sensitivity,
2. the higher surface temperatures, the lower the sensitivity; and the higher the gamma heating, the greater the sensitivity,

3. the larger the gap width the more likely local gas circulation will exist, with 0.1524 cm (0.06 in.) considered to be a safe upper limit.

Because of the high specimen temperatures desired and the substantially lower thermocouple temperatures required, a large temperature difference was required across the inner gas gap, located between the specimen and the tungsten. The selection of this gap width, 0.13716 cm (0.054 in.), was somewhat arbitrary; however, a much larger gap would tend to increase the probability of local gas convection effects without substantially increasing the temperature difference. Decreasing the gap width would increase the sensitivity to small gap errors and therefore, increasingly decrease the temperature difference, i.e. doubling the gap width may increase the temperature difference ten to twenty percent while halving the gas width may decrease the temperature 30 to 40 percent.

The maximum sensitivity and temperature difference of the gas gaps are at the position of maximum gamma heating, 40.64 cm (16 in.), with both decreasing as the gamma heating rate decreases. While the axial variation in the temperature difference of the inner gap is not as large as that of the outer gap, it had to be accounted for. However, because of the cost and complexity of stepping the inner gas gap, the temperature control was accomplished by using larger variations in the outer gap than would have otherwise been required. This method of temperature control has the disadvantage of higher thermocouple temperature towards the ends of the capsule because the outer gas gap must have higher temperature

differences at the ends of the specimen columns to account for the lower temperature differences across the inner gas gap in those areas.

The axial variation in sensitivity and temperature difference of the outer gas gap is quite large due to a number of factors.

As previously mentioned, the smaller the temperature difference across the inner gas gap, the larger the temperature difference needed across the outer gas gap and hence, the larger the gap.

The lower the gamma heating rate, the greater the thermal resistance needed to maintain the specimen temperatures and hence, the larger the gap.

The larger the gap, the less sensitive it is to change and, therefore, the gap must be increased by a larger amount to account for the larger temperature differences needed. Two examples of the sensitivity are:

1. At the axial position of 5.08 cm (2 in.), a 0.00254 cm (0.001 in.) change in the outer gap width changes the temperature difference by 1 to 3 percent.
2. At the axial position of 40.64 cm (16 in.), a 0.00254 cm change in the outer gap width changes the temperature difference by as much as 9 to 13 percent.

Because of this variation in sensitivity and temperature difference along the outer gas gap, the dimensions of the gap had to be obtained, once the gas mixture had been determined, by a process of trial and error. This process consisted of using the previous computer runs to determine the sensitivity assuming a linear temperature profile between the surfaces, the approximate temperature difference needed, and hence,

the estimated gap width required. This estimated gap change was then weighted according to its axial position so as to account for the nonlinear temperature profile which actually existed between the surfaces.

Variation of Gas Mixture and Tungsten Emissivity. In order to demonstrate one of the reasons for going through with the bench test, a set of curves were produced where the radiant emissivity of tungsten was varied and the gas mixture changed to return the specimen temperature to approximately 1232°C (2250°F) at the axial position of 40.64 cm (16 in.). The other design parameters were fixed for these calculations. These curves, Figures 2-17 and 2-18, indicate the effect on the specimen and thermocouple temperature distributions, should polished tungsten have a value of radiant emissivity greater than 0.15. As can be readily seen, the higher the value of radiant emissivity, the more nonlinear is the specimen temperature distribution and the higher the temperature on the thermocouples. Equivalent curves using the approximate gamma heating produced by an old core, when the shim rods are at their maximum height, are shown in Figures 2-19 and 2-20.

Although the value of radiant emissivity for the polished surface of the tungsten is of extreme importance, its value for the unpolished outer surface was found to be of little importance when in the expected range of 0.5 to 0.9. In fact, the temperature variation in this range was so small that it could not be easily displayed graphically.

Figures 2-21, 2-22, and 2-23 demonstrate the variation in the temperature distribution when the gas mixture is varied for tungsten emissivity values of 0.3, 0.5, and 0.8 respectively.

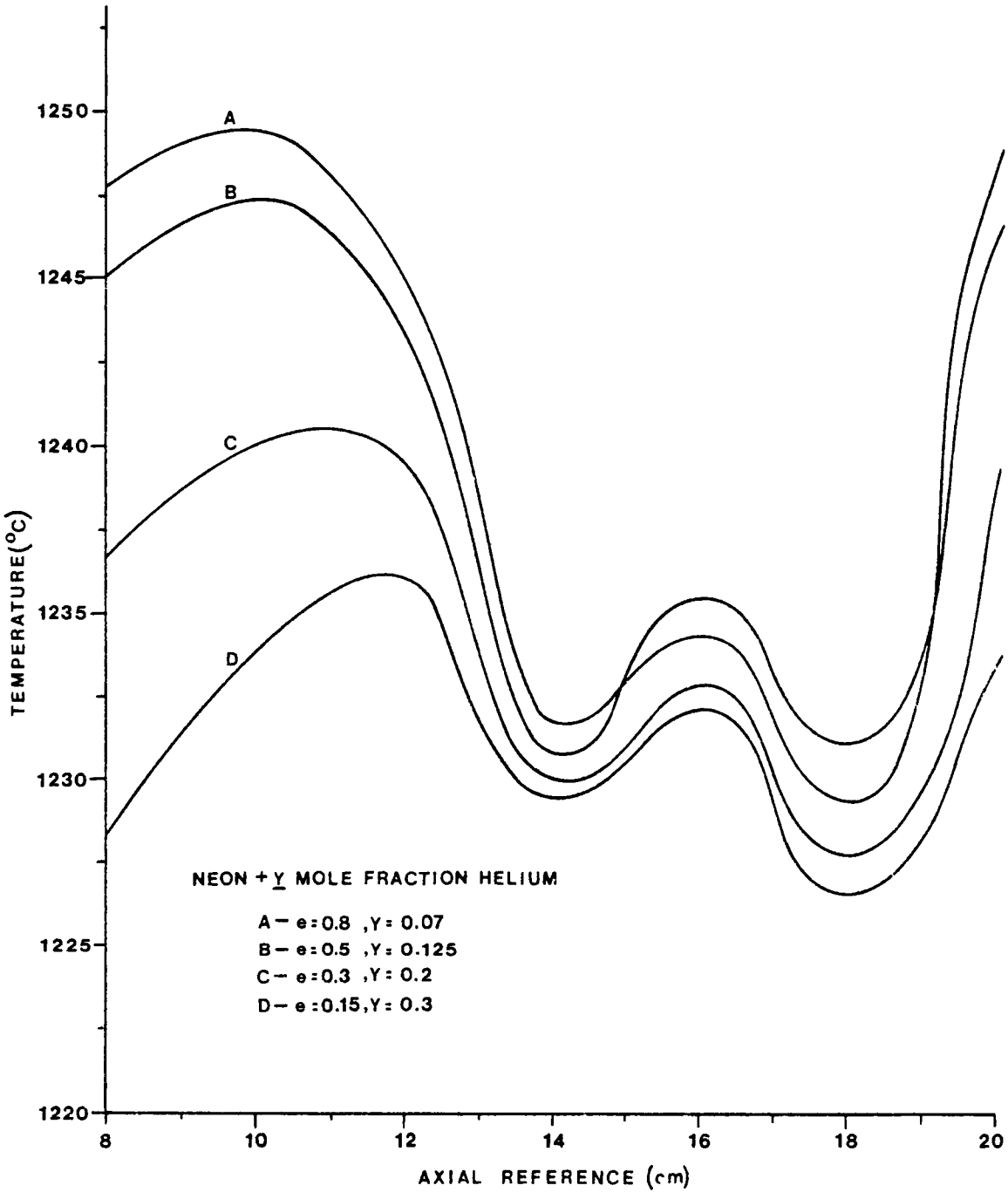



Figure 2-17. Comparison of Specimen Central Temperature Distributions for Several Polished Tungsten Emissivities and Corresponding Gas Mixtures.

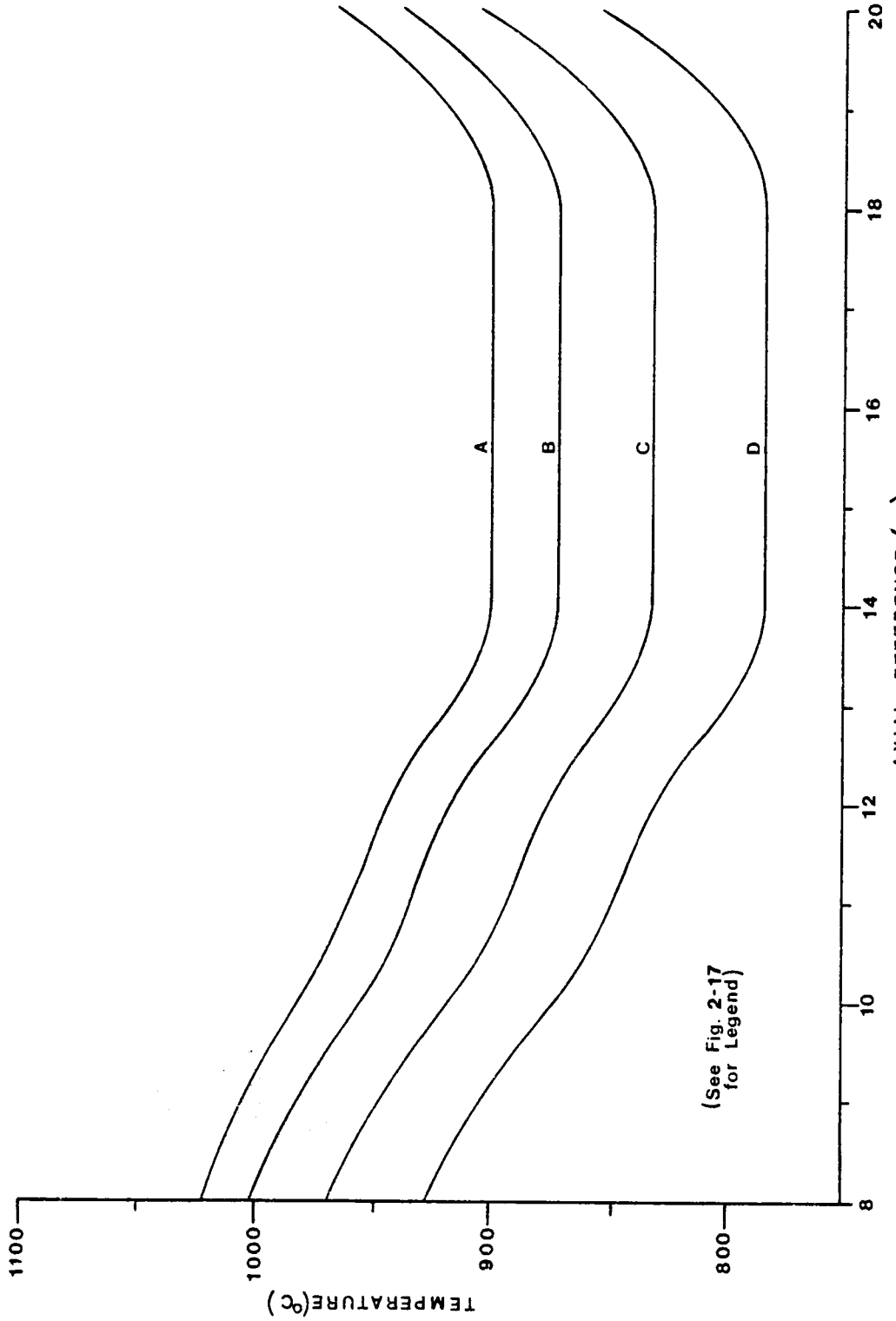



Figure 2-18. Comparison of Thermocouple Temperature Distributions for Several Polished Tungsten Emissivities and Corresponding Gas Mixtures. Distributions Obtained at a Radius of 2.896 cm Between Specimen Columns.

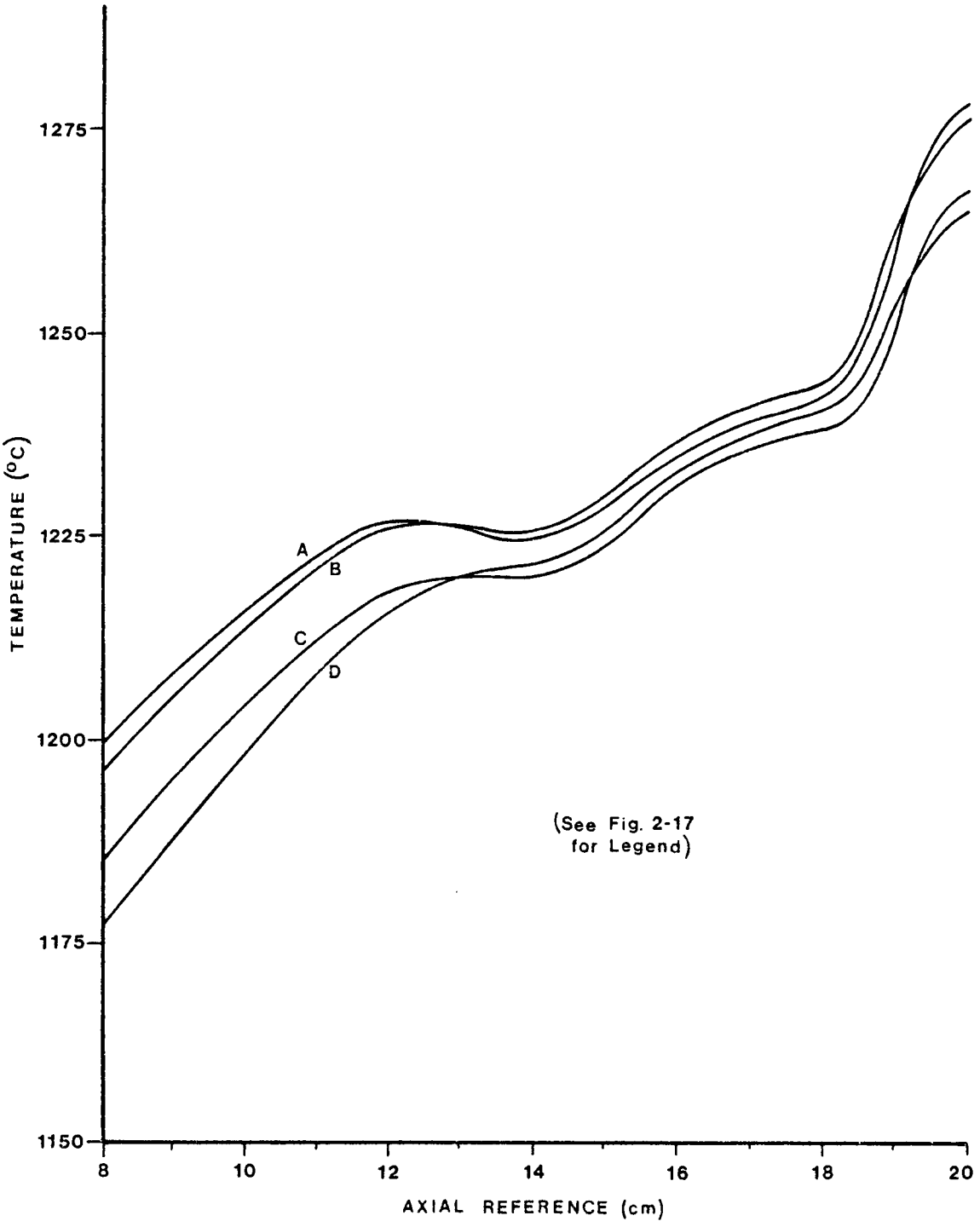



Figure 2-19. Comparison of Specimen Central Temperature Distributions for Several Polished Tungsten Emissivities and Corresponding Gas Mixtures at End of Reactor Power Cycle.

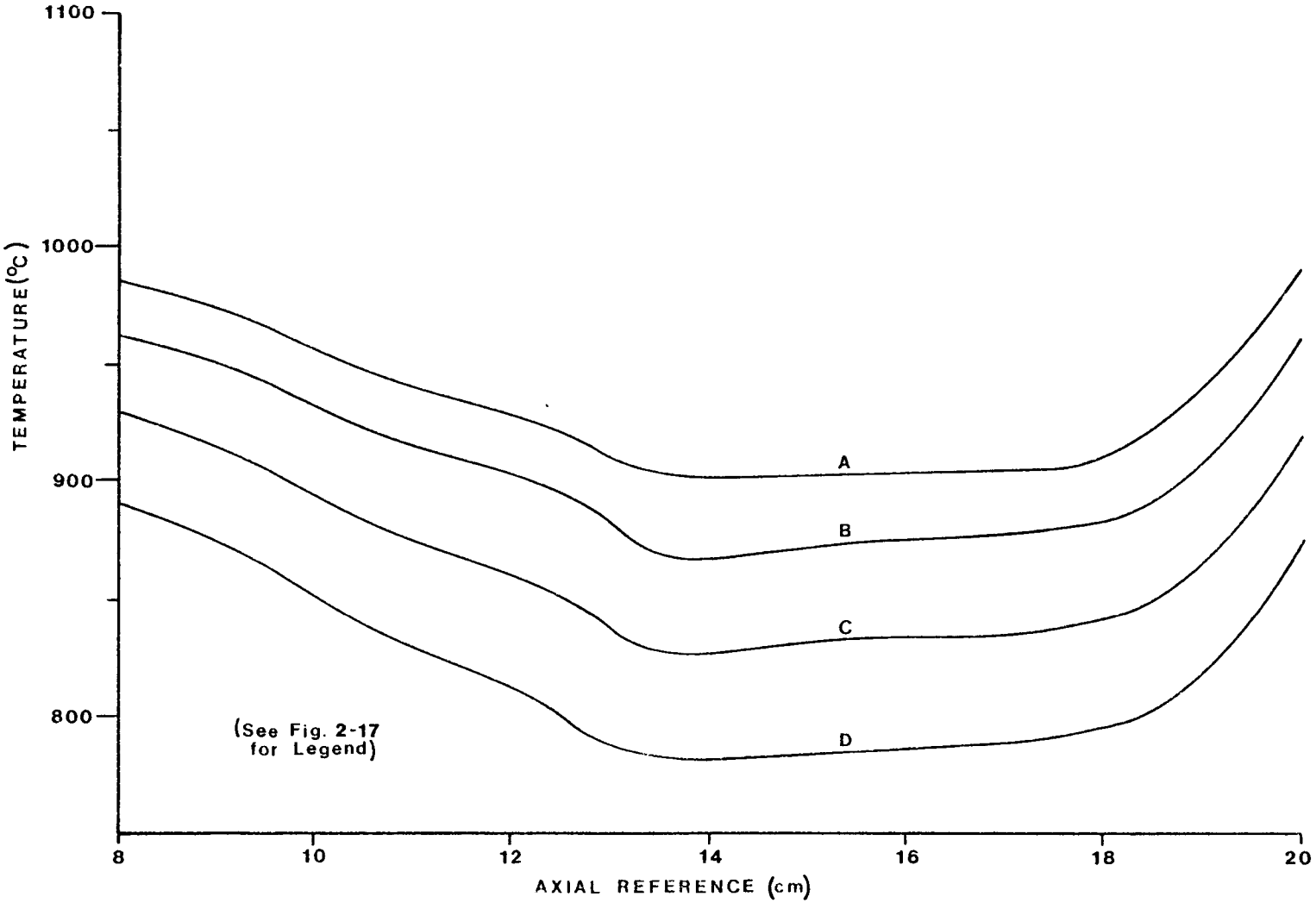



Figure 2-20. Comparison of Thermocouple Temperature Distributions for Several Polished Tungsten Emissivities and Corresponding Gas Mixtures at End of Reactor Power Cycle. Distributions Obtained at a Radius of 2.896 cm between Specimen Columns.

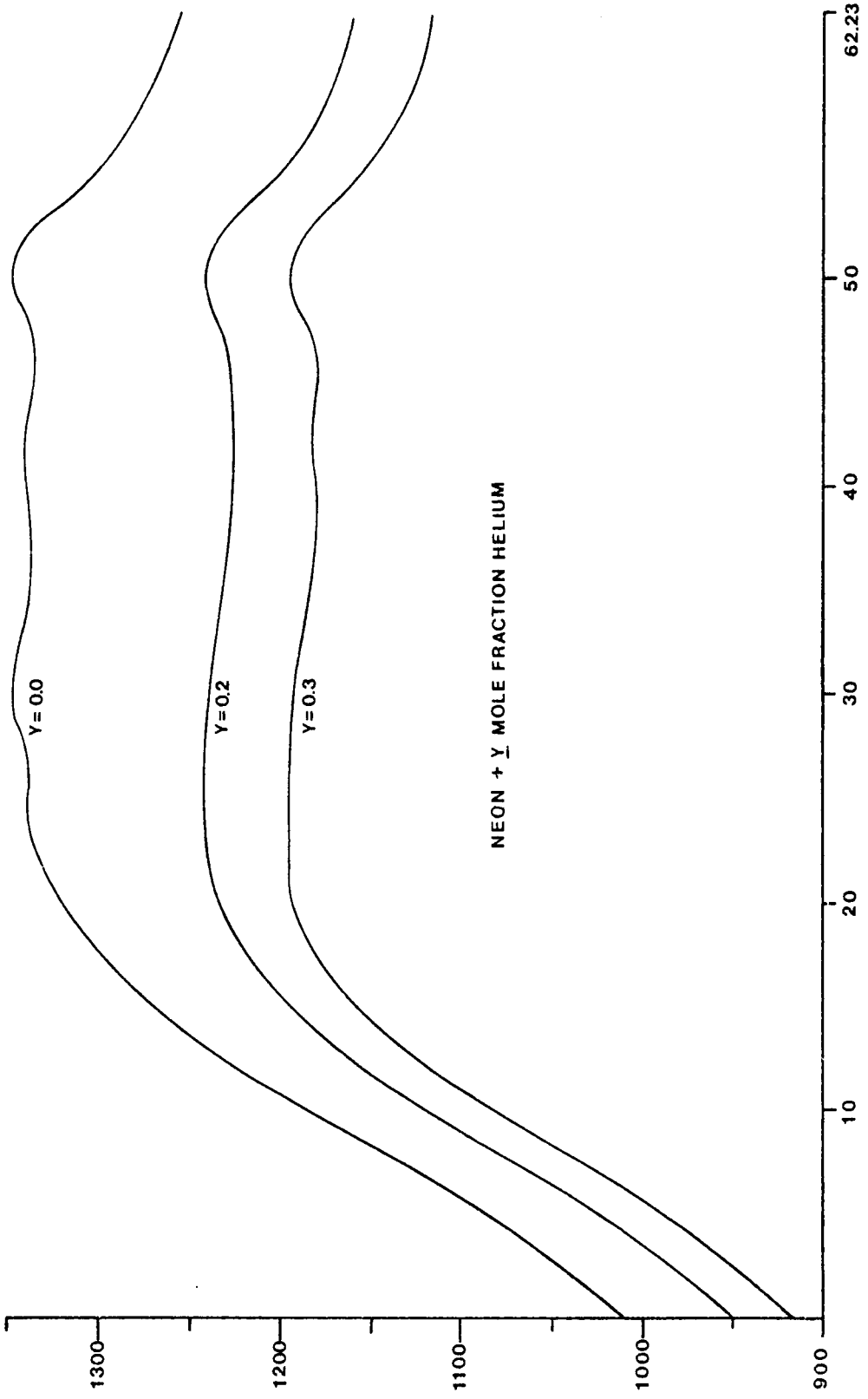



Figure 2-21. Comparison of Specimen Central Temperature Distributions for Various Gas Mixtures and Polished Tungsten Emissivity of 0.3.

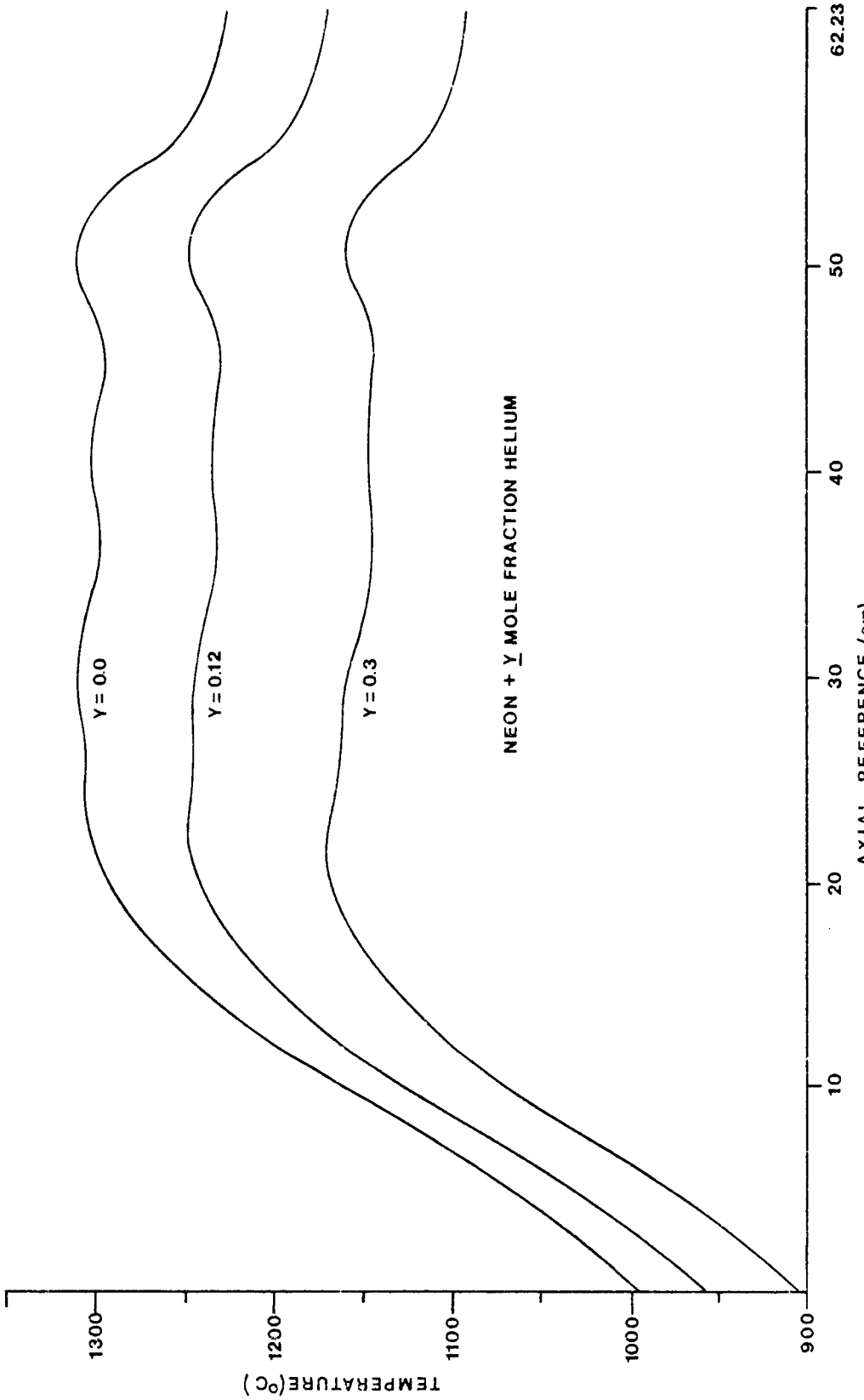



Figure 2-22. Comparison of Specimen Central Temperature Distributions for Various Gas Mixtures and Polished Tungsten Emissivity of 0.5.

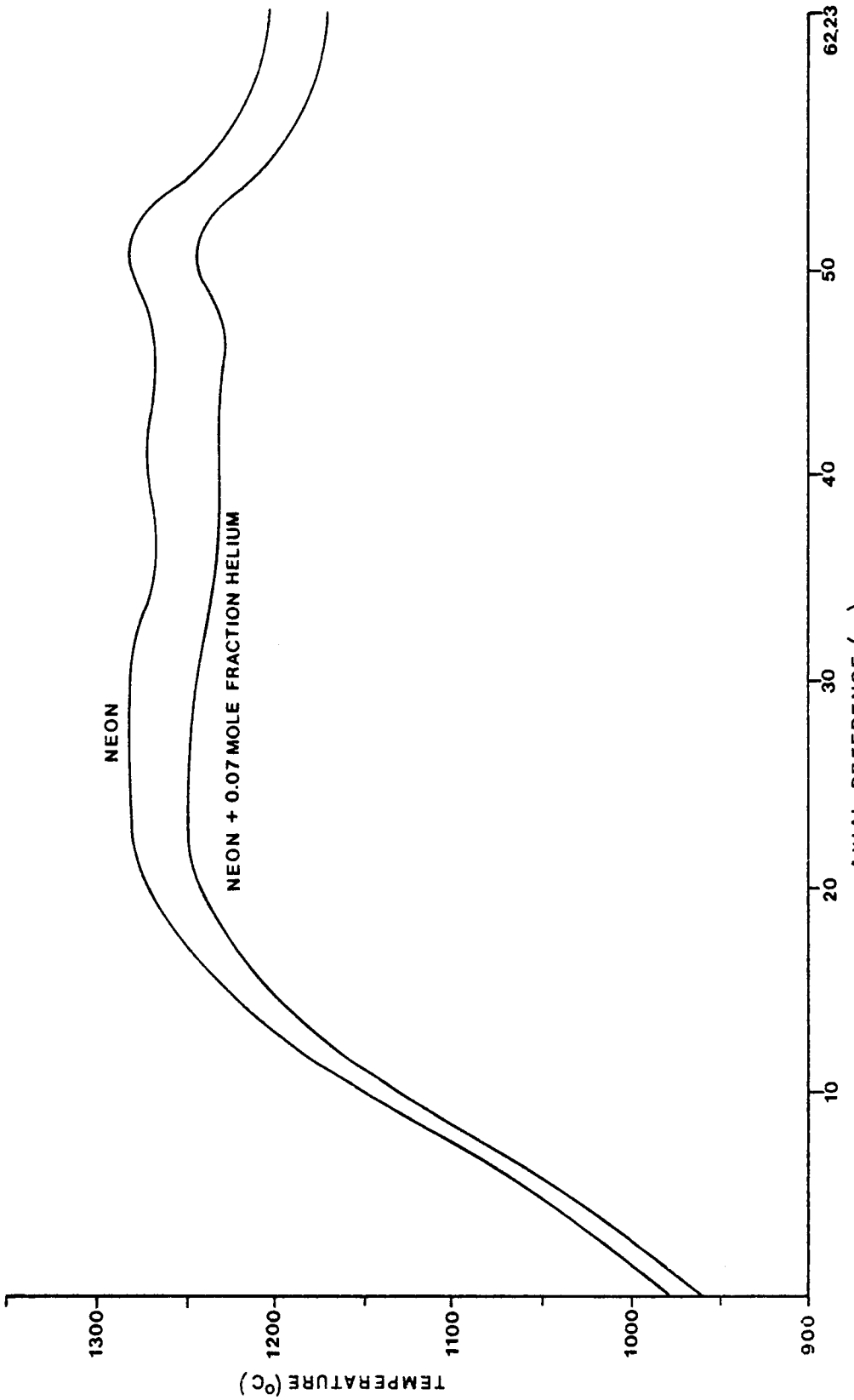



Figure 2-23. Comparison of Specimen Central Temperature Distributions for Two Gas Mixtures and Polished Tungsten Emissivity of 0.8.

Thermal Radiation Coefficient ($h_r$). As the heating codes do not provide for the direct input of the various radiant emissivities, it was necessary to calculate the thermal radiation coefficients which can be input into these codes. These calculations were made as follows, where specular reflection was neglected.

$$h_r = F_{i/o}\ (1.74 \times 10^{-9}) \quad [\text{BTU/hr - ft}^2 - {}^{o}\text{F}]$$

$$= F_{i/o}\ (2.01 \times 10^{-13}) \quad [\text{BTU/min - in}^2 - {}^{o}\text{F}]$$

where $$F_{i/o} = \frac{1}{\frac{1}{e_i} + \frac{r_i}{r_o}\left[\frac{1}{e_o} - 1\right]}$$ [unitless shape factor for concentric infinite cylinders]

i refers to the inner surface and o to the outer surface of the various gas gaps,

e is the radiant emissivity,

r is the radius of the surface and $h_r$ has been presented in consistent units for use in the heating codes.

Volumetric Heating Rate. Information on the gamma heating rate (watt/gram) for the ORR Reactor at position E-5 was initially given while the heating codes required the use of volumetric heating ($\text{BTU/in}^3$ - min). The volumetric heating rates were input by entering the gamma heating rate into the program in tabular form as an axial variable and assigning a different multiplication constant to each material, where the constant was obtained as follows:

material density [gram/$cm^3$] x 16.387 [$cm^3/in^3$] x
3.413 [BTU/watt-hr] x 0.01667 [hr/min] =
density x 0.932 [gram-BTU/$in^3$-min-watt] = Const.

This constant for each material, when multiplied by the gamma heating rate, yields the volumetric heating rate in consistent units.

Heaters. A heater consists of two wires wrapped around the graphite block four times per inch of length of capsule, where the graphite block has an outer radius of 2.812 cm (1.107 in.) and the heater region has a thickness of 0.1651 cm (0.065 in.). The equivalent volumetric heating rate for a heater power of one watt per inch of wire length (.394 watt/cm ) was determined as follows:

$$\frac{1 \text{ watt}}{\text{in. of wire}} = \frac{1 \text{ watt}}{\text{in.}} \times 2\pi(1.107 \text{ in.}) \times \frac{2 \text{ wires}}{\text{row}} \times \frac{4 \text{ rows}}{\text{in. of capsule}}$$

$$= 55.64 \text{ watt/in. of capsule}$$

$$\text{heater region volume} = \pi[(1.107 + 0.065)^2 \text{ in}^2 - (1.107)^2 \text{ in}^2]$$

$$= 0.4654 \text{ in}^3\text{/in. of capsule}$$

$$\frac{1 \text{ watt}}{\text{in. of wire}} = \frac{55.64 \text{ watt/in}}{0.4654 \text{ in}^3\text{/in}} \times 0.0569 \frac{\text{BTU}}{\text{watt-min}}$$

$$= 6.8 \frac{\text{BTU}}{\text{min-in}^3}$$

which is in consistent units.

## 2.8 Conclusion

The gross lattice thermal design of the OC-5 capsule consists of the basic design (Figures 1-2, 1-3, and 1-4, p. 4, 5, 6) with the following modifications:

1. The capsule no longer contains heaters.
2. The shifting gamma heating rate over a reactor operating cycle is accounted for by the axial shifting of the capsule which requires that the capsule be 5.08 cm (2 in.) shorter than in the basic design. This reduction in length is accomplished in the upper end of the capsule above the first specimen.
3. The specimens of most interest lie between the second and thirteenth specimens.
4. The gas gap surrounding each specimen column has a thickness of 0.13716 cm (0.054 in.).
5. A 0.13716 cm (0.054 in.) thick tungsten tube, with the inner surface polished and an inner diameter of 1.798 cm (0.708 in.), surrounds each specimen column with its outer surface a close fit with the graphite block.
6. The outer gas gap varies as in Figure 2-16 (p. 35).
7. The sweep gas is composed of neon plus 0.3 mole fraction helium.

A $45^{o}$ cross section of the capsule is shown in Figure 2-24 for a particular axial position where the thermocouples have yet to be included. Some of the temperature distributions expected with this design are shown in Figures 2-25 and 2-26. Figure 2-25 shows the

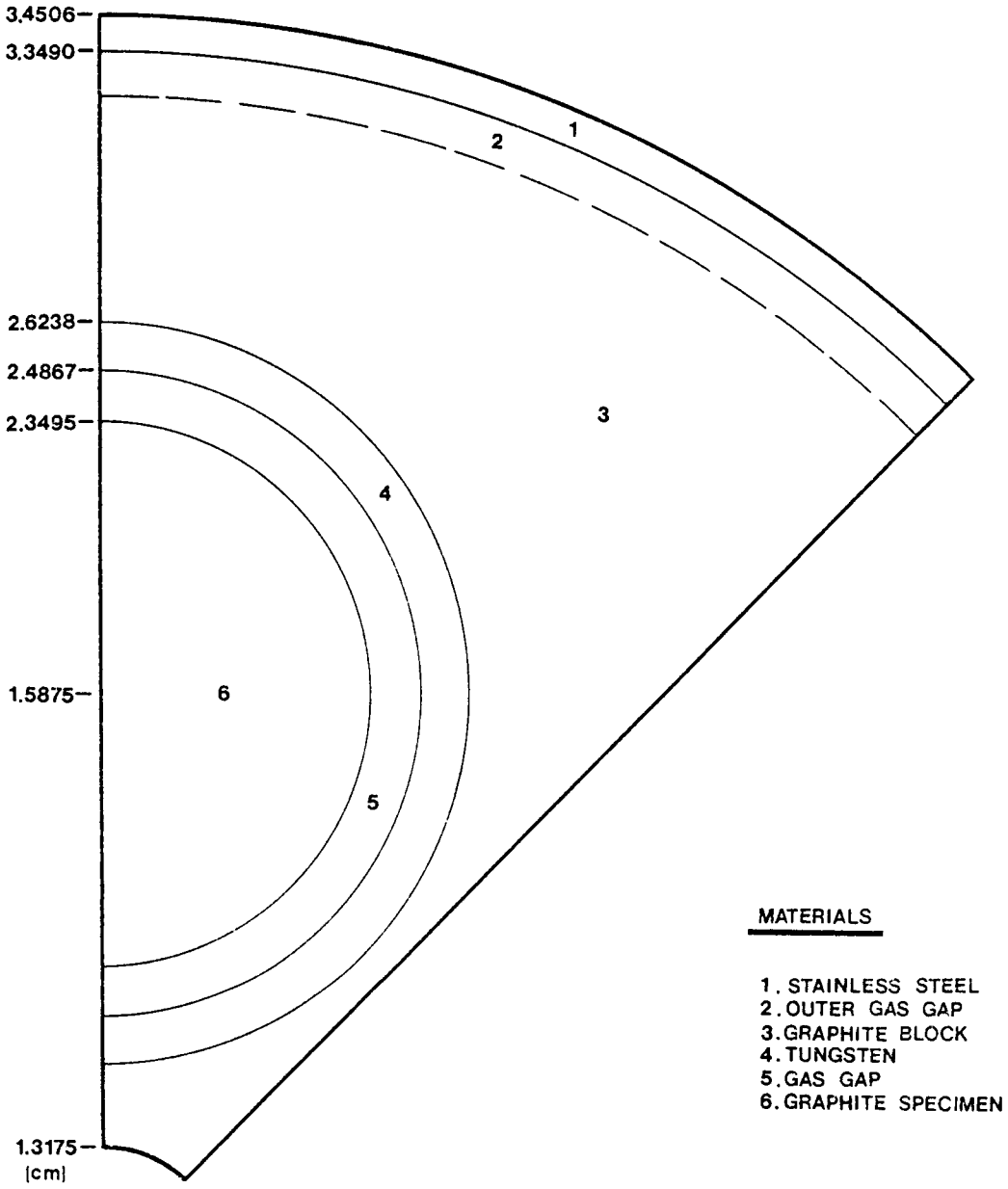



Figure 2-24. Final Simplified Model Cross Section of the OC-5 Capsule.

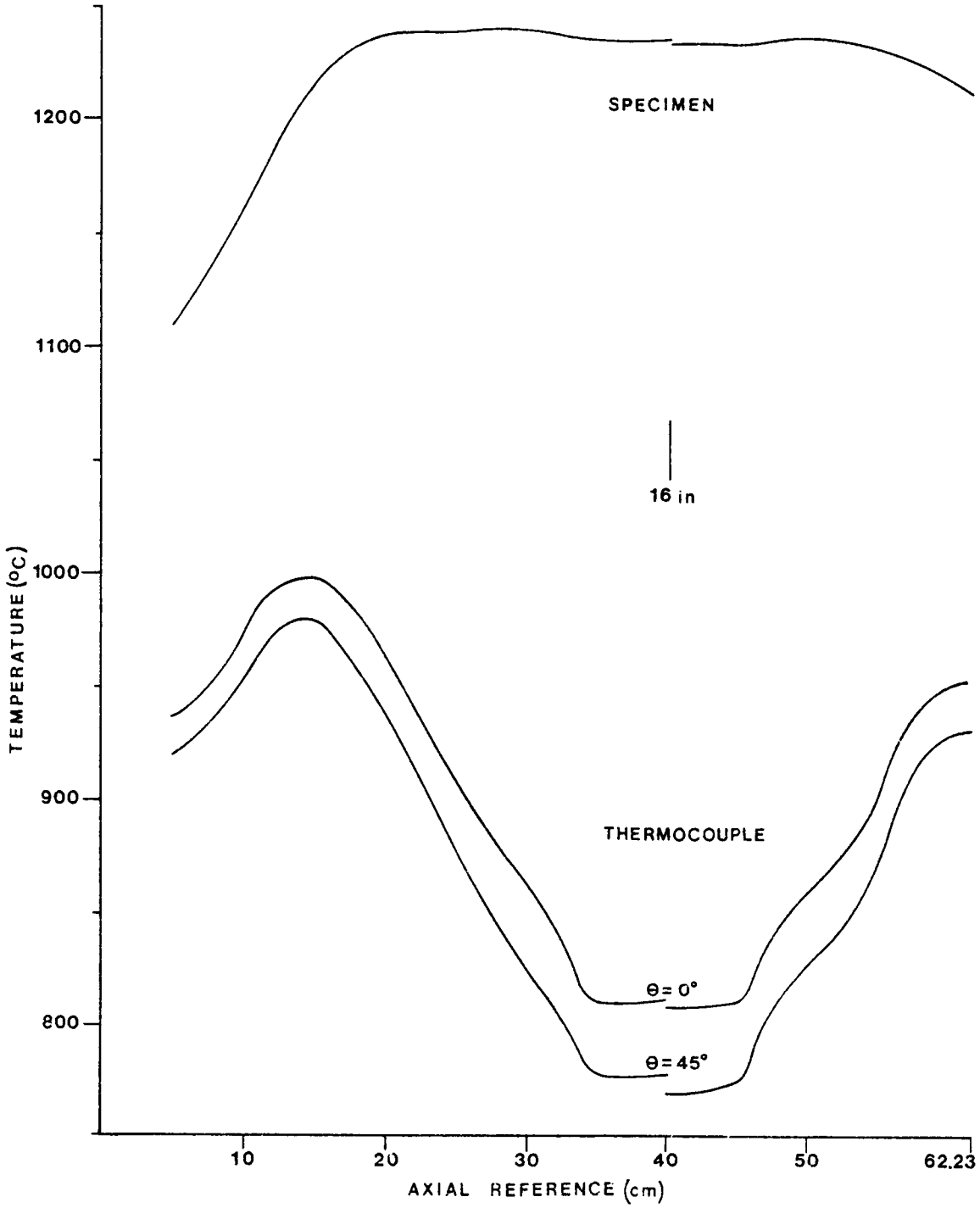



Figure 2-25. Axial Distribution of Specimen Central Temperature and Thermocouple Temperatures at Two Possible Locations. Thermocouple Locations are at a Radius of 2.896 cm.

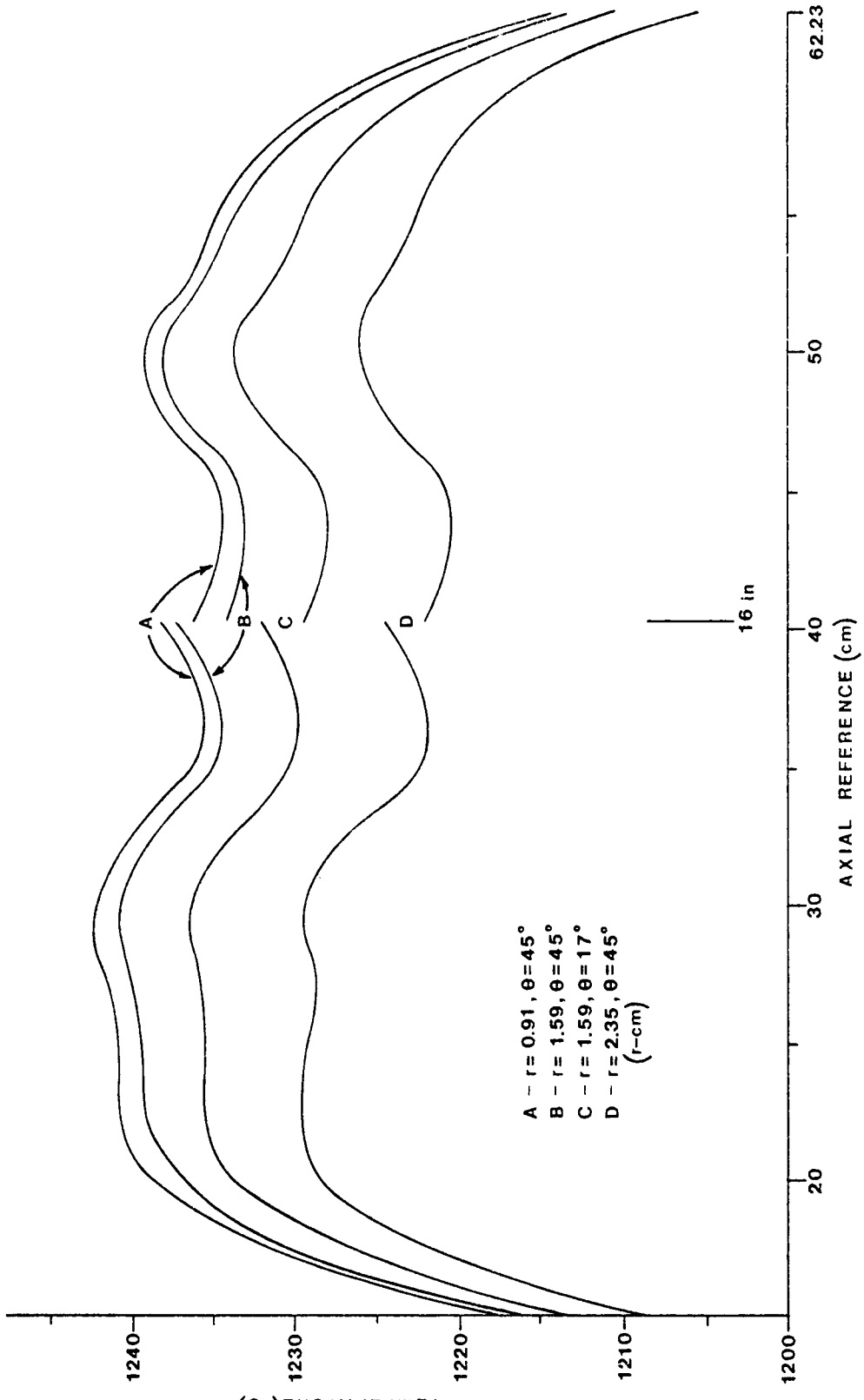



Figure 2-26. Axial Distribution of Specimen Temperature at Four Cross-Sectional Locations.

axial temperature distributions at the center of the specimens and at two possible thermocouple positions; and Figure 2-26 shows the axial temperature distributions at four positions within the specimens.

In both the 600°C and 900°C capsules the thermocouples had to be placed between the specimen columns because of the heaters. However, this restriction is no longer necessary, and it would appear that a better position would be located radially out from the center of the specimens. In this position the thermocouples would not only be less likely to overheat, because of the lower temperatures (see Figure 2-25), but would also produce better reference temperatures when using the computational temperature distributions because the capsule was more accurately modeled in this region.

The applicability of this design hinges upon the outcome of the bench test because of two crucial assumptions that were made:

1. tungsten will retain its polished surface under the OC-5 conditions, and
2. the radiant emissivity of polished tungsten is 0.15.

There are three possible outcomes of the bench test and each would lead to a different set of proceedures for completing the thermal design.

1. The first assumption is found to be invalid or the second is found to be invalid with an emissivity greater than 0.5.

In this case the capsule would have to be redesigned with a material other than tungsten which will act as a thermal radiation reflector and retain its properties under the OC-5 conditions; or the capsule could be completely redesigned if possible without the use of a thermal radiation reflector.

2. The radiant emissivity of polished tungsten is found to be a value greater than 0.15 but less than 0.5.

This will require a slight modification in the design, with the magnitude of the modification dependent upon the value found. This will require an adjustment of the outer gas gap and possibly the gas mixture. After the design has been completed by the gross lattice thermal analysis, a fine lattice study should be made.

3. Both assumptions are found to be valid.

The gross lattice analysis and design are completed in this case and a fine lattice study should be made.

# CHAPTER III

## BENCH TEST

During the thermal design of the OC-5 capsule, it became apparent that, for the desired configuration (Figure 1-2, p. 4), a specimen temperature of 1250°C could not be reached and still maintain a temperature of 950°C or less on the thermocouples between the specimens. The 300°C temperature drop from specimens to thermocouples was prohibited by the thermal radiation across the gas gap surrounding the specimen. Therefore, an alternative design had to be found which would significantly decrease this radiation without substantially increasing either the cost or complexity of construction.

One modification considered was a series of smaller gaps in place of the one large gap. This would have been an excellent method of reducing the thermal radiation except that, because of the limited space between the specimens and the thermocouples, only two gaps could be created using a 0.15 cm (0.06 in.) thick graphite sleeve. Besides the fact that two smaller gaps would not quite fulfill the requirement, the cost of milling the sleeve and the complexity of retaining it within the capsule made this possible modification less viable than that of a thermal radiation reflector.[9]

The modification chosen was that of a cylindrical thermal radiation reflector placed between the specimen column and the graphite block, and having a close fit with the graphite block (Figure 2-24). This design eliminates the need of multiple gas gaps.

The material chosen for the reflector was tungsten with the inner surface of the sleeve polished so as to further decrease the radiant emissivity. Although information about polished tungsten is somewhat scarce, previous experience indicates that, under ideal conditions and at lower temperatures, tungsten will maintain its properties and polish in the presence of graphite.[5] The radiant emissivity of tungsten is estimated to be 0.15 using a tungsten filament as the reference, and therefore, is somewhat in question.

In order to obtain greater confidence in the estimate of radiant emissivity and the characteristics of polished tungsten under the OC-5 capsule conditions, an unirradiated bench test was proposed. Final design work on the OC-5 capsule will not be completed until the results of the bench test have been obtained.

The bench test must be designed in such a way as to answer three questions:

1. Is the radiant emissivity of the tungsten in a low enough range to allow use of this design for the 1250$^{o}$C capsule?
2. Will the radiant emissivities and other properties of the tungsten tube remain constant when subjected to the conditions found in the 1250$^{o}$C Irradiation Creep Capsule?
3. How much confidence can be placed in the computational methods used?

## 3.1 Design Requirements

The answers to the first and third questions do not impose any special design requirements other than one surface of the tungsten be polished and the same computational methods be used as in the design of the OC-5 capsule. The answer to the second question does impose several requirements, namely:

1. The tungsten must be formed as a cylindrical sleeve, with the inner surface polished, and have an inner radius of 0.899 cm (0.354 in.) and an outer radius of 1.036 cm (0.408 in.).
2. A graphite sleeve must be machined so as to be a close fit with the outer surface of the tungsten sleeve at operating temperatures.
3. There must be a graphite dummy specimen with an outer radius of 0.762 cm (0.3 in.) separated from the inner surface of the tungsten sleeve by a 0.1372 cm (0.054 in.) gas gap, where the gas is a neon-helium mixture.
4. The temperature of the outer surface of the dummy specimen must be approximately 1221°C (2230°F).
5. The temperature drop across the gas gap surrounding the dummy specimen must be approximately 316°C (600°F).

Using these requirements, a cylindrical capsule was designed with the following characteristics, where the unmentioned radii, heater power, gas mixture, and coolant flow rate are to be determined by requirements four and five:

1. A heater element placed within a graphite dummy specimen which has an outer radius of 0.762 cm (0.3 in.).
2. A tungsten sleeve with a polished inner surface which has an inner radius of 0.899 cm (0.354 in.) and an outer radius of 1.036 cm (0.408 in.), with a gas gap between the dummy specimen and the tungsten sleeve.
3. A graphite sleeve made to be a close fit with the outer surface of the tungsten sleeve.
4. A stainless steel tube separated from the graphite sleeve by a gas gap.
5. A stainless steel pipe separated from the stainless steel tube by a gas gap.
6. The stainless steel pipe cooled by air at room temperature radially forced over its exterior.

## 3.2 Assumptions and Simplifications

The primary computer code used to analyze this capsule was GENGTC[10], a one dimensional heat transfer code in cylindrical coordinates on the Dec-10 computer at ORNL. The HEATING 5 code was used to check the calculations made by GENGTC, as well as for the two and three dimensional analyses.

The GENGTC code was used as the primary means of thermal analysis because of its quick response and low cost. However, to use this code, it was necessary to assume a constant convective heat transfer coefficient around the outside of the stainless steel pipe. Although this assumption was somewhat in question initially, it turned out to be a good one because the low Reynold's number required for the

coolant air indicated that the coefficient of forced convection varied only slightly.

The assumptions made during the design of the bench test capsule are as follows:

The radiant emissivity of the polished, inner, surface of the tungsten is 0.15 and the unpolished surface is 0.7, as in the OC-5 capsule.

The heater element is composed of graphite with a radiant emissivity of 0.9. This assumption is used merely to determine the power requirements of the heater and does not place restrictions on the type of heater used.

The sweep gas is stagnant. This assumption arises because of the very low flow rates involved (a few $cm^3$/min).

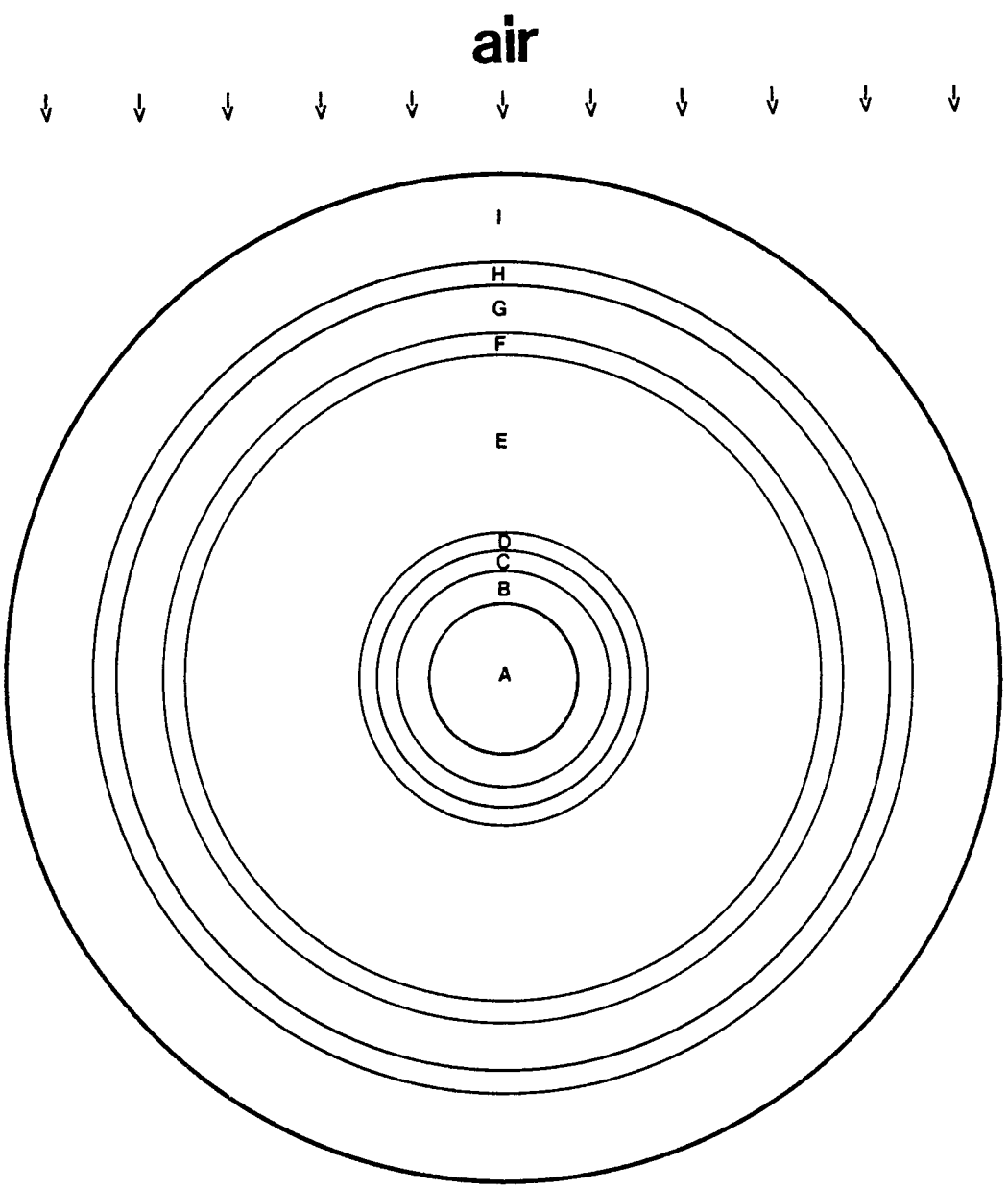
The capsule is long enough for there to be a region with an essentially flat axial temperature profile. This assumption eliminates the end effects from the analysis of the central region.

The thermocouples have a negligible effect on the temperature distribution due to their realitively small cross-sectional areas and volumes.

The material properties used are the same as those used in the analysis of the OC-5 capsule and are shown in Table 2-1 (p. 12) and Figures 2-2, 3, and 4 (p. 14, 15, 16).

## 3.3. Thermal Design

A cross section of the design obtained is shown in Figure 3-1. Table 3-1 gives temperatures at various radial positions as calculated using GENGTC and HEATING 5.




| MATERIALS | OUTER RADIUS [cm] |
|---|---|
| A. HEATER | — |
| B. GRAPHITE DUMMY SPECIMEN | 0.7620 |
| C. GAS GAP | 0.8992 |
| D. TUNGSTEN | 1.0363 |
| E. GRAPHITE SLEEVE | 2.3292 |
| F. GAS GAP | 2.4816 |
| G. STAINLESS STEEL | 2.8194 |
| H. GAS GAP | 2.9718 |
| I. STAINLESS STEEL | 3.6322 |

Figure 3-1. Simplified Bench Test Cross Section.

TABLE 3-1

RADIAL TEMPERATURE DISTRIBUTION OF THE BENCH TEST AS CALCULATED USING THE GENGTC AND HEATING 5 CODES

| Radial Position (cm) | Temperature (°C) | |
|---|---|---|
| | GENGTC | HEATING 5 |
| 0.39700 | 1236 | 1240 |
| 0.39827 | 1230 | 1231 |
| 0.76200 | 1219 | 1221 |
| 0.89916 | 864 | 868 |
| 1.03632 | 863 | 867 |
| 1.03759 | 852 | 854 |
| 2.32918 | 840 | 843 |
| 2.48158 | 735 | 737 |
| 2.81940 | 731 | 733 |
| 2.97180 | 620 | 620 |
| 3.63220 | 613 | 613 |

The capsule is approximately 45.7 cm (18 in.) long and is cooled by air at room temperature forced over the capsule perpendicular to its axis with the upstream velocity of approximately 5.85 meters per second (19.2 ft/sec). The associated Reynold's number is 28055.

A central heating element is operated at approximately 4.65 Kwatt per meter (1.418 Kwatt/ft).

A 2 in. O. D. stainless steel tube, schedule #80, is used for the inner stainless steel sleeve with the outer sleeve made from a 2 1/2 in O. D. stainless steel pipe, schedule #80. The two outer gas gaps which separate the graphite block, the stainless steel tube, and the stainless steel pipe are 0.1524 cm (0.06 in.) wide.

The cross-sectional temperature distribution obtained from this design is shown in Figure 3-2, assuming a linear profile between surfaces.

At this point, the only restrictions on the heating element used were that, it be capable of operating at 4.65 Kwatt per meter and within the graphite dummy specimen. However, it was desired to use the maximum power which could be needed as the heater rating instead of the expected operating power. Therefore, the design was temporarily modified using a radiant emissivity of 0.7 for the inner surface of tungsten and helium as the sweep gas; and, thereby, obtaining the maximum expected power of 11.43 Kwatt per meter (3.485 Kwatt/ft).

## 3.4 Angular Temperature Variation

The angular variation in temperature caused by the angular variation in the coefficient of forced convection was investigated

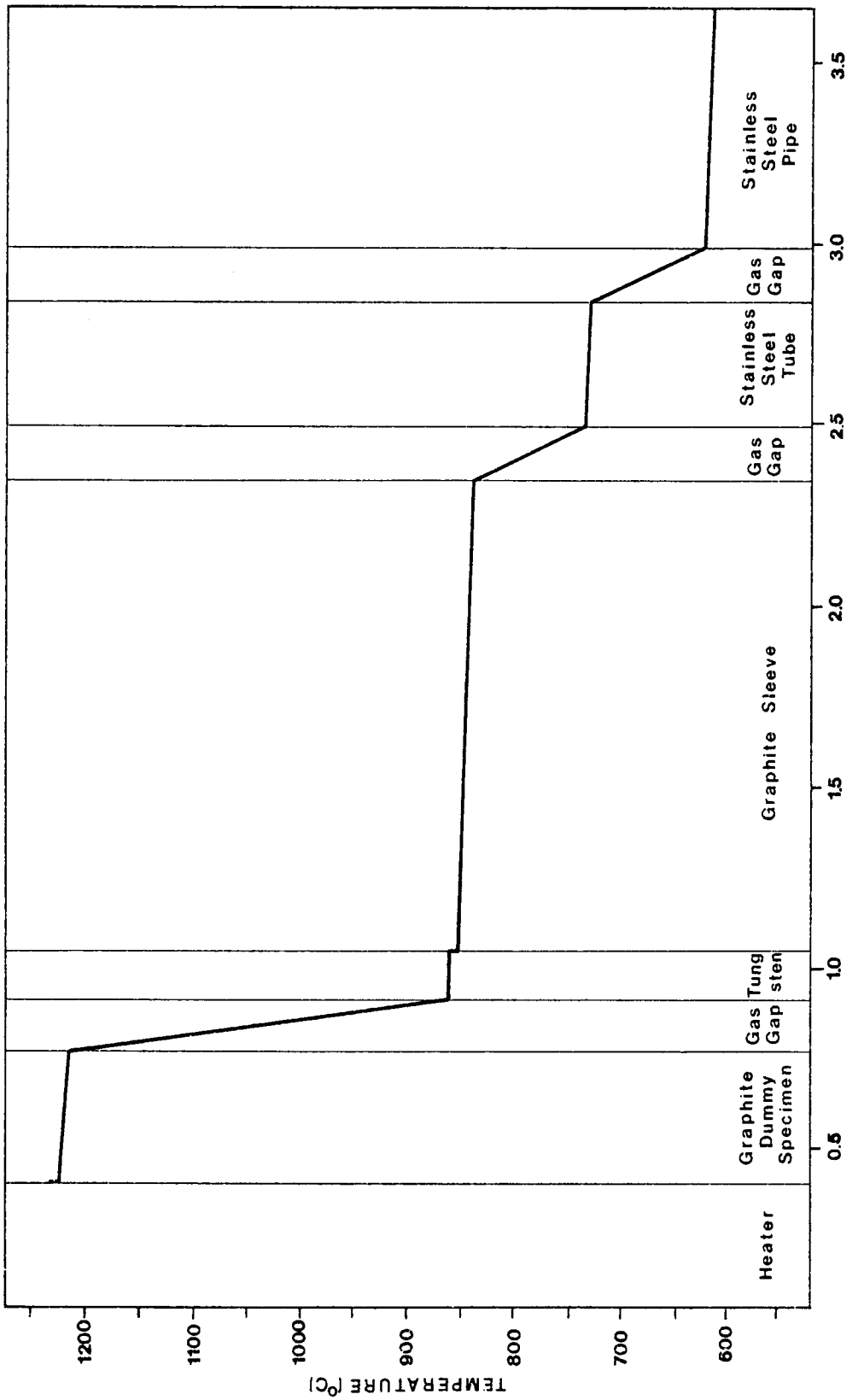



Figure 3-2. Cross-Sectional Bench Test Temperature Distribution.

using the HEATING 5 code in two dimensional cylindrical coordinates ($r$-$\Theta$). The angular average of these coefficients was assumed to be the coefficient obtained during the one dimensional analysis.

In order to obtain the angular variation in the coefficient of forced convection, tha angular variation of Nusselt's number vs. Reynold's number for a cylinder in cross flow was obtained, Figure 3-3.[11] Using the estimated variation in Nusselt's number, the estimate of the variation of the coefficient of forced convection was obtained by dividing the capsule into ten angular intervals, with symmetry about the direction of coolant flow, where the coefficient of forced convection varied as:

| Angular Variation (Radians) | Coefficient of Forced Convection, $h_{fc}$ (BTU/hr-ft$^2$-$^o$F) |
|---|---|
| 0.0 - 0.5236 | 2h = 10.31 |
| 0.5236 - 0.8727 | 1.6h = 8.248 |
| 0.8727 - 1.2217 | h = 5.155 |
| 1.2217 - 2.0944 | .75h = 3.866 |
| 2.0944 - 3.1416 | h = 5.155 |

where $\underline{h}$ was determined by using the following equation:

$$\text{Intervals} \quad \frac{\sum h_{fc}\Delta\Theta}{180} = h_{fc,ave} = \frac{6\text{BTU}}{\text{hr-ft}^2\text{-}^o\text{F}} \quad .$$

The temperature variation obtained is shown in Figure 3-4. This figure indicates that the temperature variation will wash out prior to reaching the tungsten tube.

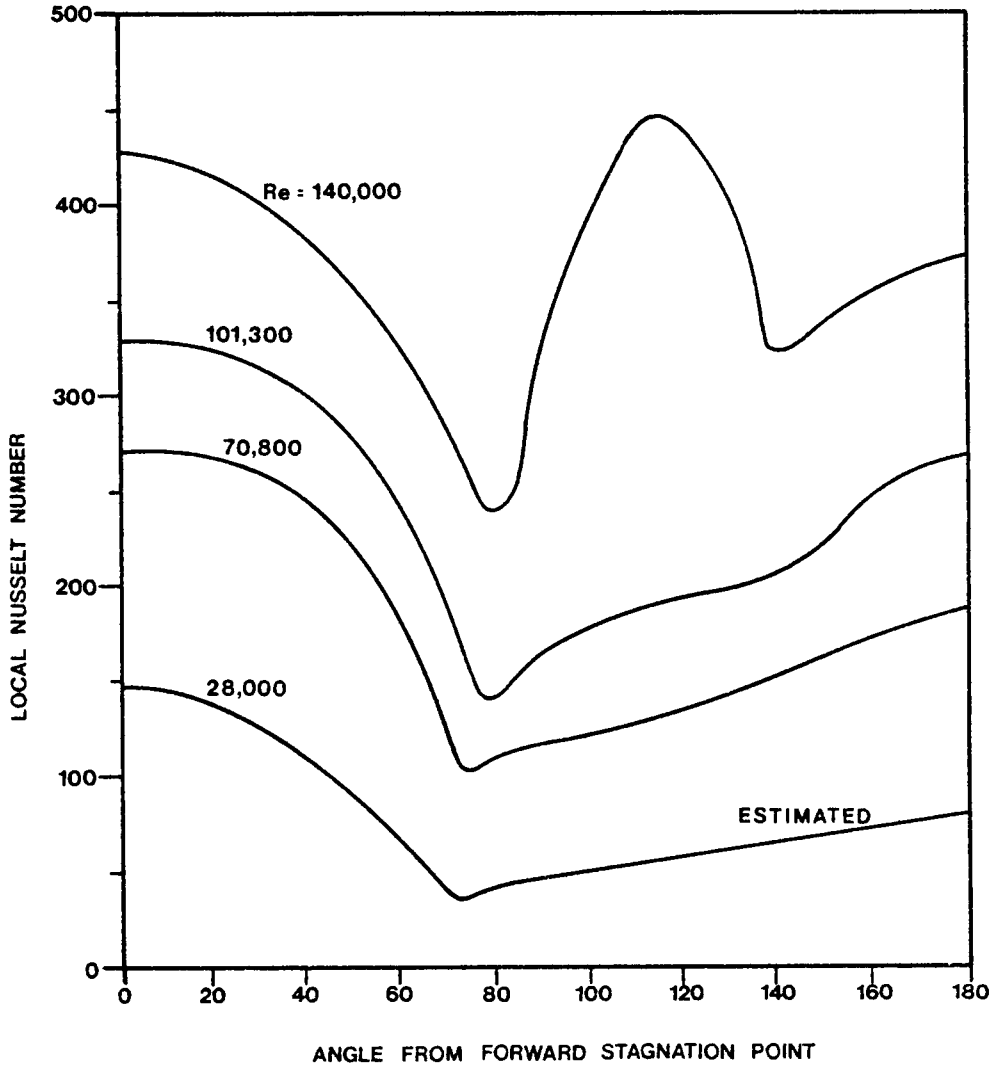



Figure 3-3. Angular Variation of Nusselt's Number vs. Reynold's Number for Cylinder in Cross Flow.

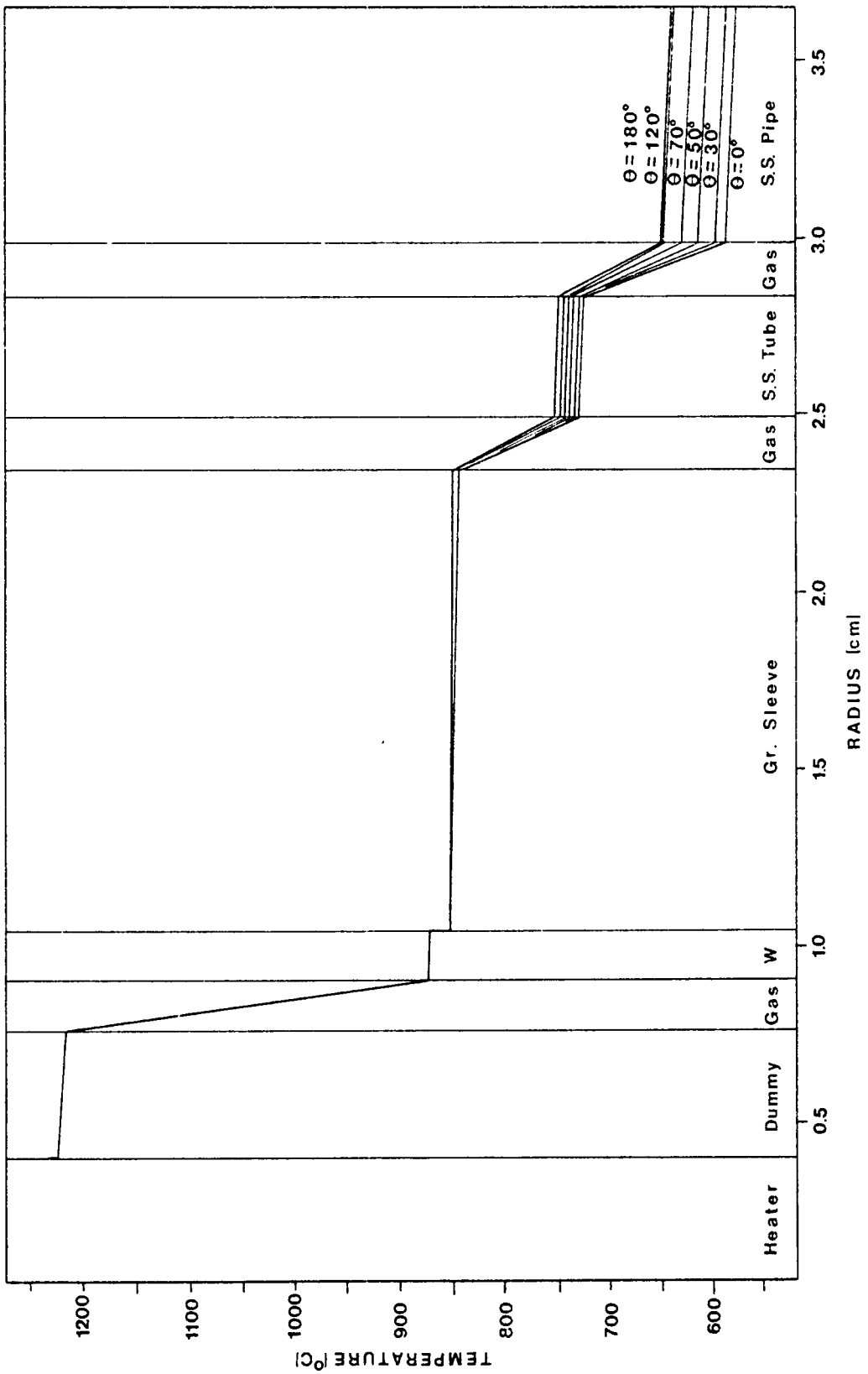



Figure 3-4. Circumferential Temperature Variation Due to Variation in Forced Convection Coefficient.

## 3.5 Thermal Effect of Discontinuities

As presently designed, the graphite dummy specimen is a tube with an outer diameter of 1.524 cm (0.6 in.) and approximately 0.3637 cm (0.1432 in.) thick and 45.7 cm (18 in.) long. This tube is very expensive to construct and difficult to handle because of its length and small cross-sectional dimensions. Hence, it was desirable to use a string of shorter tubes which would greatly decrease the cost and difficulty of construction.

In order to use this string of shorter tubes, it was necessary to determine the possible effect of these discontinuities in the dummy specimen on the temperatures of the various materials. Using the HEATING 5 code and three dimensional cylindrical geometry, the capsule was modeled with a 0.635 cm (0.25 in.) gap in the dummy specimen, which is much larger than will be physically realized as the tubes will be in contact prior to heating. Figure 3-5 illustrates that a discontinuity in the central section of the capsule will have little effect on the temperature of the materials around it.

The effect of the thermocouples and the optical pyrometer on the temperature distribution of the capsule has not been investigated because of the high computer cost involved in such a detailed analysis and because the effect is expected to be negligible.[12] However, an indication of the optical pyrometer's effect on the temperature distribution can be gained from Figure 3-5.

The optical pyrometer will be used to measure the temperature of the dummy specimen and, as such, will require a small view hole from the outside of the capsule through the tungsten sleeve. Considering

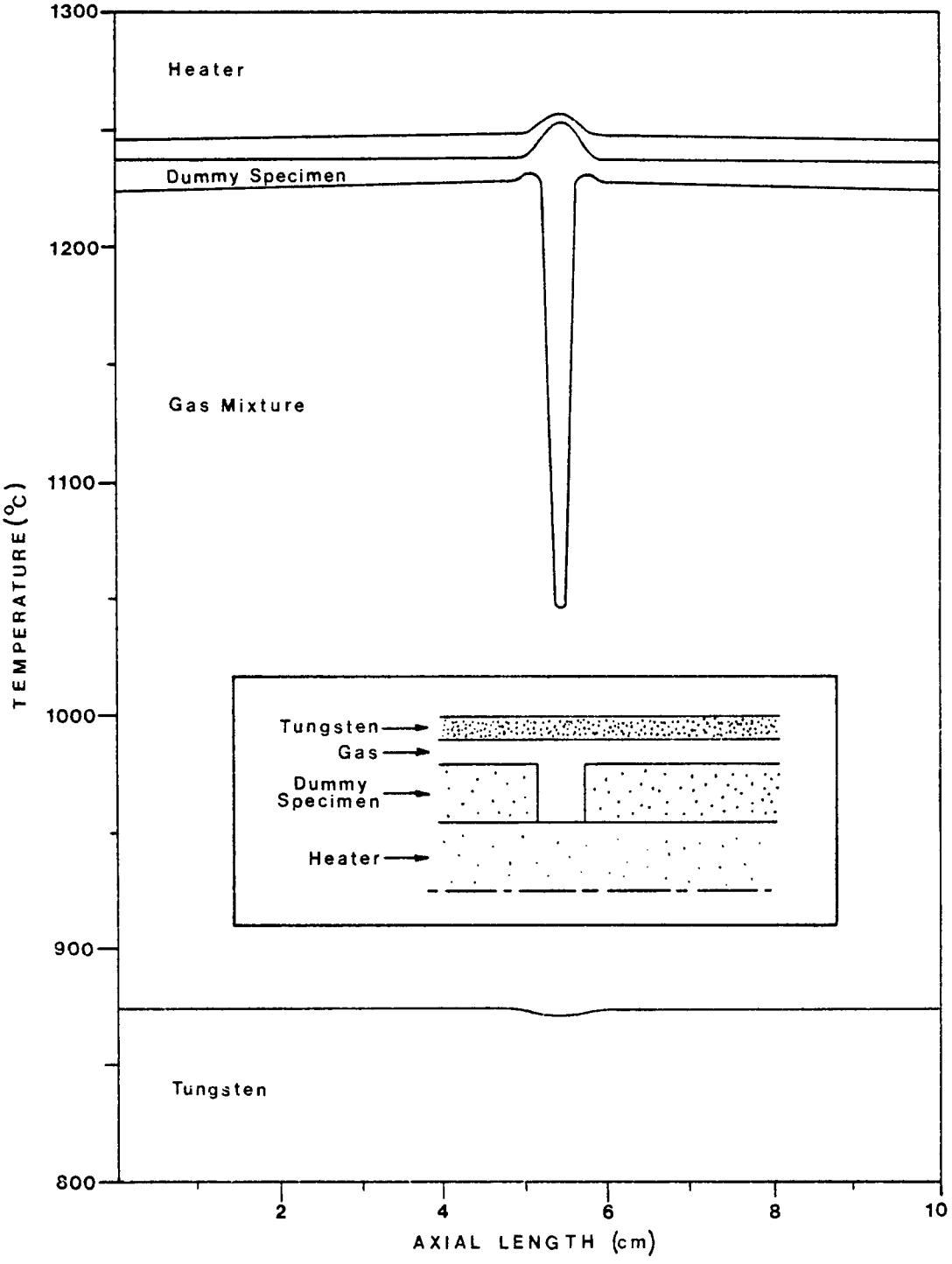



Figure 3-5. Axial Temperature Distribution with 0.638 cm Discontinuity in Dummy Graphite Specimen.

the small effect that the 0.635 cm gap had on the capsule (Figure 3-5), a smaller effect would be expected from the optical pyrometer's hole especially since it goes through materials at substantially lower temperatures.

## 3.6 Experimental Operation Guide

This section contains a series of tables and figures which were obtained during a variation of parameter analysis using the GENGTC code. It is primarily included to aid in the control of the temperature distribution during operation of the experiment.

The curves in the figures were obtained by varying the indicated parameter(s) while holding all others constant and equal to the design parameters, unless otherwise stated, where the design parameters are defined as follows:

coolant temperature = 21.1°C (70.0°F)

coolant upstream velocity = 5.85 m/sec (19.2 ft/sec)

heater power = 4.65 Kwatt/m (1.418 Kwatt/ft)

sweep gas mixture = neon + 0.4 mole fraction helium

radiant emissivity of polished tungsten surface = 0.15

radiant emissivity of unpolished tungsten surface = 0.7

radiant emissivity of graphite tungsten surface = 0.9

radiant emissivity of stainless steel = 0.7

| | Inner Diameter | Outer Diameter |
|---|---|---|
| heater | | 0.794 cm (5/16 in.) |
| graphite dummy specimen | close fit | 1.524 cm (0.6 in.) |
| tungsten | 1.798 cm (0.708 in.) | 2.07 cm (0.816 in.) |

| | | |
|---|---|---|
| graphite sleeve | close fit | 4.86 cm (1.834 in.) |
| S. S. tube | 4.96 cm (1.954 in.) | 5.64 cm (2.22 in.) |
| S. S. pipe | 5.94 cm (2.34 in.) | 7.26 cm (2.85 in.) |

Table 3-2 contains the variation of the coolant air temperature and the resultant temperature distributions. As can be seen, the coolant temperature has little effect on the temperature distribution of the capsule, within the range of probable room temperatures.

Table 3-3 contains the variation of radiant emissivity of the unpolished tungsten surface and the resultant temperature distributions. The table indicates that, should this design parameter be in error, there will be a negligible change in the temperature distribution.

Figure 3-6 indicates the effect various radiant emissivities of the polished tungsten surface will have on the temperature distribution of the capsule. During experiment operation, an examination of the temperatures and comparison with this figure should give an indication of the tungsten emissivity. Use of Table 3-4 should then help in determining the figure which will be of most help in controlling the temperature distribution.

## 3.7 Conclusion

The thermal design of the bench test, where the R-$\Theta$ cross section is shown in Figure 3-1, consists of the following:

The capsule is approximately 45.7 cm (18 in.) long and is cooled by air at room temperature forced over the capsule perpendicular to its axis at approximately 5.85

TABLE 3-2

CALCULATED RADIAL TEMPERATURE DISTRIBUTIONS FOR VARIOUS BENCH TEST COOLANT TEMPERATURES

| Radial Position (cm) | Coolant Temperature (°C) 15.6 | 21.1 | 26.7 | 32.2 |
|---|---|---|---|---|
| | Temperature (°C) | | | |
| 0.39700 | 1235 | 1238 | 1241 | 1244 |
| 0.39827 | 1227 | 1230 | 1232 | 1235 |
| 0.76200 | 1217 | 1219 | 1222 | 1225 |
| 0.89916 | 861 | 864 | 869 | 872 |
| 1.03632 | 860 | 863 | 868 | 871 |
| 1.03759 | 849 | 852 | 858 | 861 |
| 2.32918 | 837 | 840 | 846 | 849 |
| 2.48158 | 732 | 735 | 740 | 746 |
| 2.81940 | 728 | 731 | 736 | 742 |
| 2.97180 | 614 | 620 | 625 | 631 |
| 3.63220 | 608 | 613 | 619 | 624 |

TABLE 3-3

CALCULATED RADIAL TEMPERATURE DISTRIBUTIONS FOR VARIOUS RADIANT EMISSIVITIES OF THE UNPOLISHED TUNGSTEN SURFACE

| Radial Position (cm) | Radiant Emissivity | | | | |
|---|---|---|---|---|---|
| | 0.2 | 0.5 | 0.7 | 0.8 | 0.9 |
| | Temperature (°C) | | | | |
| 0.39700 | 1241 | 1241 | 1238 | 1238 | 1238 |
| 0.39827 | 1233 | 1233 | 1230 | 1230 | 1230 |
| 0.76200 | 1222 | 1222 | 1220 | 1220 | 1220 |
| 0.89916 | 867 | 867 | 864 | 864 | 864 |
| 1.03632 | 866 | 866 | 863 | 863 | 863 |
| 1.03759 | 852 | 852 | 852 | 852 | 852 |
| 2.32918 | 840 | 840 | 840 | 840 | 840 |
| 2.48158 | 735 | 735 | 735 | 735 | 735 |
| 2.81940 | 731 | 731 | 731 | 731 | 731 |
| 2.97180 | 620 | 620 | 620 | 620 | 620 |
| 3.63220 | 613 | 613 | 613 | 613 | 613 |

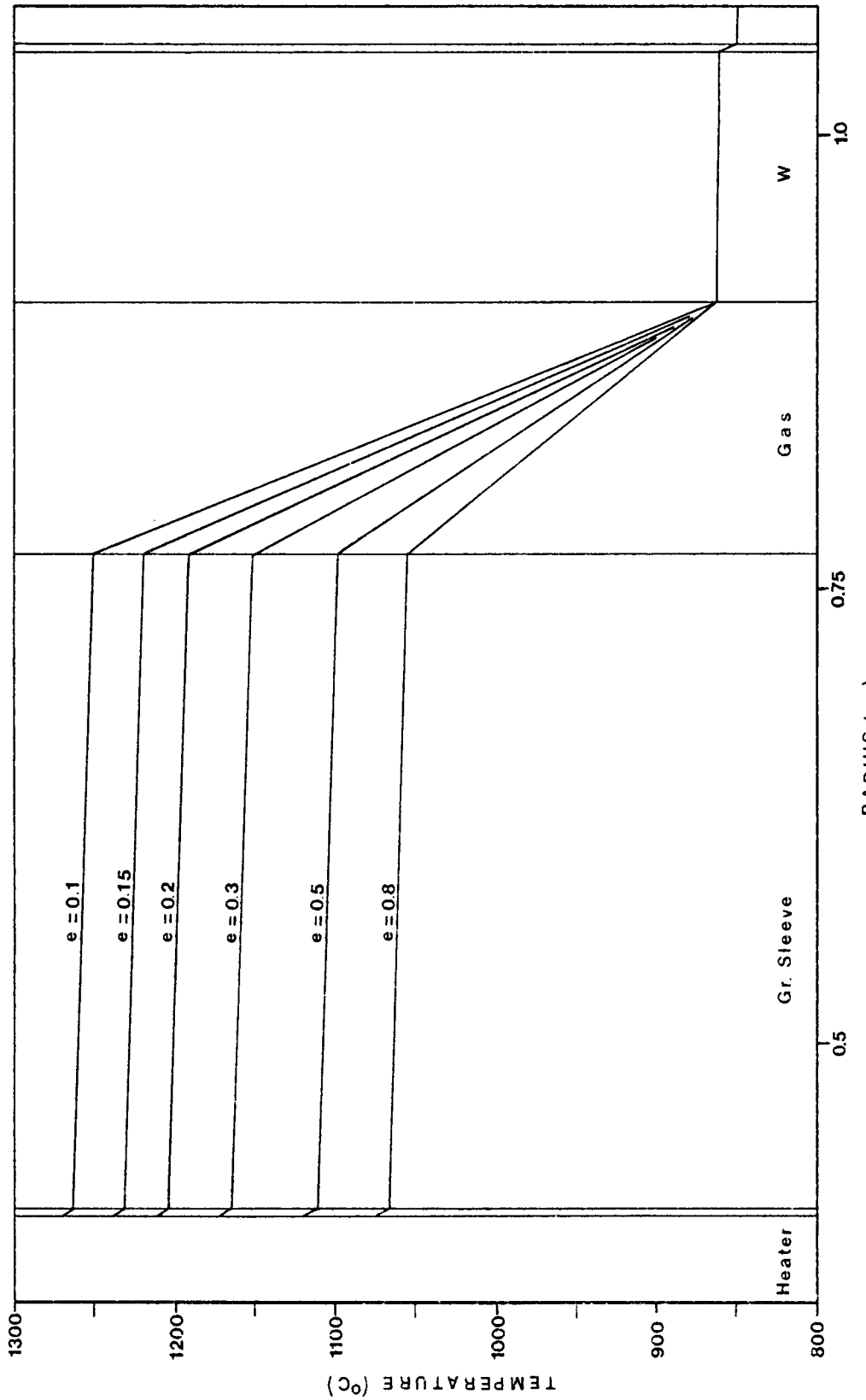



Figure 3-6. Cross-Sectional Temperature Distributions - Variation in Polished Tungsten Emissivities.

TABLE 3-4

FIGURE REFERENCE WITH PARAMETERS FOR USE IN CONTROLLING THE RADIAL TEMPERATURE DISTRIBUTION OF THE BENCH TEST DURING OPERATION

| Radial Temperature Distribution Figure # | Emissivity used for Polished Tungsten Surface 0.1,0.15,0.3,0.5 | | | | Var. Parameters: Heater Power | Coolant Velocity | Sweep Gas Mixture | Emissivity of Polished Tungsten |
|---|---|---|---|---|---|---|---|---|
| 3-7 | X | | | | X | | | |
| 3-8 | | X | | | X | | | |
| 3-9 | | | X | | X | | | |
| 3-10 | | | | X | X | | | |
| 3-11 | X | | | | | X | | |
| 3-12 | | X | | | | X | | |
| 3-13 | | | X | | | X | | |
| 3-14 | | | | X | | X | | |
| 3-15 | | X | | | | | X | |
| 3-16 | | | X | | | | X | |
| 3-17 | | | | X | | | X | |
| 3-18 | | | | | X | | | X |
| 3-19 | | | | | | X | | X |
| 3-20 | | | | | | | X | X |
| 3-21 | | X | | | X | X | | |
| 3-22 | | | X | | X | X | | |
| 3-23 | | X | | | X | X | X | |
| 3-24[a] | | | X | | X | X | | |

[a]The sweep gas mixture used in this figure was neon plus 0.2 mole fraction helium.

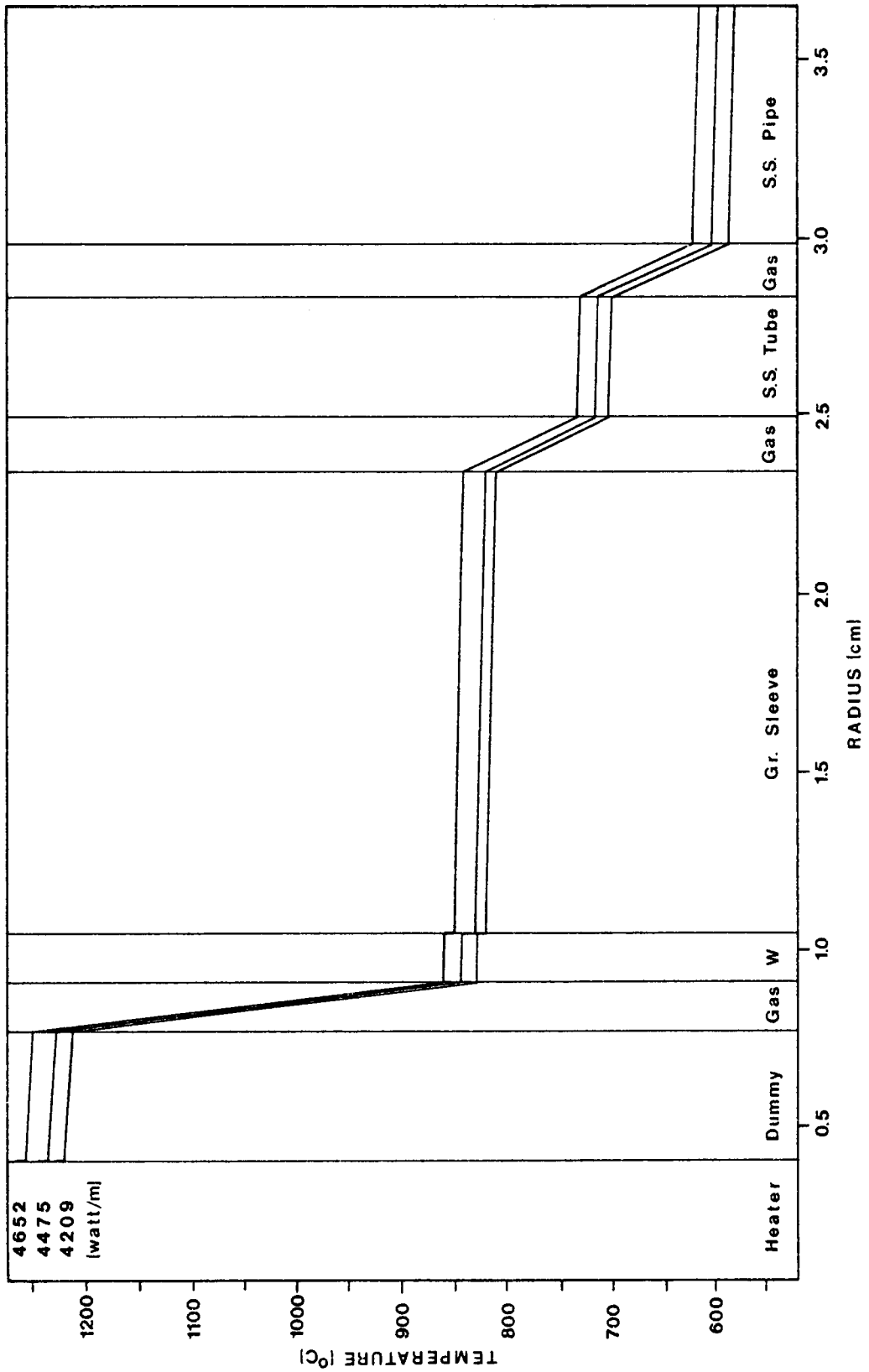



Figure 3-7. Cross-Sectional Temperature Distributions - Variation in Heater Power. Polished Tungsten Emissivity of 0.1.

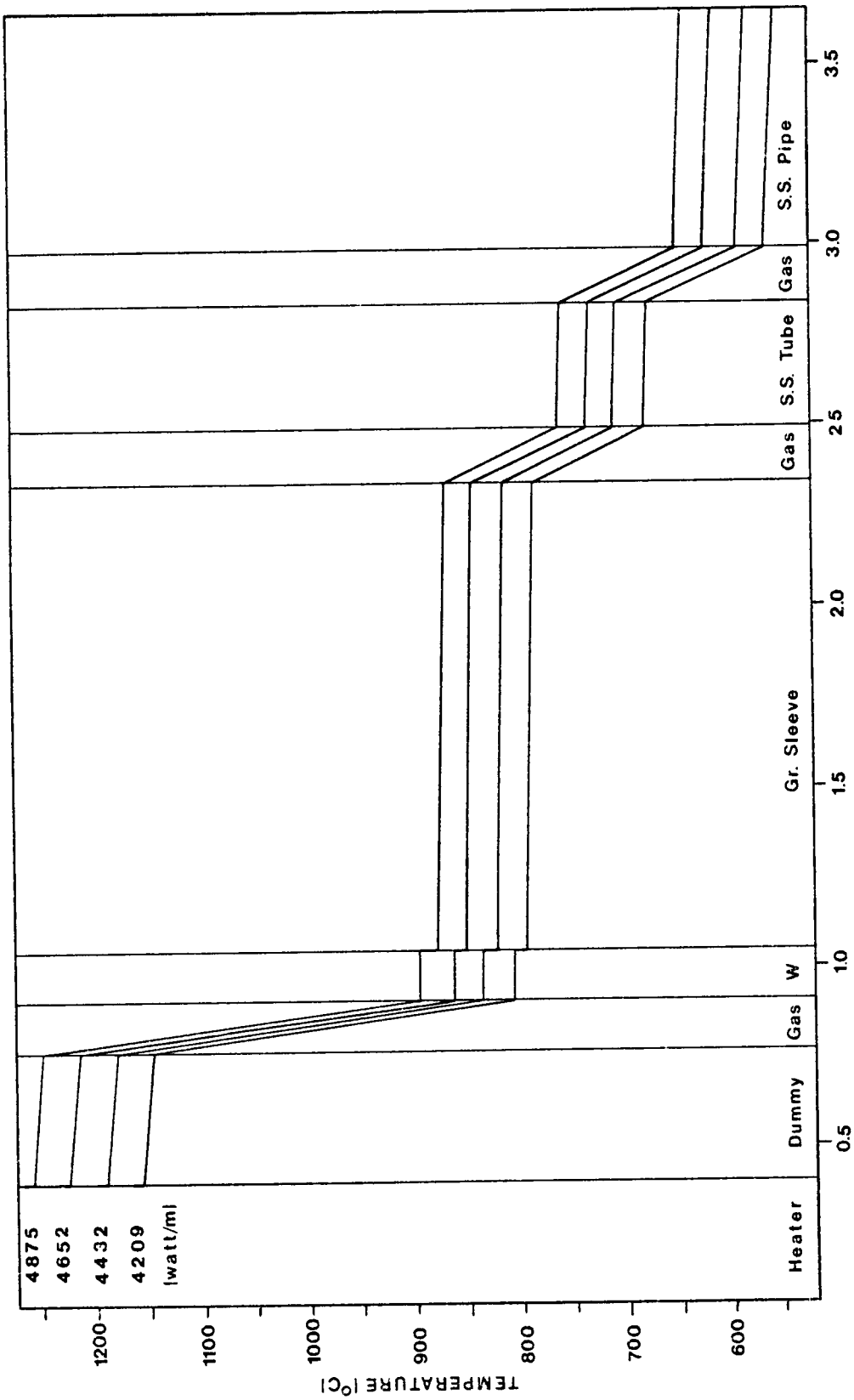



Figure 3-8. Cross-Sectional Temperature Distributions - Variation in Heater Power. Polished Tungsten Emissivity of 0.15.

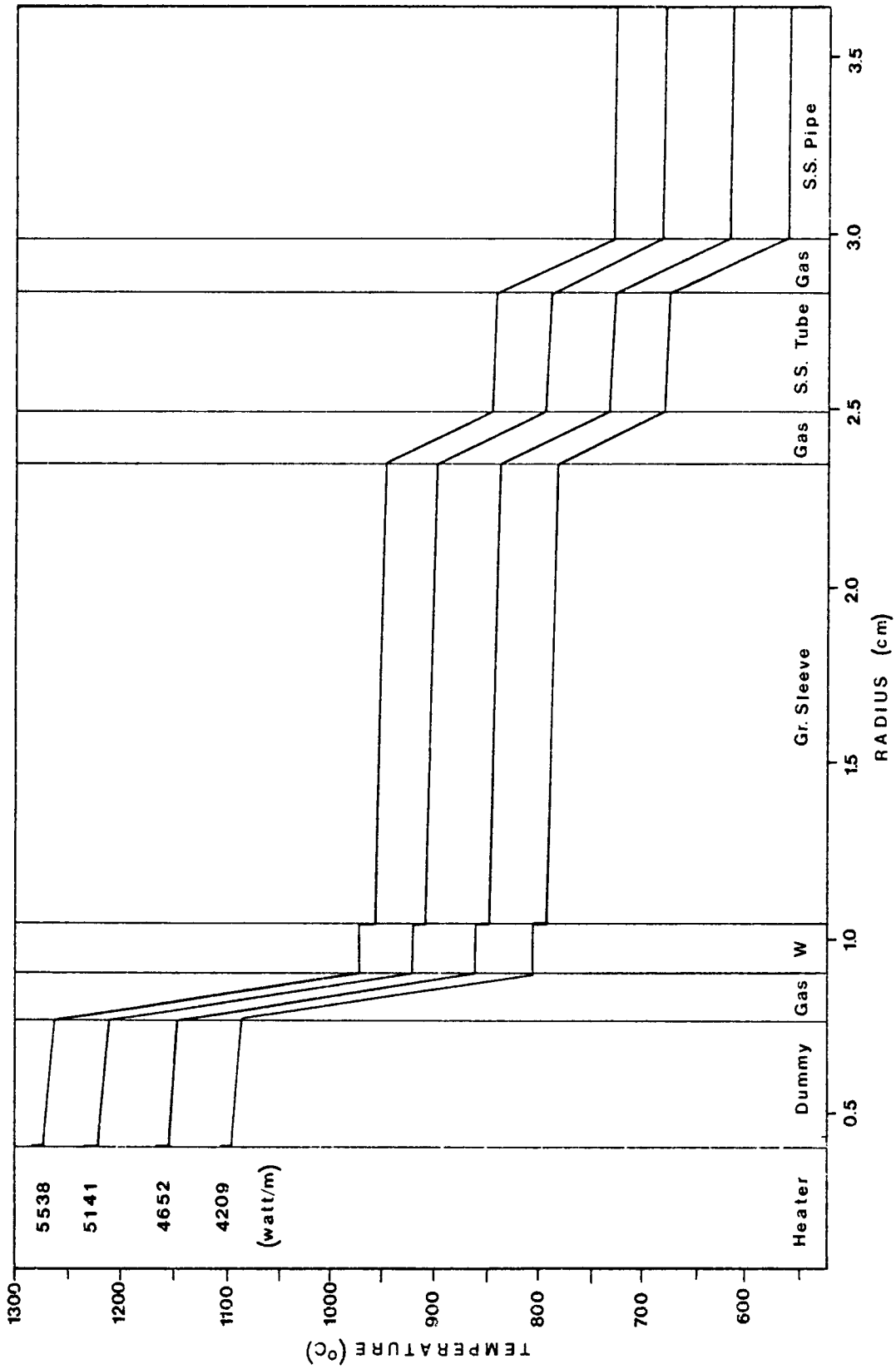



Figure 3-9. Cross-Sectional Temperature Distributions - Variation in Heater Power. Polished Tungsten Emissivity of 0.3.

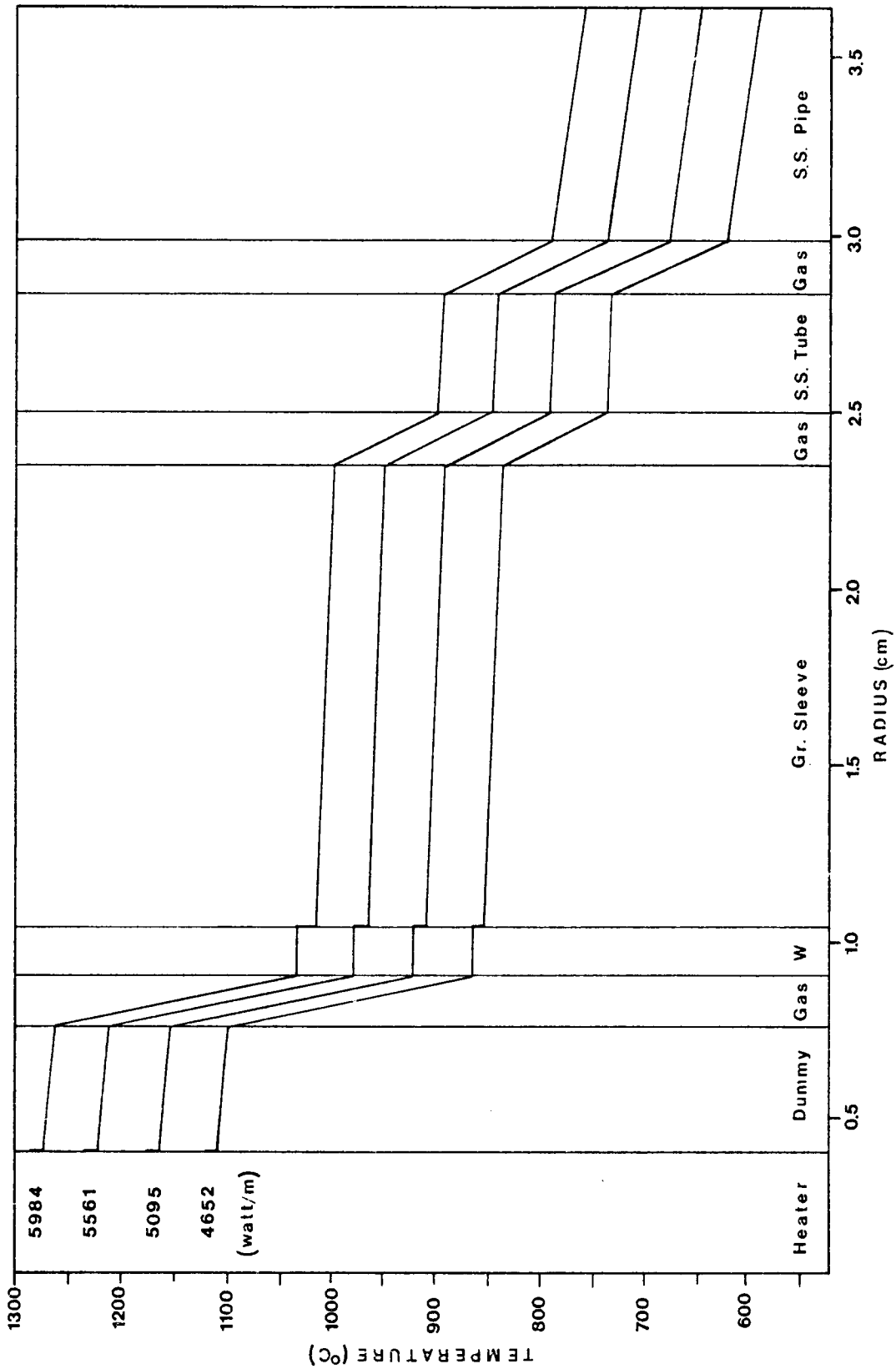



Figure 3-10. Cross-Sectional Temperature Distributions - Variation in Heater Power. Polished Tungsten Emissivity of 0.5.

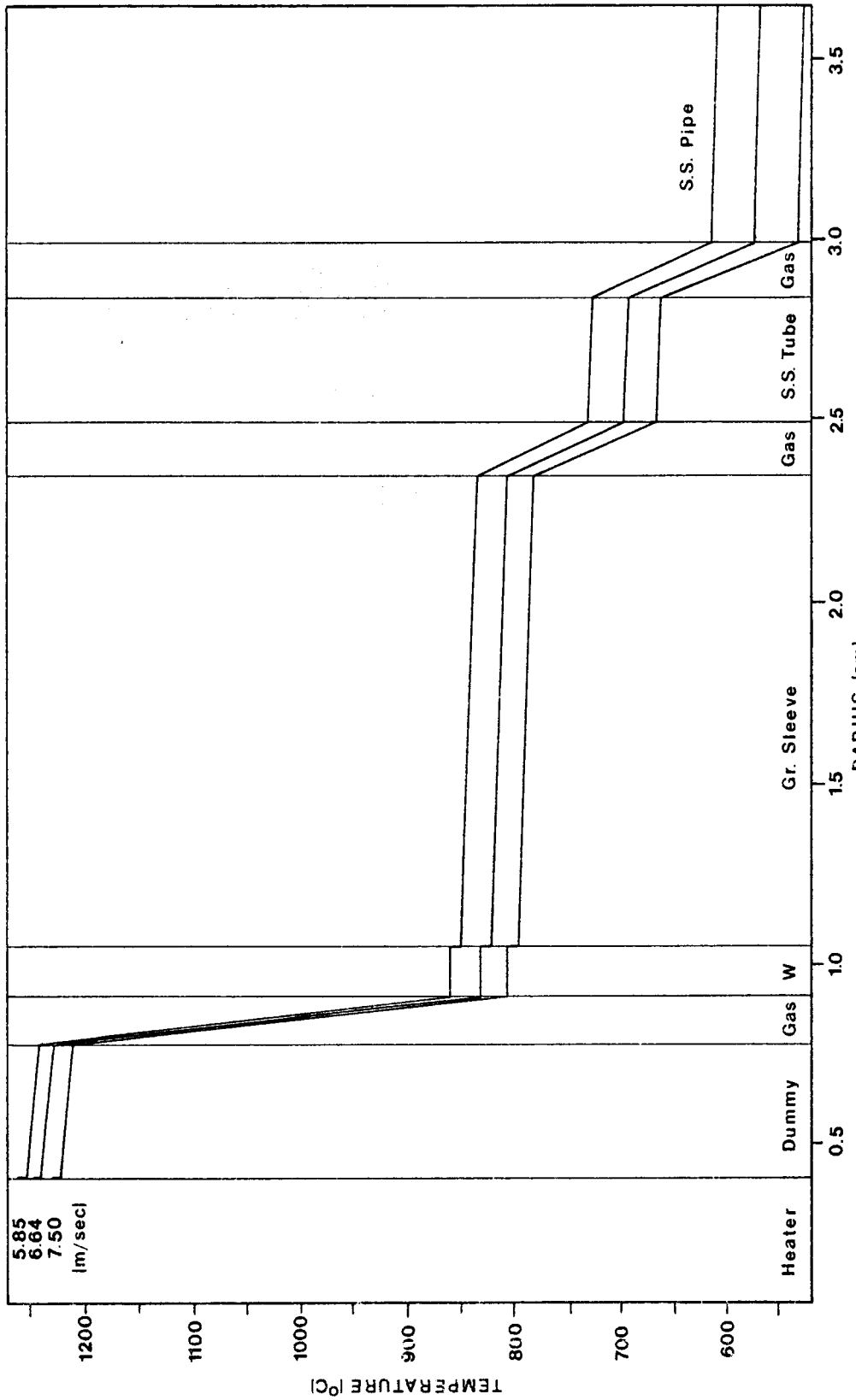



Figure 3-11. Cross-Sectional Temperature Distributions - Variation in Coolant Flow. Polished Tungsten Emissivity of 0.1.

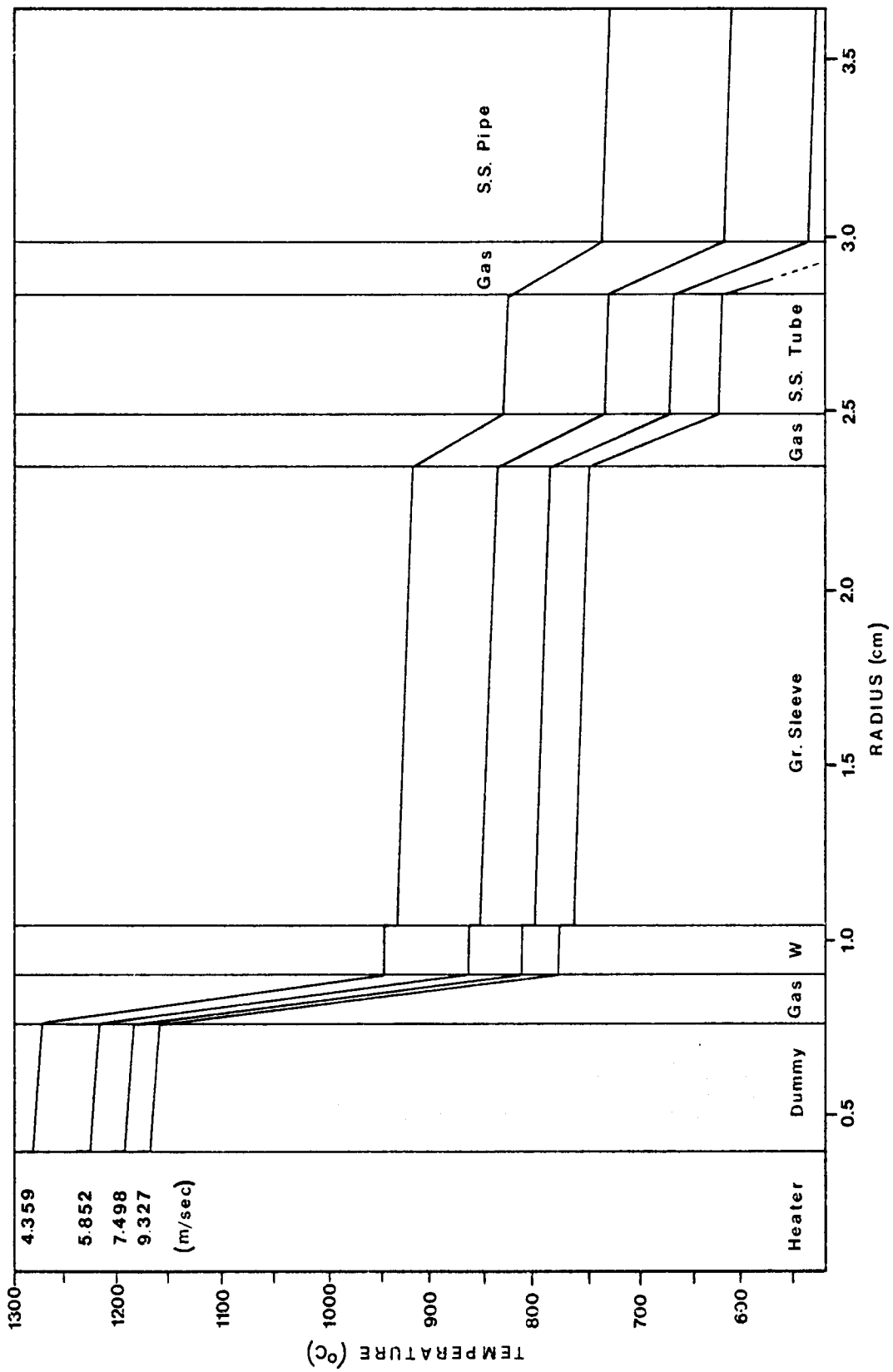



Figure 3-12. Cross-Sectional Temperature Distributions - Variation in Coolant Flow. Polished Tungsten Emissivity of 0.15.

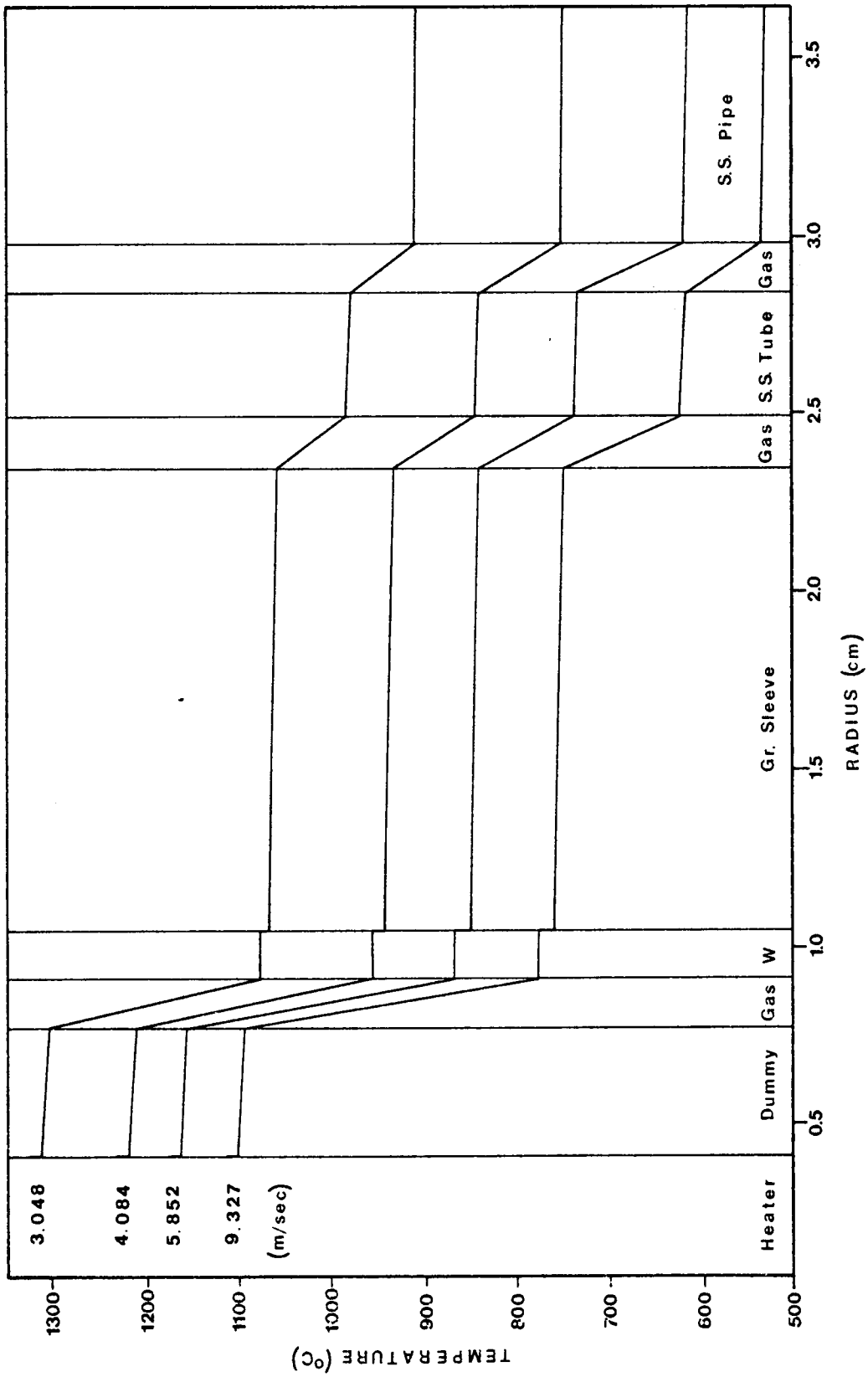



Figure 3-13. Cross-Sectional Temperature Distributions - Variation in Coolant Flow. Polished Tungsten Emissivity of 0.3.

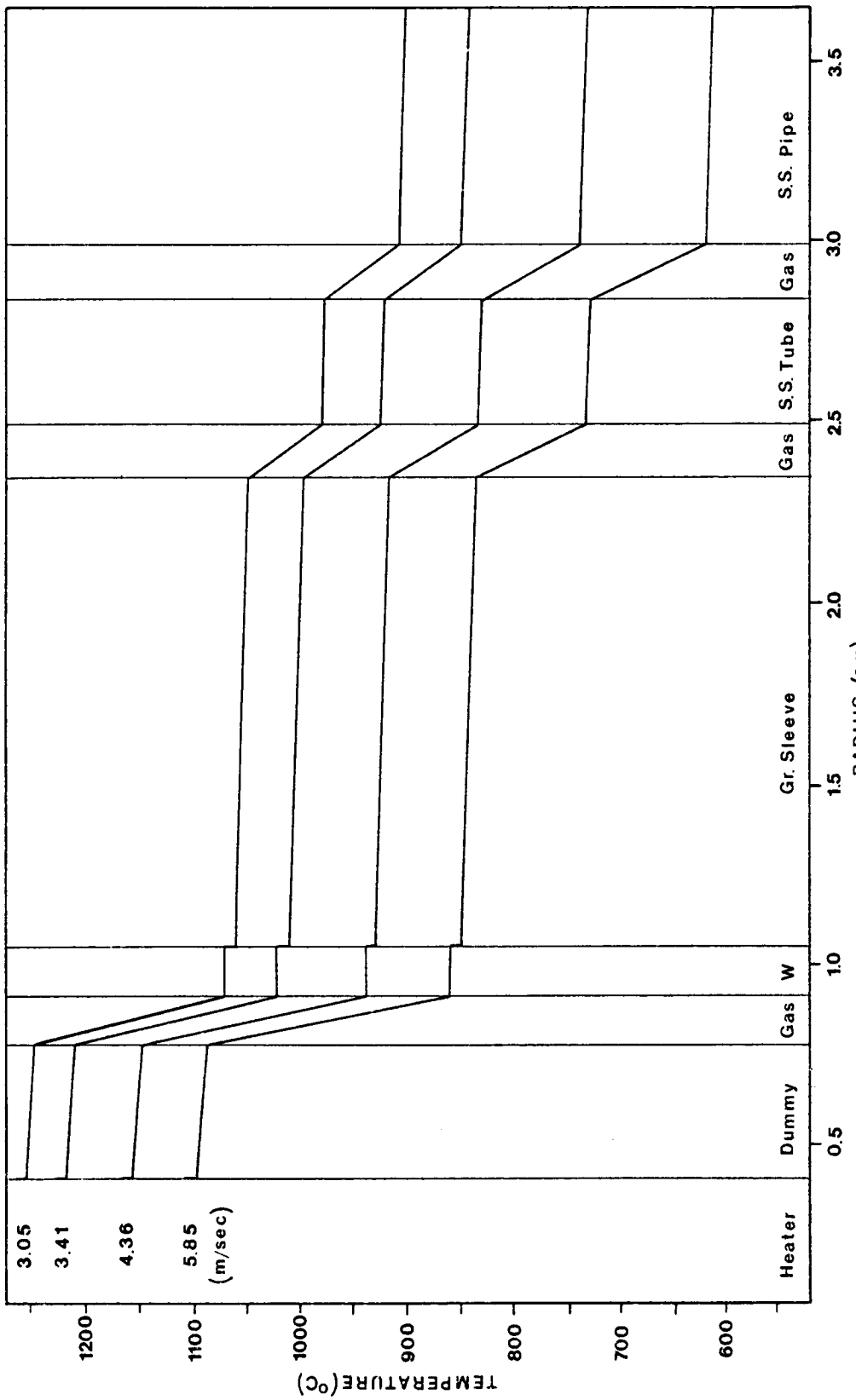



Figure 3-14. Cross-Sectional Temperature Distributions - Variation in Coolant Flow. Polished Tungsten Emissivity of 0.5.

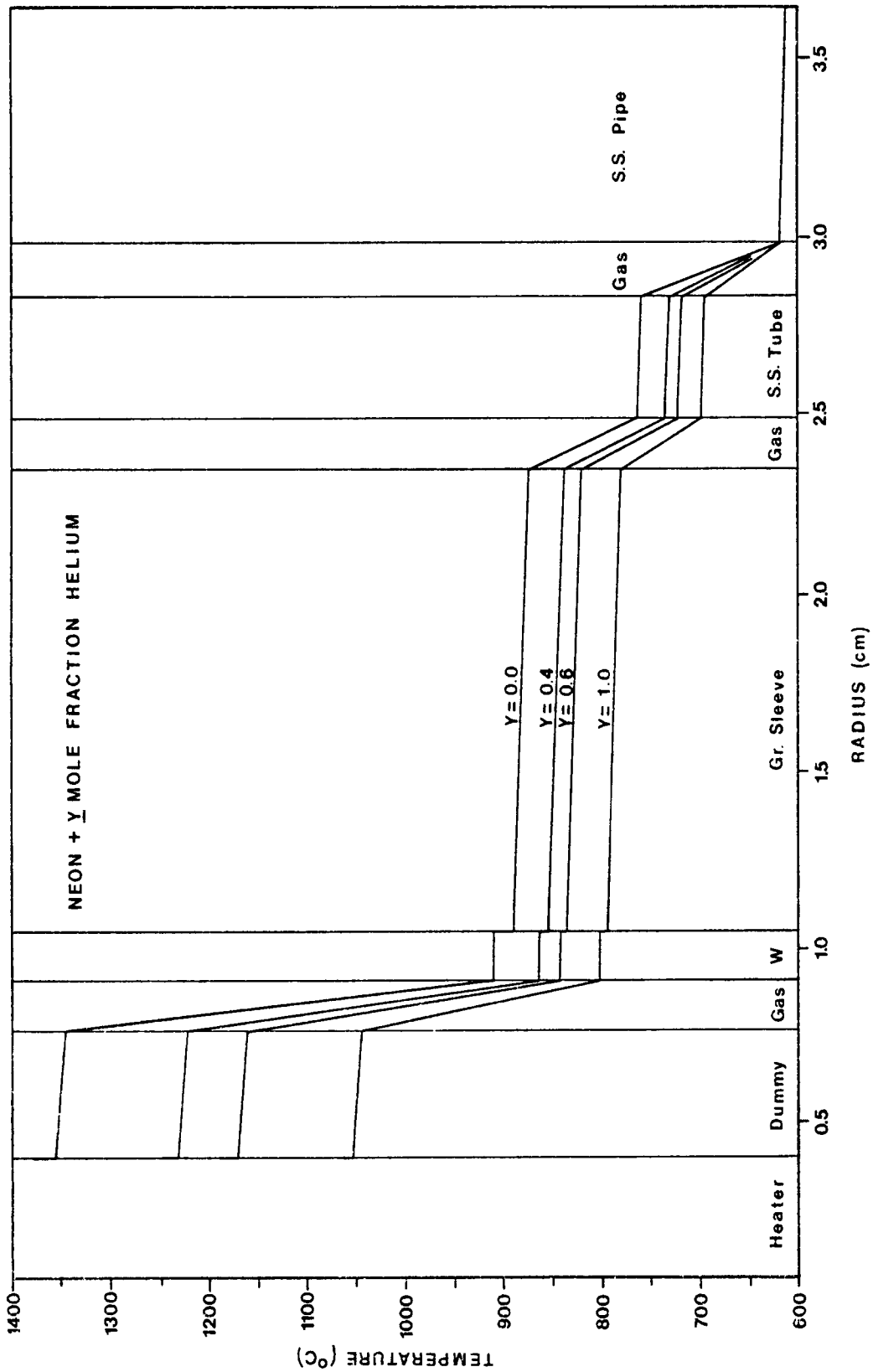



Figure 3-15. Cross-Sectional Temperature Distributions - Variation in Gas Mixture. Polished Tungsten Emissivity of 0.15.

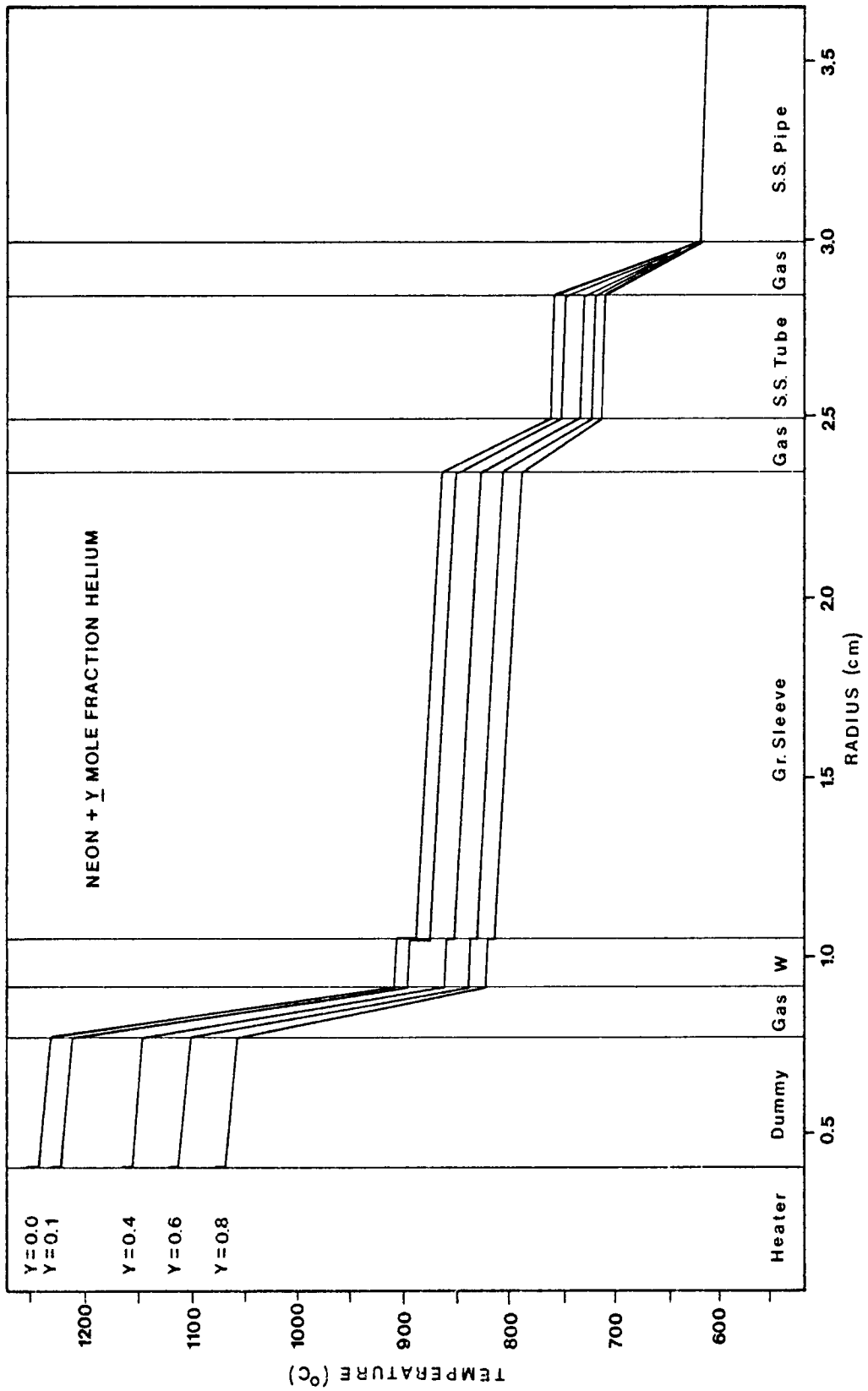



Figure 3-16. Cross-Sectional Temperature Distributions - Variation in Gas Mixture. Polished Tungsten Emissivity of 0.3.

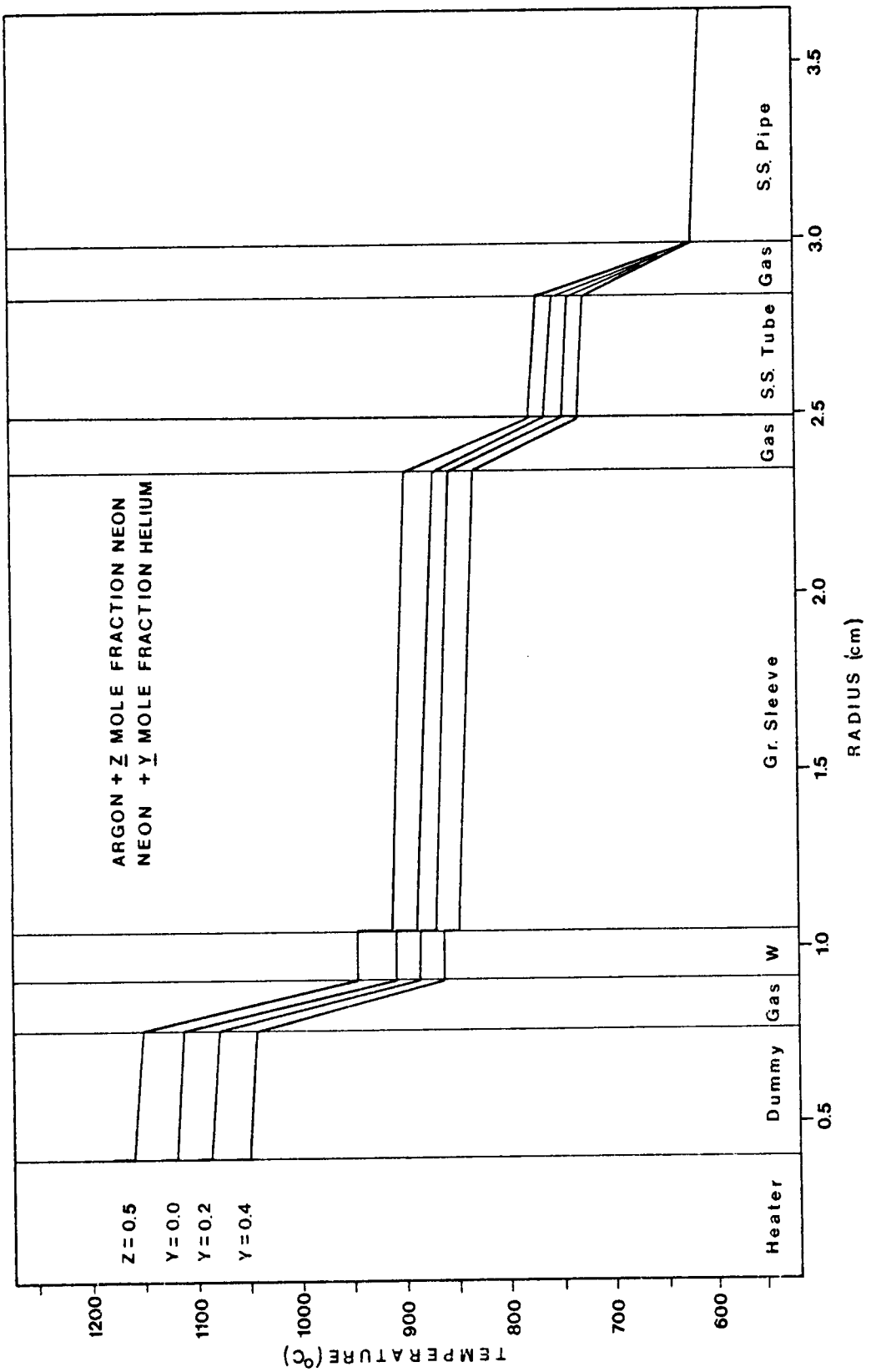



Figure 3-17. Cross-Sectional Temperature Distributions - Variation in Gas Mixture. Polished Tungsten Emissivity of 0.5.

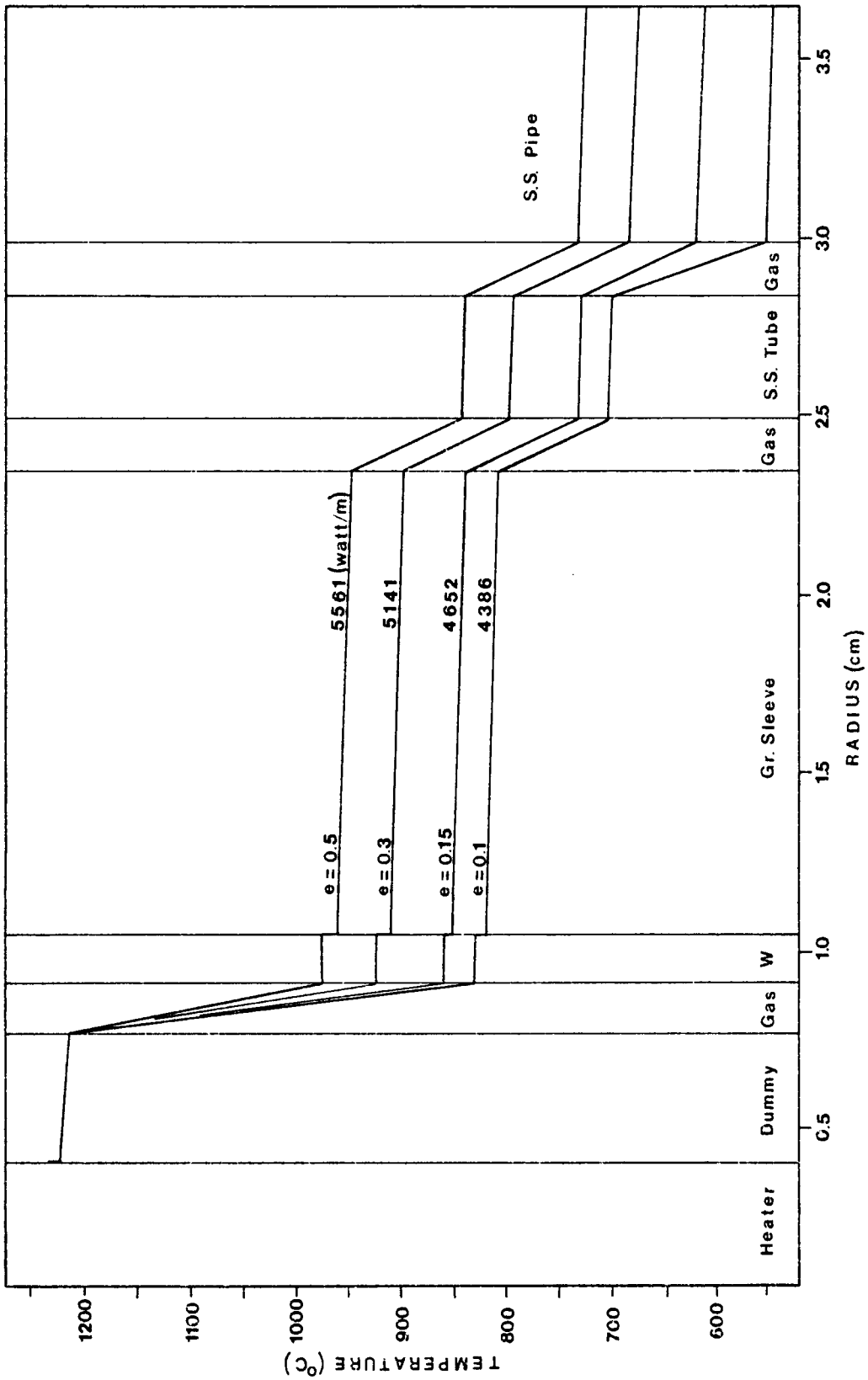



Figure 3-18. Cross-Sectional Temperature Distributions - Variation in Polished Tungsten Emissivity and Heater Power for Dummy Specimen Temperature of 1219°C.

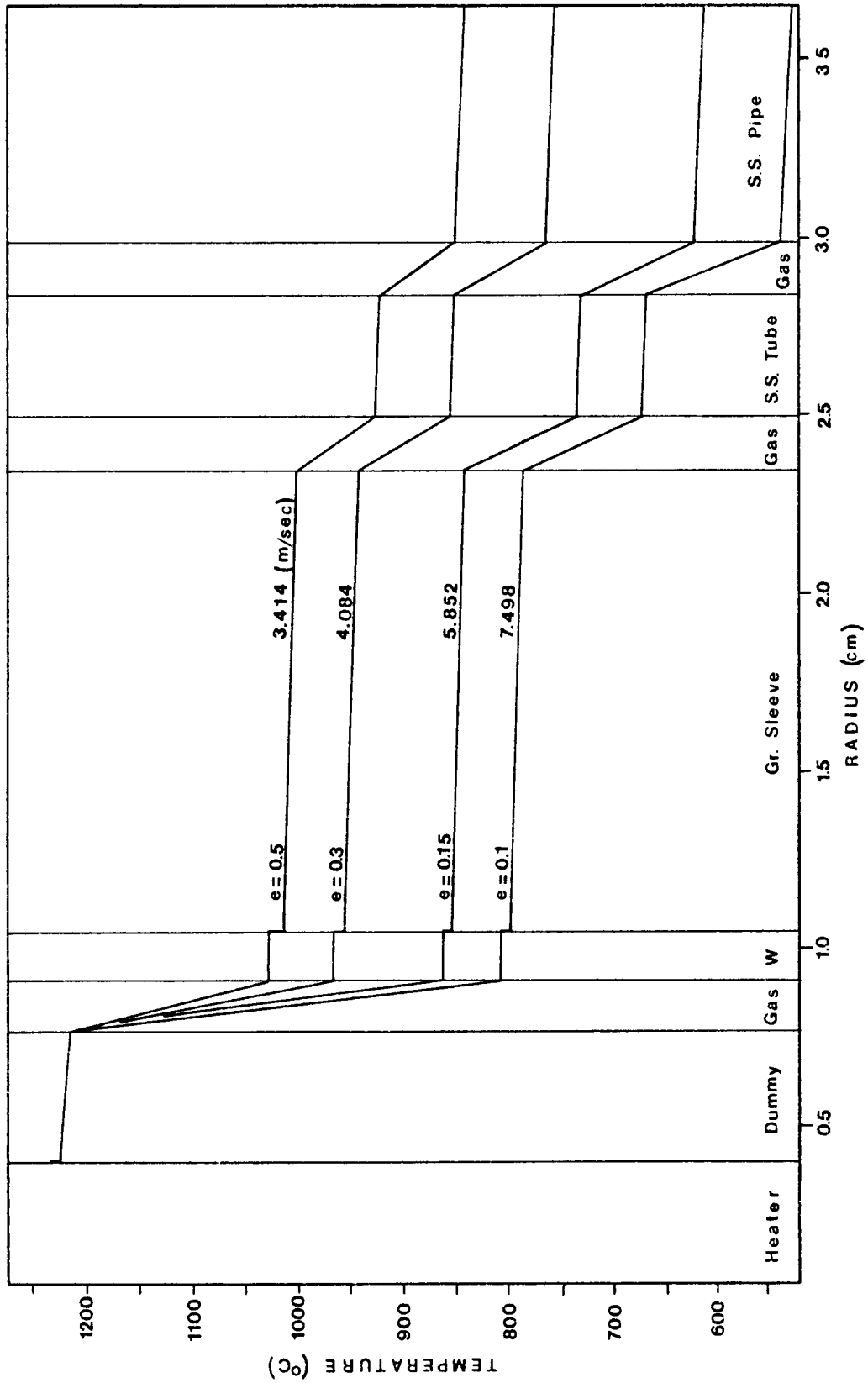



Figure 3-19. Cross-Sectional Temperature Distributions - Variation in Polished Tungsten Emissivity and Coolant Flow for Dummy Specimen Temperature of 1219°C.

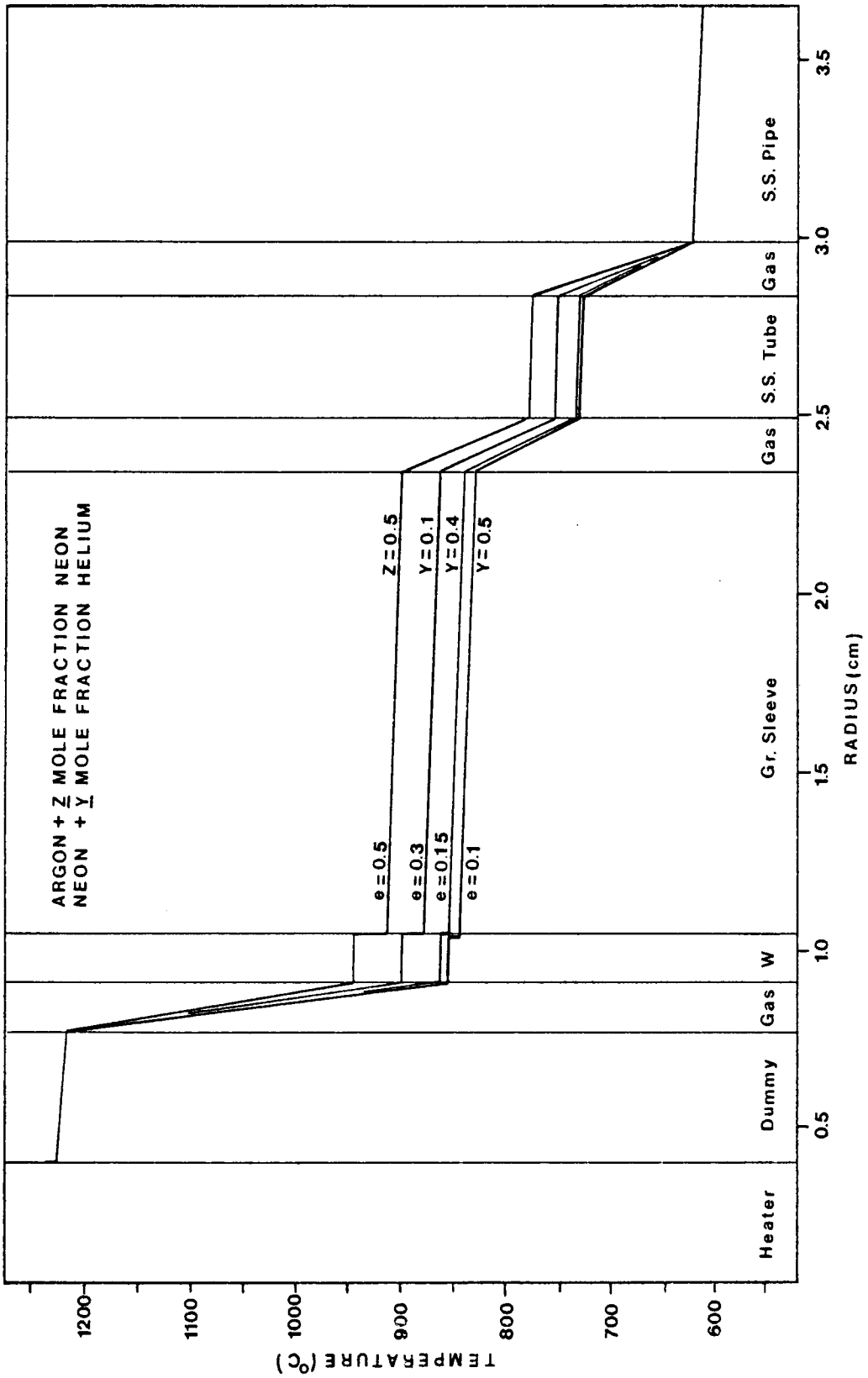



Figure 3-20. Cross-Sectional Temperature Distributions - Variation in Polished Tungsten Emissivity and Gas Mixture for Dummy Specimen Temperature of 1219°C.

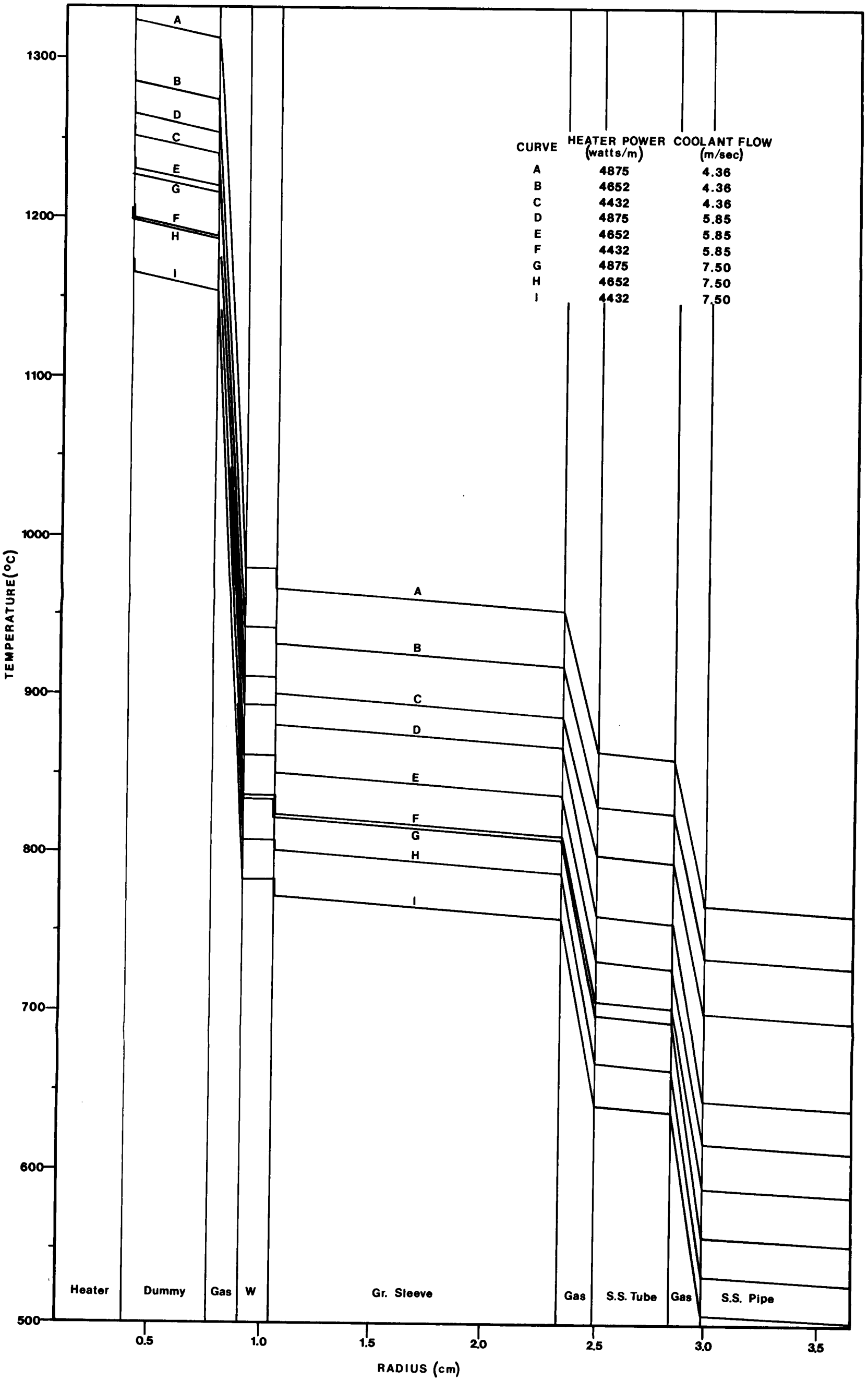



Figure 3-21. Cross-Sectional Temperature Distributions - Variation of Heater Power and Coolant Flow for Polished Tungsten Emissivity of 0.15 and Gas Mixture of Neon plus 0.4 Mole Fraction Helium.

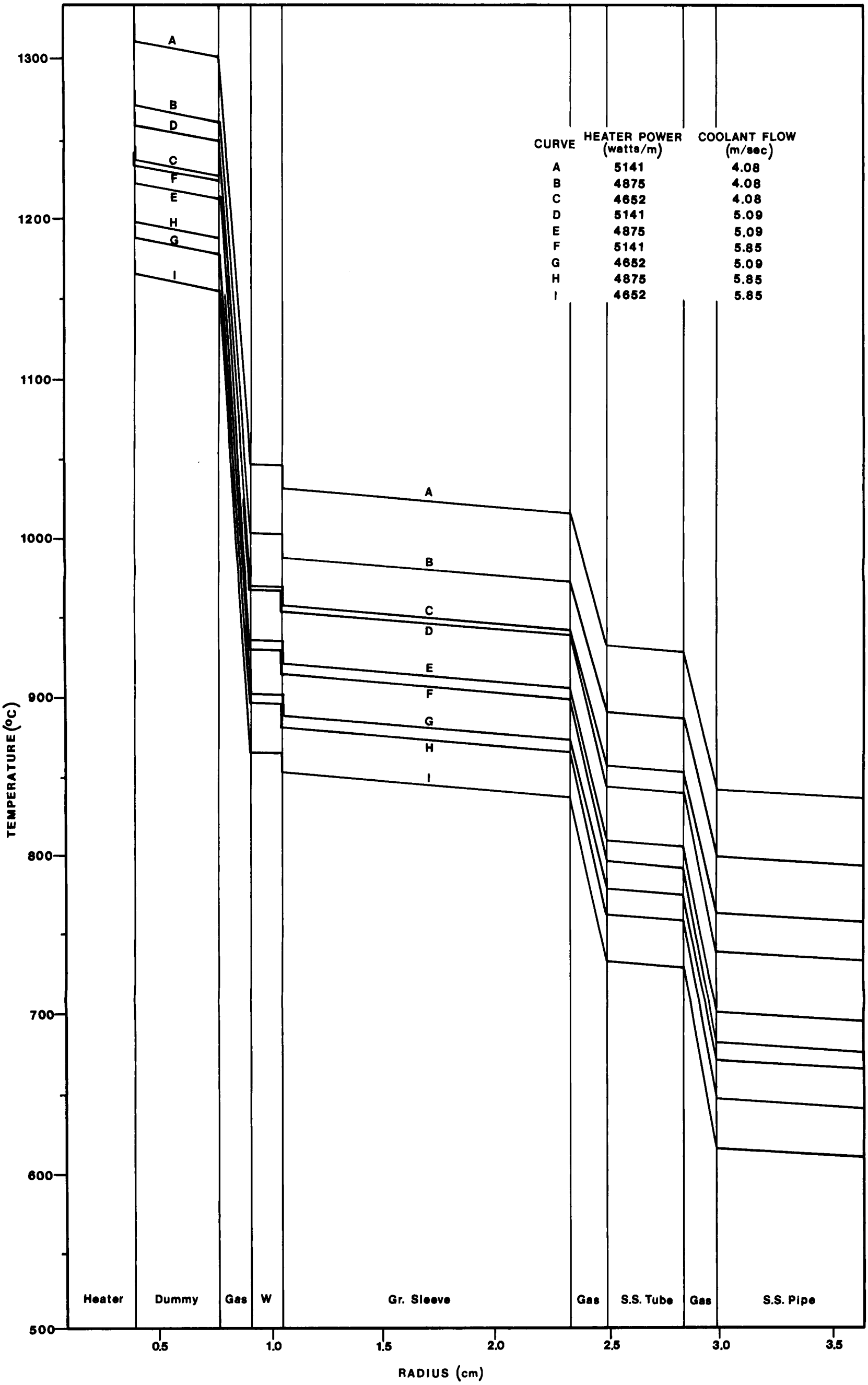



Figure 3-22. Cross-Sectional Temperature Distributions - Variation of Heater Power and Coolant Flow for Polished Tungsten Emissivity of 0.3 and Gas Mixture of Neon plus 0.4 Mole Fraction Helium.

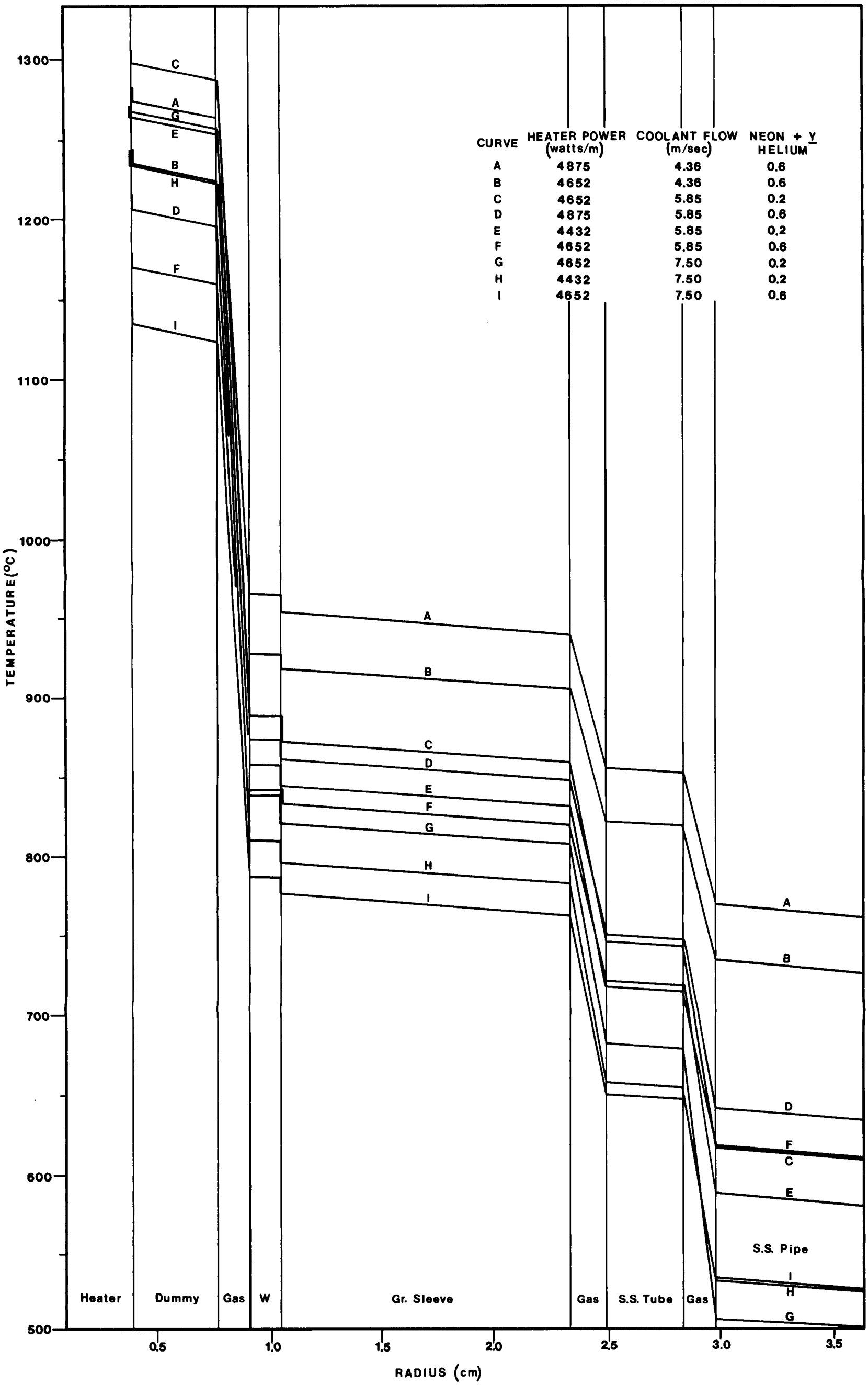



Figure 3-23. Cross-Sectional Temperature Distributions - Variation of Heater Power, Coolant Flow, and Gas Mixture for Polished Tungsten Emissivity of 0.15.

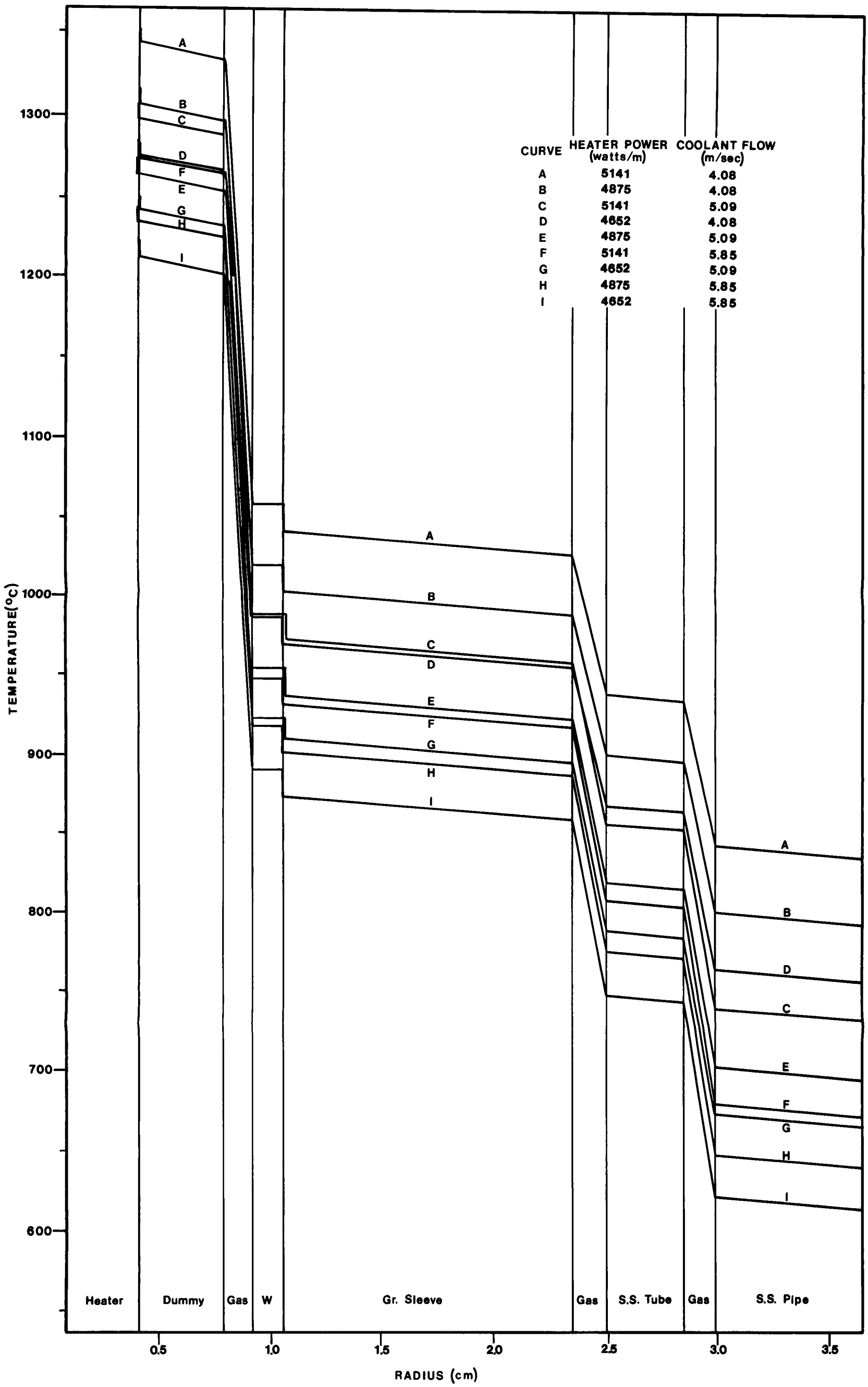



Figure 3-24. Cross-Sectional Temperature Distributions - Variation of Heater Power and Coolant Flow for Polished Tungsten Emissivity of 0.3 and Gas Mixture of Neon plus 0.2 Mole Fraction Helium.

meters per second (19.2 ft/sec), which is the upstream velocity.

A central heating element with a diameter of approximately 0.794 cm (5/16 in.) will be operated at approximately 4.65 Kwatt per meter (1.418 Kwatt/ft) but must be capable of producing a sustained power of 11.43 Kwatt per meter (3.485 Kwatt/ft).

The dummy specimen consists of three graphite tubes approximately 15.24 cm (6 in.) long with an outer diameter of 1.524 cm (0.6 in.) and an inner diameter of approximately 0.794 cm (0.3125 in.), where the precise inner diameter depends on the heater element used.

The tungsten tube has its inner surface with an inner diameter of 1.798 cm (0.708 in.) and an outer diameter of 2.07 cm (0.816 in.).

The graphite sleeve has an outer diameter of 7.86 cm (1.834 in.) and is formed to a close fit with the tungsten tube.

The 2 in. O. D. stainless steel tube, schedule #80, has an inner diameter of 4.963 cm (1.954 in.) and an outer diameter of 5.639 cm (2.22 in.).

The 2 1/2 in. O. D. stainless steel pipe, schedule #80, has an inner diameter of 5.944 cm (2.34 in.) and an outer diameter of 7.264 cm (2.86 in.).

The sweep gas is composed of neon plus 0.4 mole fraction helium.

The thermocouples are to be placed within the graphite sleeve with their location and size left to be determined. The optical pyrometer is to be used to monitor the temperature of the central dummy specimen, with its precise location and and attachment left to be determined.

The design of the ends of the capsule has not been determined as yet and therefore, the thermal analysis of the ends will not be discussed. However, a design has been proposed by Dr. Hall Roland and is shown in Figure 3-25.

This design, which is the same for each end, allows the capsule to be sealed using O rings by placing the ends approximately four inches from the heated section of the capsule and thereby greatly reducing the temperature. Another advantage of using this design is the uncomplicated way in which the series of tubes are held in place. This is accomplished by using a spring loaded retainer at each end.

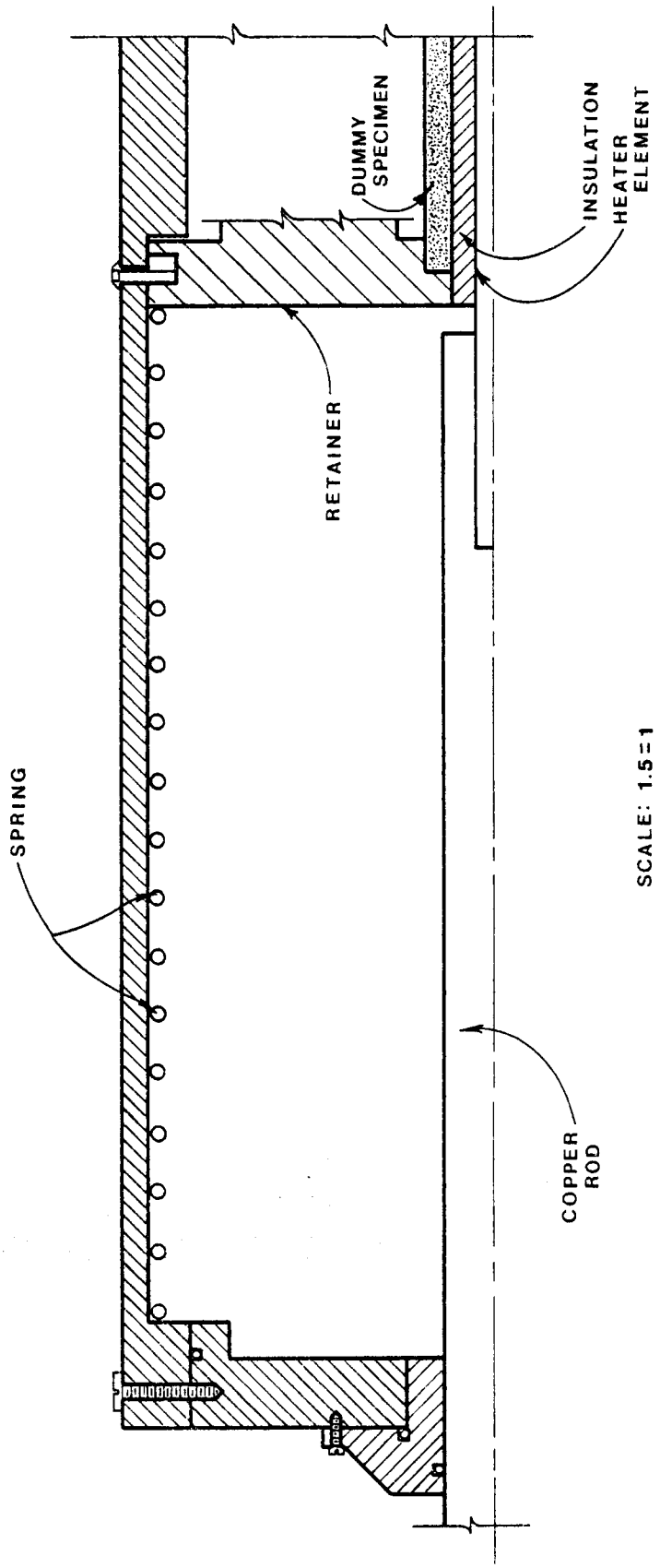



Figure 3-25. Proposed End Design of the Bench Test. Preliminary Design.

# CHAPTER IV

## SUMMARY

The preliminary thermal design of the 1250°C Irradiation Creep Capsule has been completed and conclusions are given in Section 2.8. This design was determined assuming a radiant emissivity of 0.15 for the polished inner surface of the tungsten tube and the properties of tungsten will remain constant. Therefore, further analysis must await the outcome of the bench test.

The thermal design of the bench test has been completed with the exception of the ends and conclusions are given in Section 3.7. This design was accomplished such that the bench test will answer three important questions:

1. Is the radiant emissivity of the tungsten in a low enough range to allow use of this design for the 1250°C capsule?
2. Will the radiant emissivities and other properties of the tungsten tube remain constant when subjected to the conditions found in the 1250°C Irradiation Creep Capsule?
3. How much confidence can be placed in the computational methods used?

# LIST OF REFERENCES

# LIST OF REFERENCES


1. R. J. Price, Review of Irradiation-Induced Creep in Graphite under HTGR Conditions, Gulf-GA-B12332 (November 1, 1972).

2. R. L. Senn, W. H. Cook, J. A. Conlin, and W. P. Eatherly, Design, Operation, and Initial Results from a Series of Graphite Creep Irradiation Experiments, May 5, 1976.

3. W. D. Turner and M. Simon-Tov, HEATING 3 -- An IBM 360 Heat Conduction Program, ORNL-TM-3208 (February, 1971).

4. W. D. Turner, D. C. Elrod, and I. I. Simon-Tov, HEATING 5 -- An IBM 360 Heat Conduction Program, ORNL-CSD-TM-15 (March, 1977).

5. C. R. Kennedy, Personal Conveyance (1976).

6. J. A. Conlin and R. L. Senn, Personal Conveyance (April, 1977).

7. N. M. Green et al., AMPX: Modular Code System for Generating Coupled Multigroup Neutron-Gamma Libraries from ENDF/B, ORNL-TM-3706 (March 1976).

8. W. P. Eatherly, R. L. Senn, J. A. Conlin, and H. C. Roland, Personal Conveyance (November, 1976).

9. R. L. Senn and J. A. Conlin, Personal Conveyance (1976).

10. H. C. Roland, GENGTC, A One-Dimensional CEIR Computer Program for Capsule Temperature Calculations in Cylindrical Geometry, ORNL-TM-1942 (December, 1967).

11. Frank Kreith, Principles of Heat Transfer, 3d Printing, International Textbook Co.-Scranton, 1960.

12. H. C. Roland, Personal Conveyance (1977).

# VITA

Kenneth E. Ebel was born on March 30, 1952 in New Orleans, Louisiana and lived there until September 1975, when he moved to Knoxville, Tennessee. His parents are Fred C. Ebel and Maribel S. Ebel. He attended East Jefferson High School and was graduated in May 1970.

He promptly enrolled at the University of New Orleans. After receiving the Bachelor of Science degree in Physics in August 1974, he entered graduate school to work towards a Master of Engineering degree. In September 1975, he enrolled at the University of Tennessee to work towards a Master of Science degree in Nuclear Engineering.